

IDENTIFICATION OF NOVEL GENES INVOLVED IN PLANAR CELL POLARITY
ESTABLISHMENT IN THE *DROSOPHILA* EYE

by

Duygu Koldere

B.S., Molecular Biology and Genetics, Istanbul Technical University, 2011

Submitted to the Institute for Graduate Studies in
Science and Engineering in partial fulfilment of
the requirements for the degrees of
Master of Science

Graduate Program in Molecular Biology and Genetics
Boğaziçi University
2014

IDENTIFICATION OF NOVEL GENES INVOLVED IN PLANAR CELL POLARITY
ESTABLISHMENT IN THE *DROSOPHILA* EYE

APPROVED BY:

Assoc. Prof. Arzu Çelik
(Thesis Supervisor)

Assist. Prof. Mehmet Somel

Assist. Prof. Stefan H. Fuss

DATE OF APPROVAL: 05.06.2014

To my family...

ACKNOWLEDGEMENTS

First and foremost, I would like to express my gratitude to my advisor Assoc. Prof. Arzu Çelik for her guidance, supervision and support during my study. I am grateful to her for encouraging me and providing me the opportunities to expand my vision.

I am also very grateful to Assist. Prof. Stein Aerts for his collaboration, support and valuable critics in the progress of this research work.

I would like to thank Delphine Potier from Aerts Lab for her great contribution to the bioinformatics parts of this project and also her patient guidance, useful comments and endless support whenever I needed.

I'm thankful to Assist. Prof. Mehmet Somel and Assist. Prof. Stefan Fuss for devoting their time to evaluate my thesis.

I want to send my thanks to the all members of LCB (Aerts Lab); Lotte, Valerie, Hana, Marina, Zeynep, Rekin's, Dmitry, Gert, Annelien, Katina for their help and friendship.

A huge bunch of thanks go to the great people of my lab; Ece, Gamze, Bahar, Stefan, Kaan, Rıdvan, Çağrı, Selen, Ayça, Ayşe, Gizem, Güner, Arzu A., and Güneş. They have been more than lab-mates to me. I'm thankful for all "super funny" jokes, "call from the grave" and everything else coming with their sincere friendship.

A simple 'thank you' is not enough to explain my gratitude towards Ece Terzioğlu Kara. She was always there for me with her unconditional love. I am lucky to have such a sincere friend in my life and so happy to be a member of the curlies-team!

I am more than grateful to my sincere friend Gamze Akgün for her unconditional love and support. It was a chance for me to work in the same lab and have amazing time together. I am happy to have such a lovely friend.

I would like to thank Xalid Bayramlı who has always been very helpful and such a great friend to me. Also, I would like to thank the other sister-lab members; Gizem, A.Burak, Kerem, Büşra, Yusuf, Burak and Serdar.

I also want to send my thanks to Kerem Y., Merve S., Cansu K., E. Begüm G., Burçak Ö., Merve K., Duygu D., Levent B., E. Duygu D., Aslı U., and Neslihan Z. for being great friends and making my time enjoyable in Boğaziçi.

My special thanks go to Kaya Akyüz for always making me feel better and stronger to be able to handle all situations. I am thankful for his help and friendship.

My heartfelt thanks go to my old and precious friends Aslı D., Aslı E., Ayten K. T., Buğse K., Buket A., Burcu S., Cansu E., Çağrı S., Dilay K., Esra A., Gamze Y., E. İlker Ö., Müge T., Salih T., Semiha A. and Serhat S. for their understanding, support and friendship.

My deepest thanks belong to my aunt Filiz Erdinç for being there all the time to support me with her endless love. Without her, it would not be possible for me to pursue my goals throughout the life.

And last but not least, I would like to thank my mother Çiğdem K., my father Ali K., my sister Burcu K., my grandmothers Ayşe K. and Nurten E., my grandfather Necdet E. and my aunt Funda E.C. for their everlasting love and support throughout my life. It is not possible to explain my gratitude towards them.

This project was supported by funds provided by TUBITAK Project No. 111T446 and Boğaziçi University Scientific Research Fund Projects BAP08M107 and BAP09M102.

ABSTRACT

IDENTIFICATION OF NOVEL GENES INVOLVED IN PLANAR CELL POLARITY ESTABLISHMENT IN THE *DROSOPHILA* EYE

In multicellular organisms proper functioning of tissues requires precise patterning of cells, which is acquired by apical-basal and planar cell polarization. To establish planar cell polarity (PCP), cells have to organize themselves along the plane of the epithelium. The mechanisms leading to this organization include several signalling pathways and cytoskeletal arrangements. Although general aspects of PCP have been elucidated, a complete view has not been established yet. It is known that genetic control of planar cell polarization is highly conserved among vertebrates and invertebrates. The *Drosophila* eye is a remarkable model system to study PCP, which is evident in organization of photoreceptors (PRs) into trapezoidal structures pointing to opposite directions in different halves of the eye. In the process of polarization, PR clusters require correct specification of R3/R4 cells, followed by chirality establishment and ommatidial rotation. We aimed to identify novel genes involved in PCP establishment by following two approaches. In the first approach, effects of six putative R3/R4 specific genes (*CG33259*, *cropped*, *faint sausage*, *polychaetoid*, *Stubble*, *taranis*) were analyzed by RNAi down-regulation, and *faint sausage* (*fas*) was determined as a promising candidate. Then, we generated recombinant *fas*-mutant flies to use in further mutant analyses. In the second approach, R3/R4 cells were sorted by FACS and analyzed by RNA-Seq in order to identify differentially expressed (DE) genes that might have role in PCP establishment. From this analysis, *ets domain lacking* (*edl*) appeared to be an interesting candidate. Additionally, we used this dataset to predict putative transcription factors that might be regulating differentially expressed genes. These analyses yielded six putative regulators of the DE genes in R3/R4: Trithorax-like, Grainy head, Jim, DNA replication-related element factor, Cropped, and CG7928. Furthermore, gene regulatory network data were used to dissect the Svp targetome, hypothesizing that this targetome might be containing genes contributing to PCP in the eye. Out of four putative targets that were selected for validation (*couch potato*, *bruchpilot*, *futsch*, *pebbled*), only one, *pebbled*, was verified as being regulated by Svp.

ÖZET

***DROSOPHILA* GÖZÜNDE DÜZLEMSEL HÜCRE KUTUPLAŞMASI KURULMASINDA ROL OYNAYAN YENİ GENLERİN TESPİT EDİLMESİ**

Çok hücreli organizmalarda dokular, işlevlerini düzgün biçimde gösterebilmek için apikal-bazal ve düzlemsel hücre polaritesi ile oluşturulan hatasız hücre düzenine ihtiyaç duyarlar. Düzlemsel hücre kutuplaşmasının (DHK) kurulması için hücrelerin epitel yüzey boyunca organize olması gereklidir. Bu organizasyonu sağlayan mekanizmalar, çeşitli sinyal yollarını ve hücre iskeleti düzenlemelerini içermektedir. DHK genel hatları ile aydınlatılmış olmasına rağmen henüz bir bütün halinde tanımlanamamıştır. DHK'nin genetik kontrolü omurgalı ve omurgasızlar arasında yüksek oranda korunmuştur. *Drosophila* gözü, trapezoid oluşturacak şekilde dizilen fotoreseptörlerinin gözün farklı yarılarında zıt kutupları göstermesi ile açıkça gözlenebilen DHK'yi çalışmak için mükemmel bir model sistemdir. Polarizasyon sürecinde fotoreseptör kümeleri, kiralite kurulması ve omatidyal rotasyon ile takip edilen, R3/R4 hücre farklılaşmasının düzgün biçimde gerçekleştirilmesine ihtiyaç duyar. Biz iki farklı yaklaşım ile DHK kurulmasında rol oynayan yeni genler bulmayı amaçladık. RNAi ifade düşürme yöntemi ile altı olası R3/R4-spesifik genin (*CG33259*, *cropped*, *faint sausage*, *polychaetoid*, *Stubble*, *taranis*) etkilerini incelediğimiz ilk yaklaşım sonucunda, *faint sausage* (*fas*) geninin umut verici bir aday olduğunu bulduk. İleride, mutant analizleri için kullanmak üzere rekombinant *fas*-mutant sinekleri yarattık. İkinci kısımda, gözde DHK kurulmasında rol oynayabilecekleri düşünüldüğü için, FACS ile topladığımız R3/R4 hücrelerinde farklı seviyede ifade (FI) edilen genleri, RNA-Seq ile tespit ettik ve *ets domain lacking* (*edl*)'i ilgi çekici bir aday olarak belirledik. Şimdiye dek sadece iki transkripsiyon faktörünün R3/R4 farklılaşmasında rol oynadığı belirlendiği için yenilerini bulmak üzere FI datasetini kullanıp bu bilgiyi genişletmeyi amaçladık. Analizler altı geni olası regülatör olarak gösterdi: Trithorax-like, Grainy head, Jim, DNA replication-related element factor, Cropped ve CG7928. Ancak bu çalışma süresince valide edilemediler. Gözde DHK'ye katkı sağlayabileceklerini hipotez ederek gen düzenleme ağı datasından Svp ve hedef genlerini elde ettik. Validasyon için seçilen dört hedef genden (*couch potato*, *bruchpilot*, *futsch*, *pebbled*) yalnızca birinin, *pebbled*, Svp tarafından regüle edildiğini onayladık.

TABLE OF CONTENTS

ACKNOWLEDGEMENTS	iv
ABSTRACT.....	vi
ÖZET	vii
LIST OF FIGURES	xii
LIST OF TABLES	xv
LIST OF SYMBOLS	xvi
LIST OF ACRONYMS/ABBREVIATIONS	xvii
1. INTRODUCTION	1
1.1. Eye Development in <i>Drosophila</i>	1
1.1.1. PR Specification	1
1.2. Planar Cell Polarity Establishment	5
1.2.1. PCP in the <i>Drosophila</i> Eye	6
1.2.1.1. Core Module	7
1.2.1.2. Global Module	9
1.2.1.3. Rotation Specific Module	9
1.3. Genetic Tools for <i>Drosophila</i>	11
1.3.1. Gal4/UAS System.....	11
1.1.1.1. Enhancer Trap Gal4 Line Collection.....	12
1.3.1.1. FlyLight Gal4 Line Collection	13
1.3.2. FLP/FRT System.....	13
1.4. RNA Sequencing	14
2. AIM OF THE STUDY	16
3. MATERIALS AND METHODS	17
3.1. Biological Material.....	17
3.2. Chemicals and Supplies	19
3.2.1. Chemical Supplies.....	19

3.2.2.	Buffers and Solutions	20
3.2.3.	Antibodies	20
3.2.4.	Embedding Media	21
3.2.5.	Disposable Labware	22
3.2.6.	Equipment	22
3.3.	Selection of the Candidate Lines.....	23
3.3.1.	Verification of the Expression Patterns of the Candidate Genes	23
3.4.	Experiments for Loss of Function Analyses	24
3.4.1.	Downregulation of the Candidate Genes by RNA Interference.....	24
3.4.1.1.	Visualization of the PRs by Cornea Neutralization Technique	25
3.4.2.	Clonal Analysis	26
3.4.2.1.	Generation of <i>fas</i> Mutant Lines Recombined to an FRT Site	26
3.4.2.2.	Generation of Whole Eye Mutants	27
3.4.2.3.	Generation of Mitotic Clones for Epistasis Analysis	27
3.5.	Histological Methods	28
3.5.1.	Immunohistochemistry.....	28
3.5.1.1.	Preparation of Larval Eye Imaginal Discs	28
3.5.1.2.	Antibody Staining of Larval Eye Imaginal Discs	28
3.5.2.	Visualization and Image Processing	29
3.6.	Selection of R3/R4 Specific Lines for RNA Sequencing	29
3.7.	Sorting of Cells from the Eye-Antennal Discs	30
3.7.1.	Preparation of Larval Eye-Antennal Discs for Cell Sorting	31
3.7.2.	Dissociation of the Cells	31
3.7.3.	Sorting of the Cells by the Fluorescent Activity	31
3.8.	Molecular Biological Techniques	31
3.8.1.	Isolation of RNA.....	31
3.8.2.	Preparation of cDNA Libraries	32

3.9.	RNA Sequencing and Data Analysis	32
3.9.1.	Pre-processing the Data	32
3.9.2.	Measuring Gene Expression	32
3.9.3.	GO Analysis.....	33
3.9.4.	Motif Discovery and Transcription Factor Prediction	33
3.9.5.	Validation Experiments for the Candidate Genes	35
4.	RESULTS	36
4.1.	Confirmation of the Expression Patterns of Putative R3/R4-Specific Genes	36
4.2.	Observed PCP Phenotypes After Down-regulating the Candidate Genes	39
4.3.	Mutant Analyses of the Selected Candidate <i>faint sausage</i>	44
4.4.	Generation of Whole Eye Mutants for <i>faint sausage</i>	47
4.5.	Interaction Between <i>fas</i> and <i>svp</i>	49
4.6.	Transcriptome Analysis of the R3/R4 PR Pair	50
4.6.1.	FlyLight Database Screen to Select R3/R4-Specific Lines	51
4.6.2.	Sorting of R3/R4 PR Cells	55
4.6.3.	Quality of the Extracted RNA	59
4.6.4.	Enriched Gene Ontology Terms and Possible Candidates	62
4.6.5.	Enriched Motifs and Possible Regulators of R3/R4 PR Specification ..	70
4.6.6.	Enlightening the Transcription Factor-Targetome Network of R3/R4 ..	72
4.6.7.	Validation of the Predicted Target Genes of Svp.....	75
4.6.7.1.	Selected candidate: <i>couch potato</i>	76
4.6.7.2.	Selected candidate: <i>futsch</i>	78
4.6.7.3.	Selected candidate: <i>bruchpilot</i>	79
4.6.7.4.	Selected candidate: <i>pebbled</i>	81
5.	DISCUSSION.....	83
5.1.	Correlating R3/R4 Specific Genes to Planar Cell Polarity Establishment.....	84
5.2.	Transcriptome Analysis of R3/R4 Cells	89
5.2.1.	Sorting of R3/R4 PRs by FACS	89
5.2.2.	Differential Expression Analyses.....	92

5.2.3. Predicted TFs Involved in R3/R4 Specification and PCP Establishment ...	93
5.2.4. Validation of Svp Predicted Target Genes.....	95
6. CONCLUSION	96
APPENDIX A: EXPRESSION PATTERNS OF THE ENHANCER TRAP GAL4 LINES..	97
APPENDIX B: EXPRESSION PATTERNS OF THE SCREENED FLYLIGHT GAL4 LINES	98
REFERENCES	100

LIST OF FIGURES

Figure 1.1. Schematic representation of PR specification process in the 3 rd instar larval eye disc.	3
Figure 1.2. PCP establishment in the adult <i>Drosophila</i> eye.	6
Figure 1.3. Schematic summary of R3/R4 specification through Fz/PCP signalling.	8
Figure 1.4. Interactions between the genes involved in PCP establishment.	10
Figure 3.1. Set up of cross to verify expression patterns of the enhancer trap Gal4 lines.	24
Figure 3.2. Crosses for knockdown analysis of candidate genes.	25
Figure 3.3. Crosses for generating mitotic clones of <i>svp</i> for the epistasis analysis.	28
Figure 3.4. General workflow for the RNA-Seq experiment.	29
Figure 3.5. Crossing scheme to screen FlyLight lines.	30
Figure 4.1. <i>CG33259</i> -Gal4 enhancer trap line displays a R3/R4 specific expression pattern in the 3 rd instar larval eye-antennal disc.	37
Figure 4.2. <i>Headcase</i> expression is not specific to R3/R4 in 3 rd instar larval eye disc. ..	38
Figure 4.3. R3/R4 specific expression of <i>faint sausage</i> was confirmed in 3 rd instar larval eye disc.	39
Figure 4.4. PCP defective phenotypes in adult eyes.	41
Figure 4.5. Eye structure was abnormal in <i>cropped</i> down-regulated flies.	44
Figure 4.6. PCP defective phenotypes in the eyes of heterozygous <i>fas</i> mutants.	46
Figure 4.7. Generation of whole <i>fas</i> mutant eyes in heterozygous flies.	48
Figure 4.8. <i>Svp</i> might be repressing <i>fas</i> in R3/R4 PRs.	49
Figure 4.9. Expression patterns of the screened FlyLight Gal4 lines.	53

Figure 4.11. <i>ro</i> -Gal4 FlyLight line has R3/R4 specific expression pattern in the 3 rd instar larval eye-antennal disc.	54
Figure 4.12. <i>sNPF</i> -Gal4 FlyLight line has R3/R4 specific expression pattern in the 3 rd instar larval eye-antennal disc.	55
Figure 4.13. FACS dot plots of R3/R4 cell sorting.	57
Figure 4.14. Chp-GFP expression is limited to approximately five rows at the posterior margin of the 3 rd instar eye disc.	58
Figure 4.15. rRNA measurements for <i>sNPF</i> GFP-positive and <i>chp</i> GFP-negative fractions.	60
Figure 4.16. Hierarchical graphs of enriched GO terms related to biological processes among DE genes in R3/R4.	65
Figure 4.17. Hierarchical graphs of enriched GO terms related to molecular function among DE genes in R3/R4.	67
Figure 4.18. Enriched TF binding motif associated with <i>Svp</i>	72
Figure 4.19. GO analyses of the <i>Svp</i> predicted target genes.	72
Figure 4.20. Network of <i>Svp</i> targetome.	73
Figure 4.21. The <i>Svp</i> - <i>Salm</i> interaction in R3/R4 PRs was recapitulated.	75
Figure 4.22. <i>Cpo</i> displays a homogenous expression pattern through all PRs in the 3 rd instar larval eye disc.	76
Figure 4.23. <i>Svp</i> does not affect the expression of <i>Cpo</i>	76
Figure 4.24. <i>Futsch</i> localizes to the developing axons and around the nuclei of PRs in the 3 rd instar larval eye disc.	77
Figure 4.25. <i>Svp</i> does not affect the expression of <i>Futsch</i>	78
Figure 4.26. <i>Brp</i> displays a homogenous expression pattern through all PRs in the 3 rd instar larval eye disc.	79
Figure 4.27. <i>Svp</i> does not affect the expression of <i>Brp</i>	79

Figure 4.28. Peb is expressed in all PRs in the 3 rd instar larval eye disc.	80
Figure 4.29. Svp might be affecting the expression of Peb.	81
Figure 4.30. Examination of Peb expression in mosaic eye disc by quadruple staining. ..	81

LIST OF TABLES

Table 3.1.	> <i>Drosophila melanogaster</i> strains used in this study.	17
Table 3.2.	List of chemicals used in this study.	19
Table 3.3.	Buffers and solutions used in this study.	20
Table 3.4.	Antibodies used in this study.	21
Table 3.5.	Disposable labware used in this study.	22
Table 3.6.	Equipment used in this study.	22
Table 3.7.	Summary of 72 RNA-Seq experiments of wild type and perturbed tissues of 3 rd instar larvae.	34
Table 4.1.	Number of sorted cells from the dissected eye-antennal (EA) discs.	56
Table 4.2.	RNA-Seq analyses for sNPF GFP-positive and chp GFP-negative fractions.	61
Table 4.3.	The top 40 differentially expressed genes in R3/R4 PRs.	62
Table 4.4.	Significantly enriched biological process related GO terms among DE genes in R3/R4 (FDR<0.05).	66
Table 4.5.	Significantly enriched molecular function related GO terms among DE genes in R3/R4 (FDR<0.05).	68
Table 4.6.	Enriched motifs among DE genes in R3/R4 PRs and putative TFs that bind them.	69

LIST OF SYMBOLS

g	Gram
kb	Kilobase
L	Liter
ml	Mililiter
mm	Milimeter
M	Molar
ng	Nanogram
nm	Nanometer
psi	Pound force per square inch
rpm	Revolutions per minute
v	Volume
w	Weight
μg	Microgram
μm	Micrometer
μl	Microliter

LIST OF ACRONYMS/ABBREVIATIONS

BDTNP	Berkeley Drosophila Transcription Network Project
DAPI	4',6-diamidino-2-phenylindole
DE	Differentially Expressed
DNA	Deoxyribonucleic Acid
DRSC	Drosophila RNAi Screening Center
EA	Eye-antennal
EGFR	Epidermal Growth Factor Receptor
EMA	Ethidium Monoazaide
FACS	Fluorescence-activated Cell Sorting
FC	Fold Change
FDR	False Discovery Rate
FITC	Fluorescein Isothiocyanate
FnIII	Fibronectin Type III
FRT	FLP Recombination Target
FSC	Forward Scatter
GFP	Green Fluorescent Protein
GO	Gene Ontology
GPI	Glycosylphosphatidylinositol
Ig	Immunoglobulin
IgSF	Immunoglobulin Superfamily
JNK	c-Jun N-terminal Kinase
LRR	Leucine Rich Repeat
MF	Morphogenetic Furrow
NES	Normalized E-Score
NGS	Normal Goat Serum
nt	Nucleotide
PBS	Phosphate Buffered Saline
PCP	Planar Cell Polarity

PFA	Paraformaldehyde
pH	Power of Hydrogen
PI	Propidium Iodide
PIPLC	Phosphatidylinositol-specific Phospholipase C
PR	Photoreceptor
PTM	Pavlidis Template Matching
pval	p value
PWM	Position Weight Matrix
qRT-PCR	Quantitative Reverse transcription polymerase chain reaction
RNA	Ribonucleic Acid
RNA-Seq	RNA Sequencing
RNAi	RNA Interference
RPM	Reads Per Million
SMART	Switching Mechanism at 5'-end of Ribonucleic Acid Template
SSC	Side Scatter
TaDa	Targeted DNA Adenine Methyl-transferase Identification
TF	Transcription Factor
TMH	Transmembrane Helix
UAS	Upstream Activating Sequence
VDRC	Vienna Drosophila RNAi/Resource Center
wt	Wild-type

1. INTRODUCTION

1.1. Eye Development in *Drosophila*

Although eyes can be structurally different among species, most of the genes involved in eye development are well conserved. Light-absorbing molecules, namely opsins can be given as an example for these common molecules as they have not been subjected to so much environmental pressure throughout evolution. However, necessities to fit the environment made organisms develop several types of eyes that can be classified as simple and compound. Vertebrate eyes have a simple eye structure made up of a single optical system. On the other hand, most of the insects have compound eyes that consist of multiple eye-like structures named ommatidia. Each individual eye unit receives one part of the image and sends it to the center, where the entire image is created by putting the parts together (Litzinger and Rio-Tsonis, 2002).

The *Drosophila* compound eye is composed of approximately 800 ommatidia, which are aligned in a precise pattern. Each ommatidium is composed of eight photoreceptor cells (PRs), which are classified as outer (R1-R6) and inner PRs (R7, R8). Additionally, there are 12 accessory cells including cone, pigment and bristle cells. An accurate organization of the cells composing each ommatidium and alignment of all ommatidia throughout the eye are crucial for the fly to be able to achieve proper vision (Cagan and Ready, 1989; Heberlein and Moses, 1995).

1.1.1. PR Specification

As *Drosophila* progresses through its developmental stages, the eye also undergoes several molecular and cellular changes (Charlton-Perkins and Cook, 2010). Formation of the eye pattern is a multi-step event that requires many factors; however, the interaction network has not been completely elucidated yet. The gene *eyeless* (*ey*), a homologue of mammalian *Pax6*, is one of the master regulators of *Drosophila* eye development and

required for development of the eye primordium; therefore, its absence results in a total loss of the eye. The other master regulators that can be considered as early retinal genes are *sine oculis (so)*, *twin of eyeless (toy)*, *eyes absent (eya)*, *dachshund (dac)*, and *teashirt (tsh)* (reviewed in Şahin and Çelik, 2013).

The progressive formation of the eye pattern starts at the third instar of larval development in the eye-antennal imaginal discs. This imaginal disc can be defined as a monolayer epithelial sheet made up of a posterior and anterior part from which the eye and the antenna are derived, respectively. A wave of differentiation morphogenetic furrow (MF) is initiated at the posterior margin of the eye disc by Hedgehog (Hh) signalling. Decapentaplegic and Ecdysone are other signalling molecules playing a role in this initiation process (Niwa *et al.*, 2004). Once the MF is triggered, it sweeps across the disc towards the anterior part as it leaves differentiated cells posterior to it. A feedback loop between Hh and Atonal (Ato) plays a role in the progression. Hh molecules are secreted from the differentiating cells and induce *atonal (ato)* expression throughout the MF and nearby undifferentiated cells. Hh secretion is promoted by Ato in those cells and as a response to Hh signalling, the cells anterior to the MF secrete Dpp that leads cells to proneurogenesis. The MF, therefore, progresses through these recursive interactions (Lopes and Casares, 2010).

Since migration does not take place in the cells posterior to the MF, initial specification events define the eventual pattern (White and Jarman, 2000). The first PR to be specified is R8, a founder cell that recruits the other PRs subsequently. Every R8 is selected from an evenly spaced *ato*-expressing cell group that resides right after the MF. In these clusters Ato activates *senseless (sens)*, which encodes a zinc-finger transcription factor necessary to ensure R8 differentiation. Then, Notch-mediated lateral inhibition decreases the number of *ato*-expressing cells to one for each cluster and these selected cells are defined as R8 precursors. *sens* continues to be expressed in these cells and represses *rough (ro)* to maintain the R8 fate (Frankfort *et al.*, 2001; Pepple *et al.*, 2008).

After their specification, R8 precursors recruit the other PRs sequentially in the following order: R2/R5, R3/R4, R1/R6, and R7. Although how this recruitment happens is not fully understood, the EGFR signalling plays the major role. At first, the EGFR ligand

Spitz is activated in R8 cells, and then the signal is relayed to R2/R5 precursors, resulting in Spitz production in R2/R5. In this way, all non-R8 precursors receive and transmit the EGFR signal (Bao, 2010; Roignant and Treisman, 2009). However, the same signal triggers different responses in these PR subtypes and this variation is very likely to be related with differential expression of particular genes in each subtype (Bao, 2010).

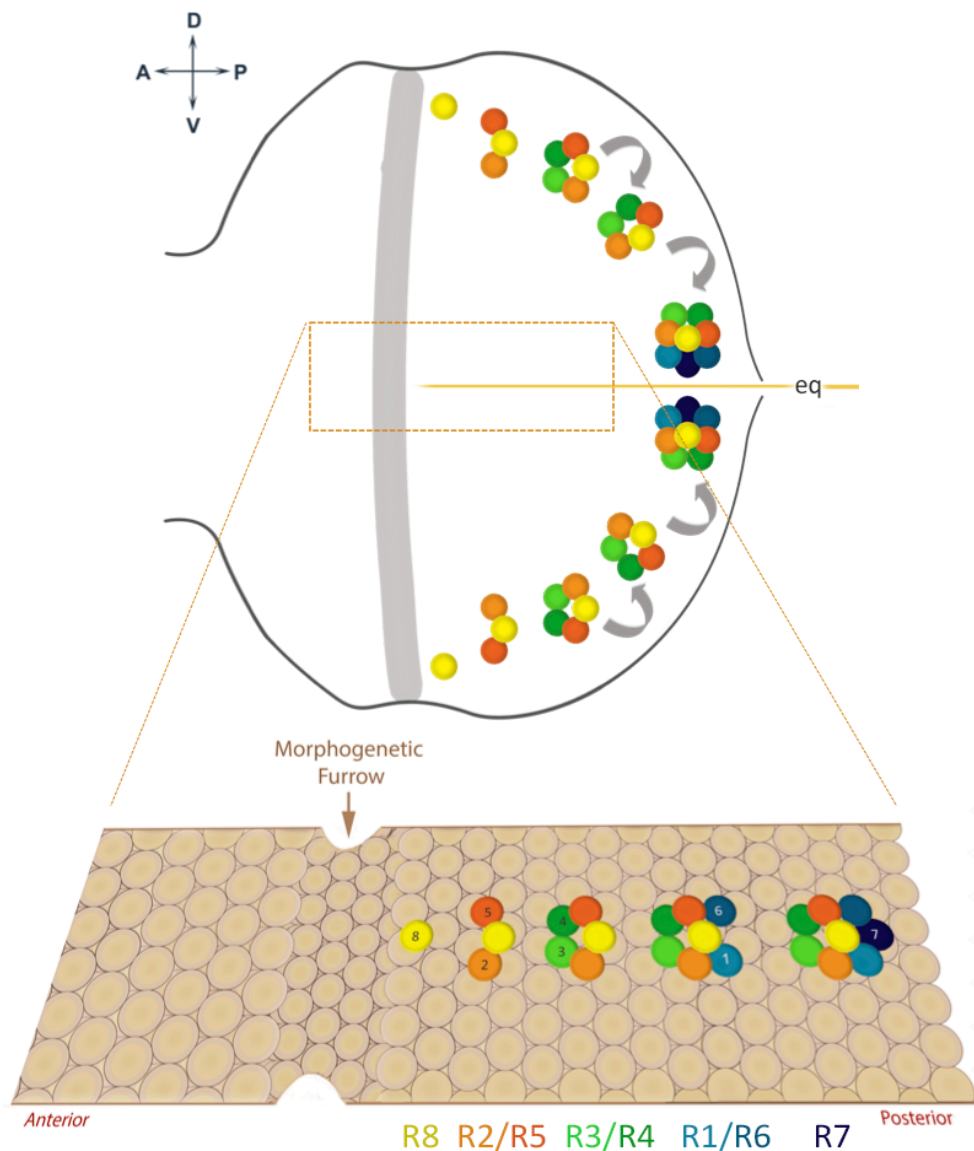


Figure 1.1. Schematic representation of PR specification in the 3rd instar larval eye disc. MF is initiated at the posterior site and moves towards the anterior leaving differentiating cells in its wake. The R8 is specified first, then recruits the other PR pairs in the order: R2/R5, R3/R4, R1/R6, R7. Dorsal is up, anterior is to the left, eq represents equator.

The first recruited PR pair, R2/R5, highly expresses *ro*, which encodes a homeodomain transcription factor that represses the R8-specific transcription factor Senseless in R2/R5 precursor cells and thus prevents them from becoming R8 cells (Frankfort *et al.*, 2001; Kimmel *et al.*, 1990). After the recruitment of R2/R5, PRs R3 and R4 join to form a five-cell pre-cluster. The essential gene for R3/R4 fate choice is the nuclear hormone receptor *seven-up* (*svp*), which is highly expressed in that cell pair. In the absence of Svp, cells adopt the R7 cell fate (Mlodzik *et al.*, 1990). Additionally, the *spalt* (*sal*) gene complex is also crucial in this process as it regulates the expression of *svp* through encoding two transcription factors, Spalt-major (Salm) and Spalt-related (Salr), that initiate *svp* expression in R3 and R4 precursors. Then Svp represses Sal via negative regulation and prevents cells to adopt the inner cell fate (Domingos *et al.*, 2004). Moreover, a non-canonical Wnt pathway, Fz/PCP, plays a role in R3/R4 cell fate choice through interactions between Wnt ligand and the membrane protein Frizzled (Fz). After activation of the Fz/PCP signalling pathway the cell closer to the equator becomes R3 and *svp* ensures the proper interpretation of the signal in R3 by preventing it to become R7 (Fanto *et al.*, 1998; Tomlinson and Struhl, 1999; Zheng *et al.*, 1995). The received signal gives rise to up-regulation of Delta (Dl) expression in R3, which then leads to initiation of Notch signalling in the neighboring cell. Notch (N) activation represses Dl in this neighbor cell and as a result, it gets specified as R4 (Cooper and Bray, 1999; Fanto and Mlodzik, 1999).

After the five-cell cluster of PRs is established, R1 and R6 precursors join the cluster. Svp is required for specification of the R1/R6 cell fate; otherwise, these precursor cells prefer to adopt either R7 or R8 cell fates (Mlodzik *et al.*, 1990). The other transcription factors important for the specification of the R1/R6 pair are the homeodomain proteins BarH1 and BarH2 (Higashijima *et al.*, 1992). In addition to these, Ras/Raf pathway-dependent expression of a nuclear receptor Phyllopod (Phyl) is involved in precise specification of R1 and R6 cells (Miller *et al.*, 2008).

R7 is the last PR that is recruited. It requires *bride-of-sevenless* (*boss*) expression in R8 cells. Boss has a non-autonomous effect and activates the receptor tyrosine kinase Sevenless (Sev) residing on the membrane of the R7 precursor cell. Except R7 cells, Sev expression is described in R1/R6 and R3/R4 cells; however, the receptor Sev on the

presumptive R7 cell membrane is the one that interacts with the Boss signal from the R8 cell (Reinke and Zipursky, 1988). R1 and R6 cells also play a role in R7 specification by expressing the Delta ligand that activates the Notch signalling pathway. In the absence of Sev in R7 precursors, the cells prefer a non-neuronal cell fate and become cone cells. Moreover, R7 precursors lacking Notch signalling adopt the R1/R6 cell fate. In addition to Notch signalling, receptor tyrosine kinase signalling also contributes to the specification of R7 PRs. R7 precursors express *phyl* as a result of high levels of receptor tyrosine kinase signalling. Interaction between Phyl and Seven in absentia (Sina) forms a complex that acts in degradation of Ttk88, which functions as repressor of a number of neuron-specific genes. One of the genes is *pros*, which can be regarded as an R7 marker. It was shown that receptor tyrosine kinase signalling activates Pointed (Pt) and Lozenge (Lz) TFs to regulate the expression of Pros (Daga *et al.*, 1996; reviewed in Raabe, 2000).

All these specification steps require specific transcription factors and several signalling pathways. However, still many of the involved factors and interaction networks are waiting to be elucidated.

1.2. Planar Cell Polarity Establishment

Most of the tissues and organs require a correct anatomy to execute their function properly. For this reason, their cells have to be organized throughout both their apical-basal axis and the axis orthogonal to it. The latter is called planar cell polarity (PCP) or tissue polarity, which can be further defined as the arrangement of a sheet of cells within the epithelial plane (Eaton, 1997). However, it is also observed in a rare number of mesenchymal cells (reviewed in Thomas and Strutt, 2012).

The precisely aligned bristles of an insect, *Rhodnius*, has urged attention of Wigglesworth (1940); afterwards, lots of studies have been done to unravel the underlying mechanisms of this kind of arrangements, which were later referred to as planar cell polarity. Subsequent studies in vertebrates revealed high conservation among animals (reviewed in Singh and Mlodzik, 2012). Moreover, connections between disrupted PCP signalling and several human diseases such as cystic kidney disease, congenital heart

disease, neural tube defects and deafness have been established (reviewed in Simons and Mlodzik, 2008).

Based on genetic and molecular studies, molecules contributing to PCP via distinct signalling pathways are grouped into three modules: core module, global module, and tissue-specific module (Tree *et al.*, 2002; Wong and Adler, 1993). Most of the insights into PCP modules were gained through studies in *Drosophila* organs such as the eye, wing, and thorax. While there is quite some insight, lack of a complete picture of interactions between these modules leaving this open to discussions and controversial interpretations. (Lawrence and Casal, 2013).

1.2.1. PCP in the *Drosophila* Eye

In the adult *Drosophila* eye, PCP can be observed as the mirror symmetrical arrangement of PRs in two chiral forms relative to the dorso-ventral midline, the equator (Figure 1.2). However, this regular arrangement based on the earlier organization begins at the third instar larval eye disc and is very closely linked to the specification process of the R3 and R4 PRs (Fanto *et al.*, 1998; Singh and Mlodzik, 2012). The mechanisms will be further explained in detail as three modules in terms of the eye:

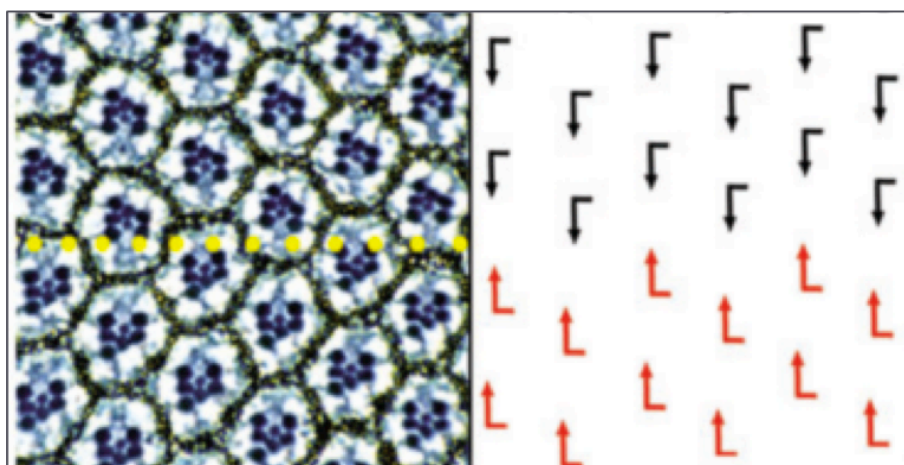


Figure 1.2. PCP establishment in the adult *Drosophila* eye. PR clusters adopt different chiral forms at dorsal and ventral half and generates mirror symmetry along the equator (dotted yellow line). Black and red arrows represent orientations of the ommatidia at dorsal and ventral, respectively (Simons and Mlodzik, 2008).

1.2.1.1. Core Module. The proteins involved in core PCP module are a seven-pass transmembrane Wnt receptor Frizzled (Fz), cytosolic proteins Dishevelled (Dsh), Prickle (Pk), and Diego (Dgo), Van Gogh/Strabismus (Vang/Stbm), a seven-pass transmembrane cadherin Flamingo (Fmi). They are conserved from invertebrates to mammals and act via Fz/PCP signalling in various tissues as well as in the *Drosophila* eye. These proteins localize asymmetrically within cells and allowing interactions with neighboring cell to receive and transmit polarization signals (reviewed in Peng and Axelrod, 2012; Strutt *et al.*, 2002). The major role of Fz/PCP signalling in the eye is to ensure correct specification of R3/R4 PRs for a proper determination of chirality, which subsequently affects direction of rotation (Fanto *et al.*, 1998).

As previously mentioned, PRs differentiate in a step-wise manner posterior to the MF. After the second pair of cells, the R3/R4 precursors, are recruited all recruited cells together form a five-cell precluster. At this stage the core module proteins localize to the apical membrane of these PRs. Then, Fz/Dsh complex becomes enriched in R3 and Vang/Stbm/Pk is enriched in R4 at the R3/R4 membrane boundary (Strutt *et al.*, 2002). It is thought that this asymmetry and polarization is driven by a gradient of a diffusible signalling molecule from the equator, most likely a Wnt ligand that can interact with the Fz receptor. However, such a Wnt molecule has not been found to interact with Fz in the *Drosophila* eye yet (reviewed in Strutt and Strutt, 2002).

It is anticipated that this unknown ligand of Fz is present at high levels along the equator. Therefore, the strength of the signal received by cells depends on their localization in the eye disc. Hence, the cell closer to the midline receives the Fz signal at a higher level and expresses Dl, which in turn activates N expression in the neighboring cell. This results in the R3 cell fate choice in the equatorial cell while the polar cell adopts the R4 cell fate (Cooper and Bray, 1999; Fanto and Mlodzik, 1999) (Figure 1.3). Fmi, together with its interaction partner Dgo, is also important in this process as becomes enriched in R4 and down-regulates Dl expression (Das *et al.*, 2002).

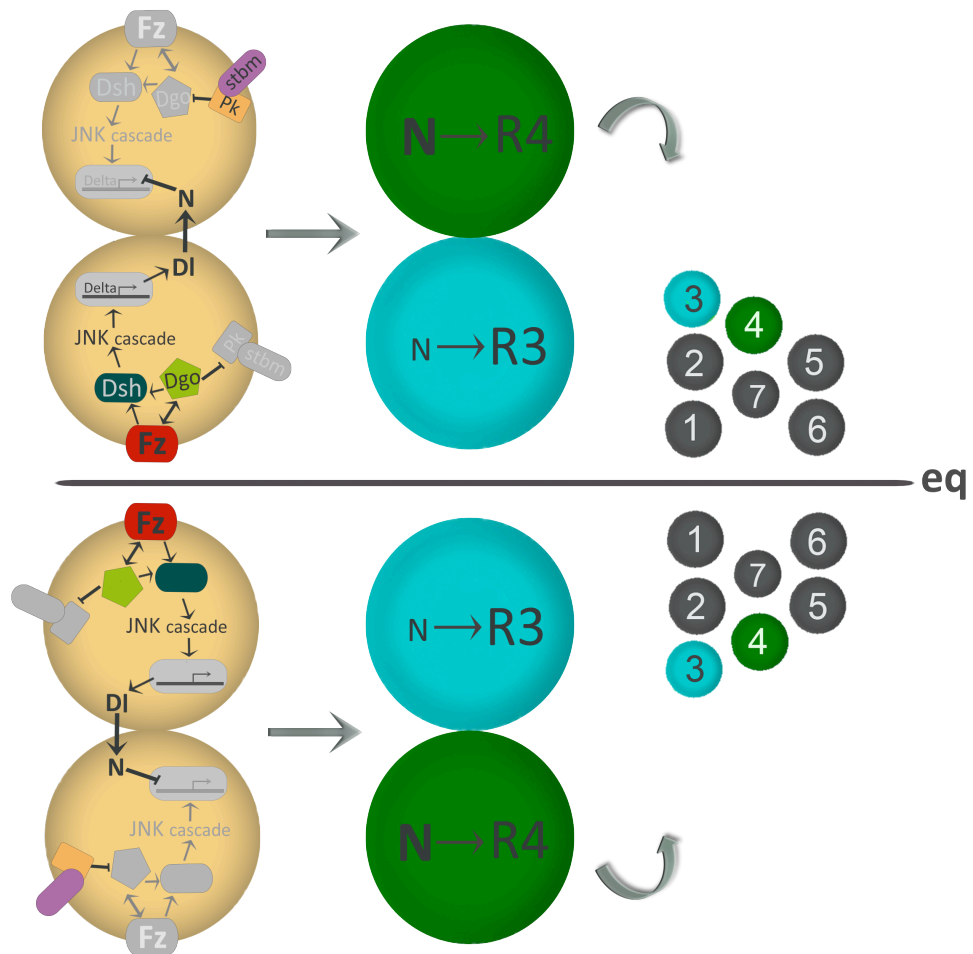


Figure 1.3. Schematic summary of R3/R4 specification through Fz/PCP signalling. The unknown Fz ligand is predicted to be found at high levels along the equator, decreasing gradually towards polar sides. The cell closer to the equator is subjected to the Fz signal more than its neighbor, which in turn generates an asymmetric DI/N expression pattern between this cell pair.

It should be noted that correct cell fate choice of R3/R4 is crucial to determine correct chirality of PRs. As loss of function studies have revealed, *fz* has a role in both chirality and ommatidial rotation, it is very important for PCP establishment in the eye. Additionally, a Notch domain interacting with the cytosolic signal transducer Dsh has been identified. Considering the low N activity in the cell in which the Fz/Dsh complex is enriched, it is believed that this interaction has a repressive effect on N signalling. Thus, Fz/PCP signalling and its downstream effector Notch are crucial to exert proper chirality and rotation (Strutt *et al.*, 2002).

1.2.1.2. Global Module. The molecules that are included in the global module are the players of the Ft/Ds/Fj signalling pathway. These include the atypical cadherins Fat and Dachshous, and a Golgi protein kinase Four-jointed (Fj). Large transmembrane proteins Ft and Ds form heterodimers by binding each other at cell surfaces. It is known that Fj regulates binding via phosphorylating their extracellular cadherin repeats, which results in an increment in the affinity of Ft for Ds and a decrement in the affinity of Ds for Ft. In tissues gradients of Fj and Ds are opposite to each other, which in turn provides directional information (reviewed in Matis and Axelrod, 2013; Tissir and Goffinet, 2013). Additionally, the gradients of these three molecules are defined by the graded distribution of Wg, which is high at the poles and low at the equator and Notch and JAK/STAT signals, which are low at the poles and high at the equator (Yang *et al.*, 2002; Zeidler *et al.*, 1999).

The core PCP module provides local polarity; however, the cells need directional cues to be polarized along the tissue axes properly. It is very likely that this kind of cue could be a diffusible signal molecule that provides a gradient throughout the tissue. Since Fat (Ft) and Dachshous (Ds) generate such a gradient, they are thought to provide the necessary cue. However, there is a controversy on the interaction of these two modules, so it is still not known if the global module interacts with the core module as an upstream regulator or as a parallel mechanism (reviewed in Matis and Axelrod, 2013).

1.2.1.3. Rotation Specific Module. Ommatidial rotation is one of the aspects of PCP, which is the least understood compared to the other aspects (R3/R4 specification and chirality establishment). However, it is evident in the third instar larval eye disc as it occurs in a two-step process by the activity of PCP genes after cell fate determination of R3 and R4. In the first step, at about row six, PR clusters rotate 45 degrees clockwise in the dorsal half and counter clockwise in the ventral half of the eye disc. After several rows, these rotations continue with another 45 degrees in the same directions. Thus, the initial symmetry through the eye disc is changed into mirror symmetry by the overall 90-degree rotation in the opposite directions at different halves of the eye disc (Fanto and Mcneill, 2004; Mlodzik, 1999; D. Strutt *et al.*, 2002).

Although the cellular mechanisms of ommatidial rotation are poorly understood, it is reported that some effectors downstream of Fz/PCP signalling such as Rho-associated

kinase dROK (Fiehler and Wolff, 2007) Myosin II (Zipper), and Spaghetti squash (Sqh) (Winter *et al.*, 2001) have a role in rotation (Figure 1.4). It was also shown that cell adhesion molecules DE-Cadherin and DN-Cadherin have regulatory roles, promoting and restricting rotation, respectively (Mirkovic and Mlodzik, 2006).

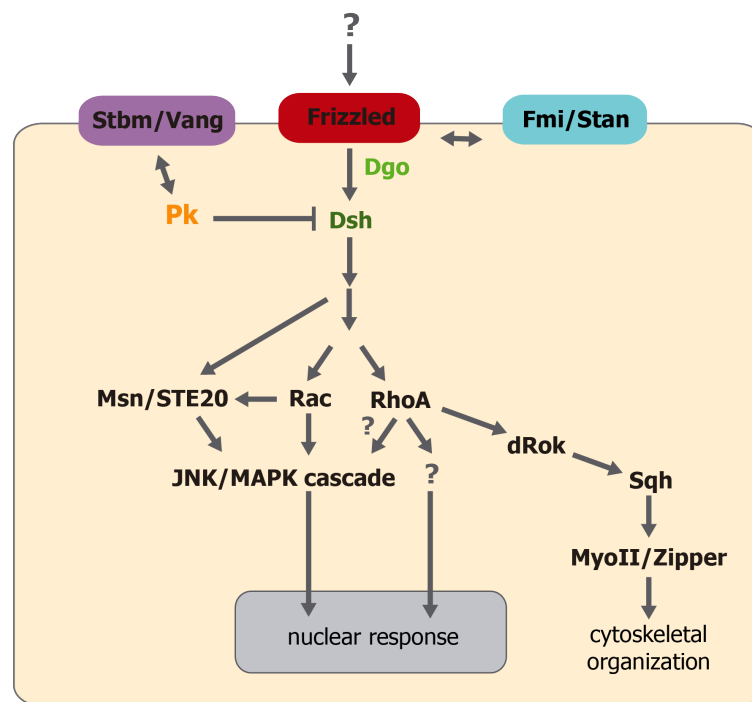


Figure 1.4. Interactions between the genes involved in PCP establishment. Activation of Fz/PCP signalling may results in a nuclear response or cytoskeletal rearrangements through interactions within or between the elements of the core module and the rotation specific module (Adapted from Jenny, 2010; Mlodzik, 2005).

Besides these factors, a small number of rotation-specific genes has been identified by performing mutant analysis; however, it is still not known how they act in the rotation process. As several studies revealed, some of the PR clusters rotate by unusual degrees while direction of rotation, R3/R4 specification, and therefore, chirality are not affected (Gaengel and Mlodzik, 2003). Examples of such genes are *nemo* (*nmo*), *roulette* (*rlt*), and *scabrous* (*sca*) (Choi and Benzer, 1994; Chou and Chien, 2002). Among these, the best-characterized one is *nemo*, which encodes a mitogen-activated protein kinase (reviewed in Singh and Mlodzik, 2012). It is believed that Nemo interacts with the β -catenin/E-Cadherin complex and promotes cell movements by phosphorylation and, therefore, drives ommatidial rotation. Moreover, it is also likely that it interacts with signalling pathways

involved in PCP, such as Fz/PCP, N, and EGFR (Mirkovic *et al.*, 2011; Muñoz-Soriano *et al.*, 2013).

1.3. Genetic Tools for *Drosophila*

Drosophila melanogaster stands out as one of the best model organisms for various biological studies due to the availability of sophisticated tools that allow investigations in a broad range of topics (Ryder and Russell, 2003). In the light of a study by Rubin and Spradling (1982) to generate transgenic lines using P-elements, new genetic tools have started to be developed through combining transposable elements and gene expression systems (reviewed in Ryder and Russell, 2003). Some of the available tools, which were also used in this study, will be further explained.

1.3.1. Gal4/UAS System

Among the systems used to generate genomic tools for functional studies in *Drosophila*, the most common one is the Gal4/UAS binary system that was derived from the yeast *Saccharomyces cerevisiae*. It is based on the ability of the yeast Gal4 transcription factor to bind DNA and activate transcription. Gal4 directly binds to DNA specifically at Upstream Activating Sequences (UAS). UAS are similar to enhancers in eukaryotic genomes and necessary for activation of the transcription of downstream genes upon Gal4 binding (Duffy, 2002).

In 1993, a breakthrough study of Brand and Perrimon revealed that the Gal4/UAS system could be used for spatiotemporal control of targeted gene expression. This control is achieved by cloning a specific promoter and/or enhancer region to the upstream of the Gal4 gene. Thus, Gal4 is expressed in a manner that reflects the cloned regulatory element normally driving the expression of its target gene(s).

On the other hand, a transgenic line having a UAS construct placed upstream of a target gene can also be generated. These two constructs are brought together by crossing a

Gal4-driver line to a UAS-responder line, and the effect can be observed in the offspring (reviewed in Duffy, 2002).

Taking advantage of the Gal4/UAS binary system, several fly line collections bearing Gal4 and UAS constructs have been generated. In this study, we used two Gal4 line collections generated by different groups: Enhancer trap collection by Çelik and Desplan, and FlyLight collection by the team of Rubin.

1.1.1.1. Enhancer Trap Gal4 Line Collection. The study of Brand and Perrimon has also pointed out a novel method called enhancer-trap that provides enhancer site discovery by using the Gal4/UAS system. In this method, a minimal promoter and Gal4 containing P-element vector is introduced into the fly genome. The generated fly line is crossed to a line bearing constitutively active transposase. Thus, the P-element is mobilized by transposase and randomly integrates itself into the genome. If the landing site is close to a regulatory element, such a nearby enhancer can activate Gal4 expression. In order to identify the tissues or cells in which these enhancers are active, the established transgenic lines are crossed to UAS-reporter lines and screened to determine the expression patterns (Brand and Perrimon, 1993).

Since the method has been established, various groups have generated several enhancer trap collections. However, it was revealed that P-element-based enhancer trapping was not efficient to cover the entire genome because of the bias of P-elements to insert themselves into the hot-spot regions or places near local P-elements (Ryder and Russell, 2003). Using different transposable elements with higher tendency for random integration into the genome, alternative tools have been generated. One of these tools was a lepidopteran-derived transposable element *piggyBac* (Horn *et al.*, 2003). In order to discover novel genes that may have a role in PR specification and differentiation in the *Drosophila* eye, Çelik and Desplan generated an enhancer trap Gal4 line collection based on the *piggyBac* transposable element (unpublished data). The expression patterns of the generated Gal4 lines were classified after crossing to UAS-reporter lines according to their expression patterns (Öztürk, 2010).

1.3.1.1. FlyLight Gal4 Line Collection. Although transposable element based Gal4 lines have allowed detecting novel enhancers and labelling subsets of cell groups, they could not

respond to the demand to label specific cell types or small groups of cells. In order to overcome this difficulty, a new Gal4 collection has been generated by the team of Gerry Rubin at Janelia Farm (reviewed in Jones, 2009).

The team has generated a library of fragments, which are on average 3kb in length and overlap by around 1kb, covering almost the whole enhancers of the *Drosophila* nervous system. As a first step, genes related to the nervous system were selected and the fragments were produced out of their intronic (larger than 300bp) and flanking upstream and downstream intergenic regions by PCR. After verifying their sequences, they were cloned into a vector for being placed at the upstream region of a synthetic core promoter, which has a Gal4 sequence at its downstream region. All of these generated constructs having various enhancer sites were inserted into the same location in the fly genome by site-specific integration (Pfeiffer *et al.*, 2008). In order to reveal the expression pattern driven by these fragments, the Gal4 lines were crossed to UAS-GFP reporter lines and nervous system dissections were performed for embryonic, larval, and adult stages. Confocal microscopy imaging showed that this Gal4 collection allows labeling of small groups of cells. A large data set of images were collected and stored in the FlyLight database, which can be accessed online. Therefore, it has become possible for anyone to investigate the expression patterns generated by the particular genomic fragments (Jenett *et al.*, 2012; Jory *et al.*, 2012).

1.3.2. FLP/FRT System

Another useful system is based on FLP/FRT, which allows performing conditional genomic manipulations by recombination. The FLP gene derived from yeast encodes a site-specific recombinase that recognizes FLP recombination target (FRT) sequences and triggers site-specific recombination between FRT sites. This system was applied to fly genetics by generating transgenic lines carrying the FLP gene under the control of tissue- and/or time-specific promoters and FRT sequences flanking the region of interest (Golic and Lindquist, 1989; reviewed in Johnston, 2002).

In 1991, Golic investigated if mitotic recombination can also be mediated by FLP recombinase in *Drosophila*. He showed that FLP induced recombination can take place

between the FRT sites located on different chromosomes (Golic, 1991). Subsequently, combining this system with the Gal4/UAS system and using specific drivers and reporters, diverse genetic tools have been developed. Therefore, mitotic clones and whole tissue mutants can be generated through spatiotemporal regulation (Johnston, 2002).

1.4. RNA Sequencing

In recent years, remarkable innovations have emerged in sequencing technology and carried biological research one step further. The next-generation technologies not only provide high resolution and massive scale sequencing of the whole genome and transcriptome, but also shorten the time and reduce the costs of the experiments (Marguerat *et al.*, 2008).

RNA sequencing (RNA-Seq) is one of these high-throughput technologies, which is replacing the previous technology of microarrays with an advantage of not requiring prior knowledge of sequences to design hybridization probes. It is now possible to perform *de novo* transcript discovery and reveal the whole repertoire of RNA content in a cell at a specific stage and condition. An additional advantage of RNA-Seq is that it allows making comparative analysis of different experiments through a simplified data normalization procedure which is quite difficult to apply for microarray data (reviewed in Ozsolak and Milos, 2011; Wang *et al.*, 2009). Moreover, in this technique, DNA fragments are sequenced directly without the requirement of cloning into a vector as is done for traditional Sanger sequencing (Wilhelm and Landry, 2009).

There is a general workflow for RNA-Seq experiments based on the Illumina platform; however, differences can be seen in the applications of other platforms. In this workflow, the first step is to extract RNA from the cells to prepare cDNA libraries. Then, fragmentation of cDNA is performed and adaptors are ligated to both ends of the cDNA fragments. The sample is then loaded to the lane and placed into the sequencing machine in which the reactions take place as the fragments start to attach randomly to the surface of the Illumina flow cell by the help of the adaptor sequences. Attached fragments make single stranded bridges on the surface. In order to generate clusters of these fragments,

bridge amplification and denaturation follow this step. After that, fluorescent-labeled nucleotides are added to the reaction and laser excitation is applied to detect the signal of each base while they are incorporated to the amplifying strand. Finally, the sequence data is presented and can be used for further analysis (Wilhelm and Landry, 2009).

2. AIM OF THE STUDY

Previously, expression patterns of the *piggyBac* enhancer trap Gal4 lines generated by Çelik and Desplan (unpublished data) were determined through immunostainings on several *Drosophila* tissues from this collection. In this screen, several lines with R3/R4 PR-specific expression in 3rd instar larval eye disc were identified (Öztürk, 2010). The genomic position of the *piggyBac* transposable elements in these lines were localized by inverse PCR and the corresponding genes were identified as *CG33259*, *faint sausage*, *headcase*, *polychaetoid*, *taranis*, *Stubble*, and *cropped* (Öztürk, 2010).

It is known that R3/R4 PRs are crucial for planar cell polarity establishment in the *Drosophila* eye. Thus, it was hypothesized that these specifically expressed genes could have a role in R3/R4 specification and/or ommatidial rotation processes that lead to planar cell polarization. Therefore, we aimed to determine if these genes are involved in the polarization processes in the eye. Additionally, since the expression of enhancer-trap lines do not always fully represent the expression pattern of the genes they have inserted into in a second aim we intended to identify novel genes using an unbiased, high-throughput approach, RNASeq.

3. MATERIALS AND METHODS

3.1. Biological Material

Flies were kept at 25°C in incubators at 80% humidity and a 12:12 day:night cycle unless otherwise stated. Commercially available fly food (Nutri-Fly™ Bloomington Formulation) was used with an addition of 6 ml of propionic acid per liter.

Table 3.1. *Drosophila melanogaster* strains used in this study.

Name of line	Chr. No.	Description
Gal4 Drivers		
<i>ey</i> -Gal4	2	Expresses Gal4 under the control of <i>ey</i> enhancer
<i>IGMR</i> -Gal4	2	Expresses Gal4 under the control of <i>IGMR</i> enhancer
AC711-Gal4	3	Enhancer trap line with Gal4 insertion in the first intron of <i>polychaetoid</i>
AC724-Gal4	3	Enhancer trap line with Gal4 insertion at the ~2.3 kb upstream of <i>headcase</i>
AC748-Gal4	3	Enhancer trap line with Gal4 insertion at the ~40 kb upstream of <i>CG33259</i>
AC1048-Gal4	3	Enhancer trap line with Gal4 insertion in the first intron of <i>taranis</i>
<i>Appl</i> -Gal4	3	FlyLight line expresses Gal4 under the control of <i>Appl</i> enhancer (R65B07)
<i>argos</i> -Gal4	3	FlyLight line expresses Gal4 under the control of <i>argos</i> enhancer (R24C05)
<i>CadN</i> -Gal4	3	FlyLight line expresses Gal4 under the control of <i>CadN</i> enhancer (R31E03)
<i>CG14510</i> -Gal4	3	FlyLight line expresses Gal4 under the control of <i>CG14510</i> enhancer (R55F01)
<i>CG30143</i> -Gal4	3	FlyLight line expresses Gal4 under the control of <i>CG30143</i> enhancer (R91H10)

Table 3.1. *Drosophila melanogaster* strains used in this study (cont.).

<i>phyl</i> -Gal4	3	FlyLight line expresses Gal4 under the control of <i>phyl</i> enhancer (R51E01)
<i>psc</i> -Gal4	3	FlyLight line expresses Gal4 under the control of <i>psc</i> enhancer (R29F04)
<i>ro</i> -Gal4	3	FlyLight line expresses Gal4 under the control of <i>ro</i> enhancer (R94D11)
<i>Sema-5c</i> -Gal4	3	FlyLight line expresses Gal4 under the control of <i>Sema-5c</i> enhancer (R71F07)
<i>sba</i> -Gal4	3	FlyLight line expresses Gal4 under the control of <i>sba</i> enhancer (R82H04)
<i>sNPF</i> -Gal4	3	FlyLight line expresses Gal4 under the control of <i>sNPF</i> enhancer (R20D06)
<i>stan</i> -Gal4	3	FlyLight line expresses Gal4 under the control of <i>stan</i> (<i>fmi</i>) enhancer (R30F01)
UAS Constructs		
UAS-Dicer2	1	Expresses Dicer2 under the control of UAS
UAS-GFP.nls	2	UAS fusion to cDNA of GFP with a nuclear localization signal
UAS-GFP.nls	3	UAS fusion to cDNA of GFP with a nuclear localization signal
UAS- <i>fas</i> -RNAi	2	Expresses double stranded RNAi of <i>faint sausage</i> under the control of UAS
UAS- <i>sal</i> -RNAi	2	Expresses double stranded RNAi of <i>spalt</i> gene complex under the control of UAS
UAS- <i>svp</i> -RNAi	2	Expresses double stranded RNAi of <i>svp</i> under the control of UAS
UAS- <i>Sb</i> -RNAi	2	Expresses double stranded RNAi of <i>Stubble</i> under the control of UAS
UAS- <i>tara</i> -RNAi	2	Expresses double stranded RNAi of <i>taranis</i> under the control of UAS
UAS- <i>CG33259</i> -RNAi	3	Expresses double stranded RNAi of <i>CG33259</i> under the control of UAS
UAS- <i>fmi</i> -RNAi	3	Expresses double stranded RNAi of <i>flamingo</i> under the control of UAS
UAS- <i>pyd</i> -RNAi	3	Expresses double stranded RNAi of <i>polychaetoid</i> under the control of UAS
General Stocks		
<i>y w</i>	1	Yellow body color and white eye phenotype
<i>w</i> ¹¹¹⁸	1	White eye phenotype
<i>svp</i> ::GFP::FLAG	2	Transgenic <i>svp</i> construct with GFP and FLAG tags
<i>fas</i> ¹	2	Null mutant allele of <i>faint sausage</i>

Table 3.1. *Drosophila melanogaster* strains used in this study (cont.).

<i>fas</i> ⁰⁵⁴⁸⁸	2	Hypomorphic allele of <i>faint sausage</i> with LacZ insertion in the upstream
FRT42D	2	FLP recombination target site on 42D map position
FRT42D, <i>GMR-hid</i>	2	Expresses eye-specific cell-death gene, <i>hid</i> , recombined to an FRT site on 42D map position
FRT82B, <i>svp</i> ^{E22}	3	<i>svp</i> null mutant allele recombined to an FRT site on 82B map position
FRT82B, <i>GMR-myrGFP</i>	3	Expresses eye-specific membrane-targeting GFP recombined to an FRT site on 82B map position
Chp-GFP	3	1 st intron of Chp fused to cDNA of GFP with a nuclear localization signal
Rh1-GFP	3	Rhodopsin 1 promoter fused to GFP
Balancers and Markers		
CyO	2	Balancer chromosome with curly wings
sp	2	Supernumerary bristles marker
TM2	3	Balancer chromosome with large halteres and/or with bristles on halteres
TM6B	3	Balancer chromosome with humeral and tubby markers

3.2. Chemicals and Supplies

Chemicals used in this study were obtained from Fisher Scientific, Sigma Aldrich, Molecular Probes or Roche unless stated otherwise.

3.2.1. Chemical Supplies

The chemicals used in this study are listed in Table 3.2.

Table 3.2. List of chemicals used in this study.

Chemical	Manufacturer
Bovine Serum Albumin	Sigma-Aldrich, USA (A9647)
Normal Goat Serum (NGS)	Millipore (S26-100ML)
NuSieve® GTG® Agarose	Lonza, USA
Paraformaldehyde	Sigma-Aldrich, USA (P6148)

Table 3.2. List of chemicals used in this study (cont.).

RNA Series II 6000 Pico Kit	Agilent Technologies, USA
RNAqueous Micro Kit	Ambion, USA (AM1931)
Sf-900 Medium	Invitrogen, USA (10967-032)
SMARTer Ultra Low RNA Kit for Illumina Sequencing	Clontech, Japan (634935)
Sodium Deoxycholate	Sigma-Aldrich, USA (30970)
Triton X-100	AppliChem, USA (A4975)
Tween 20	Roche, USA (11332465001)
Trypsin-EDTA 0.05%	Sigma-Aldrich, USA (59417C)

3.2.2. Buffers and Solutions

Buffers and solutions in this study are listed in Table 3.3 with their contents.

Table 3.3. Buffers and solutions used in this study.

Buffer/Solution	Content
Formaldehyde Solution (16%)	8 g paraformaldehyde in 50 ml dH ₂ O 1M NaOH until solution becomes transparent pH 7.4
PaxDG	10 g BSA 3 g Sodium Deoxycholate 3 ml Triton X-100 50 ml Normal Goat Serum 100 ml 10X PBS dH ₂ O to 1 L
PBS (1X)	137 mM NaCl 2.7 mM KCl 10 mM Na ₂ HPO ₄ 1.8 mM KH ₂ PO ₄
PBX3	0.3% Triton X-100 in 1X PBS

3.2.3. Antibodies

Primary and secondary antibodies used in the immunohistochemistry experiments are listed with their dilution ratios in Table 3.4. All primary antibodies were kept at 4°C

and the secondary antibodies were kept at -20°C.

Table 3.4. Antibodies used in this study.

Name	Antigen	Species	Dilution	Source
Primary Antibodies				
Anti-β-gal	β-galactosidase	Rabbit	1:5000	Cappel
Anti-Brp	Bruchpilot	Mouse	1:100	DSHB (nc82)
Anti-Chp	Chaoptin	Mouse	1: 50	DSHB (24B10)
Anti-Cpo	Couch potato	Rabbit	1:2500	Bellen, H., BCM, USA
Anti-Elav	Elav	Mouse	1:20	DSHB (9F8A9)
Anti-Elav	Elav	Rat	1:20	DSHB (7E8A10)
Anti-Fmi	Flamingo/Starry night	Mouse	1:10	DSHB (#74)
Anti-Futsch	Futsch	Mouse	1:50	DSHB (22C10)
Anti-GFP	GFP	Chicken	1:1000	Abcam (ab13970)
Anti-GFP	GFP	Rabbit	1:500	Torrey Biolabs (TP401)
Anti-Hdc	Headcase	Mouse	1:3	DSHB (U33)
Anti-Hnt	Hindsight/Pebbled	Mouse	1:10	DSHB (1G9)
Anti-Pros	Prospero	Mouse	1:20	DSHB (MR1A)
Anti-Ro	Rough	Mouse	1:20	DSHB (62C2A8)
Anti-Salm	Spalt major	Rabbit	1:10000	Schnorrer, F., IMP, Germany
Anti-Svp	Seven-up	Mouse	1:10	Hiromi, Y., NIG, Japan
Anti-Svp	Seven-up	Rabbit	1:200	Cripps, R.M., UNM, USA
Secondary Antibodies				
Alexa 488	Chicken	Goat	1:200	Invitrogen
Alexa 488	Rabbit	Goat	1:800	Invitrogen
Alexa 488	Rabbit	Donkey	1:800	Invitrogen
Alexa 555	Mouse	Donkey	1:800	Invitrogen
Alexa 555	Rabbit	Goat	1:800	Invitrogen
Alexa 633	Rat	Goat	1:800	Invitrogen
Alexa 647	Rat	Donkey	1:800	Invitrogen
Alexa 647	Rabbit	Goat	1:800	Invitrogen
Cy3	Mouse	Goat	1:800	Invitrogen

3.2.4. Embedding Media

Vectashield Embedding Medium (Vector Laboratories, Inc) was used to embed tissues, which were processed by fluorescent immunohistochemistry.

3.2.5. Disposable Labware

Disposable labware used during this study are given in Table 3.5.

Table 3.5. Disposable labware used in this study.

Material	Manufacturer
Filter Tips	Greiner Bio-One, Belgium
Microscope cover glass	Fisher Scientific, UK
Microscope slides	Fisher Scientific, UK
Petri Dishes, 60 x 15 mm	TPP Techno Plastic Products AG, Switzerland
Pipette Tips	VWR, USA
Test Tubes, 0.5 ml	Citotest Labware Manufacturing, China
Test Tubes, 1.5 ml	Citotest Labware Manufacturing, China
Test Tubes, 2 ml	Citotest Labware Manufacturing, China
Test Tubes, 15 ml	Becto, Dickinson and Company, USA
Test Tubes, 50 ml	Becto, Dickinson and Company, USA

3.2.6. Equipment

Equipment used in this study is listed in Table 3.6.

Table 3.6. Equipment used in this study.

Equipment	Manufacturer
Autoclave	Astell Scientific Ltd., UK
Bioanalyzer 2100	Agilent Technologies, USA
Centrifuges	Eppendorf, Germany (Centrifuge 5424, 5417R)
Confocal Microscope	Leica Microsystems, USA (TCS SP5)
Fluorescence Stereomicroscope	Leica Microsystems, USA (MZ16FA)

Table 3.6. Equipment used in this study (cont.).

BD FACSAria™ III cell sorter	BD Biosciences, USA
Freezers	Arçelik, Turkey
Incubator	Weiss Gallenkamp, USA (Incubator Plus Series)
Inverted Microscope	Zeiss, USA (Axio Observer, Z1)
Laboratory Bottles	Isolab, Germany
Micropipettes	Eppendorf, Germany
Microwave oven	Vestel, Turkey
pH meter	WTW, Germany (Ph330i)
Refrigerators	Arçelik, Turkey
Stereo Microscope	Olympus, USA (SZ61)
Vortex Mixer	Scientific Industries, USA (Vortex Genie2)

3.3. Selection of the Candidate Lines

An enhancer trap screen with *piggyBac* insertions was previously performed to find novel genes that may be involved in PR differentiation in the *Drosophila melanogaster* eye (Çelik and Desplan, unpublished data). Expression patterns of a subset of these lines were shown by Arzu Öztürk (2010). Since specification of R3/R4 PR pair is crucial for the establishment of planar cell polarity, lines having R3/R4 specific expressions were selected by considering the location of PR cells in ommatidia.

3.3.1. Verification of the Expression Patterns of the Candidate Genes

Previously, expression patterns of the enhancer trap Gal4 lines, namely AC lines were shown by staining with antibodies detecting neuronal cells and GFP, which is reflecting the expression pattern of the enhancer-trap line and likely the gene into which

the P-element has inserted (Öztürk, 2010). In order to confirm that the candidate lines are expressed in R3/R4 cells, stainings were repeated with the addition of antibodies that are specific to R3/R4 PRs. The antibody stainings were done on 3rd instar larval eye discs with the genotype shown in Figure 3.1. Additionally, LacZ lines and antibodies for the candidates were obtained and used to verify previously shown expression patterns.

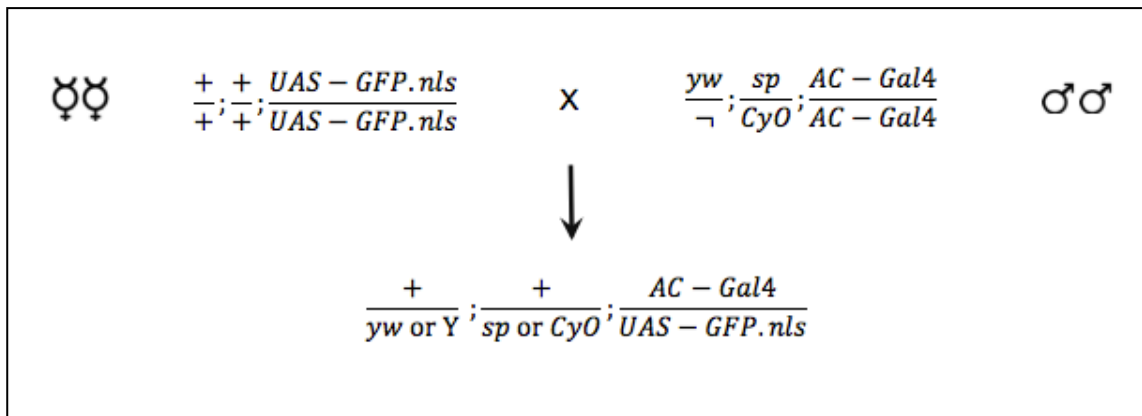


Figure 3.1. Set up of cross to verify expression patterns of the enhancer trap Gal4 lines. AC-Gal4 represents enhancer trap Gal4 lines, which are crossed to UAS-GFP.nls construct bearing reporter line to detect expression patterns.

3.4. Experiments for Loss of Function Analyses

3.4.1. Downregulation of the Candidate Genes by RNA Interference

In order to knockdown the candidate genes, UAS-RNAi lines (Dietzl *et al.*, 2007) were ordered from the Vienna Drosophila RNAi/Resource Center (VDRC). Tissue specific downregulation was done by using eye specific drivers *ey*-Gal4, which is active starting from embryonic stages and *IGMR*-Gal4, which is active starting from larval stages and maintained throughout adulthood. Additionally, UAS-Dicer2 was used to enhance RNAi activity (Dietzl *et al.*, 2007). Crosses were set up as shown in Figure 3.2.

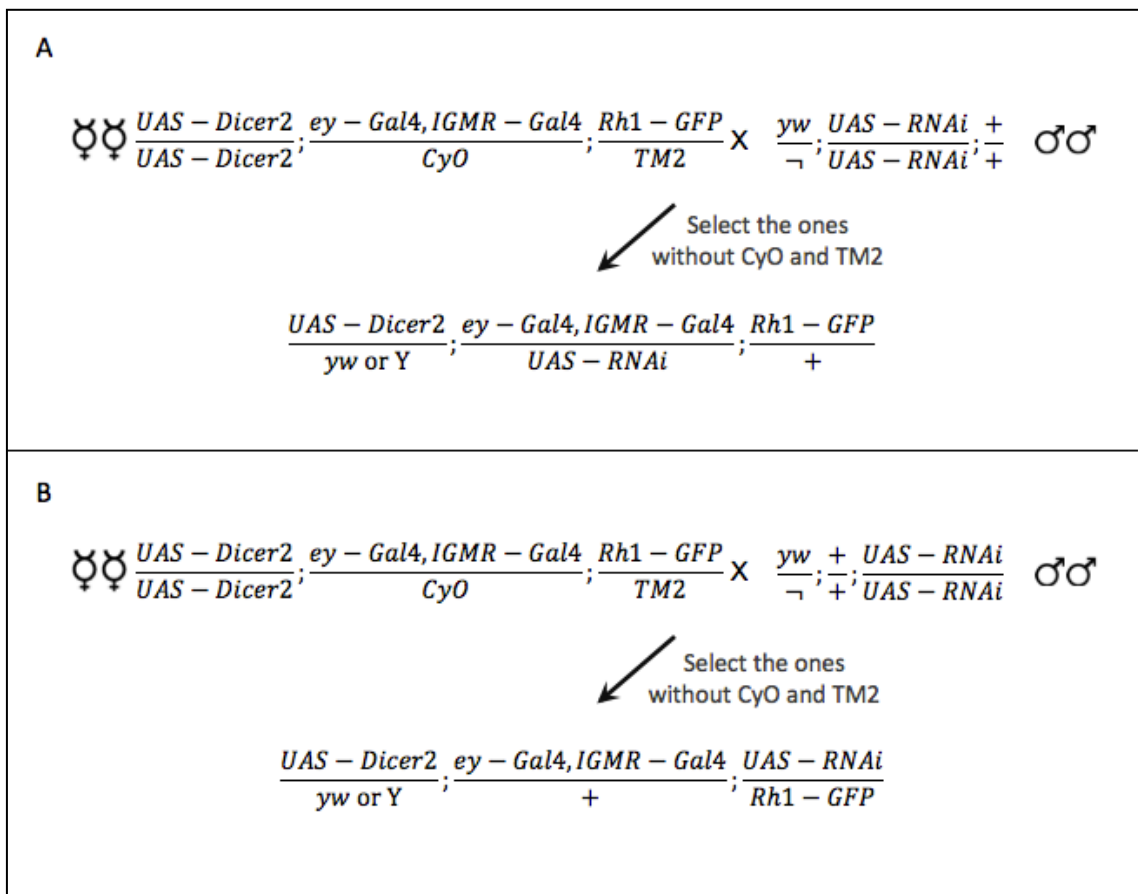


Figure 3.2. Crosses for knockdown analysis of candidate genes. Lines having relevant UAS-RNAi construct either on the second chromosome (A) or on the third chromosome (B) were crossed with the driver line.

3.4.1.1. Visualization of the PRs by Cornea Neutralization Technique. In order to detect the phenotypes in the fly eye, the cornea neutralization technique was applied by water immersion (Pichaud and Desplan, 2001). Petri dish covers were used as they properly fit into the stage of the confocal microscope. 2% low melt agarose was poured into the cover of a petri dish. Once the agarose started to cool, flies were fixed by embedding their body into the agarose while keeping one of their eyes on the surface looking upwards. After the agarose gel solidified, flies were covered with water in order to neutralize the cornea and the ommatidia were visualized under the confocal microscope with a 40x water immersion objective.

This method requires being fast and precise in terms of fixing flies into the agarose gel with a correct angle. Additionally, it only provides a limited area across the petri dish

for visualization. Considering these, few modifications have been done to apply the technique more efficiently. For this purpose, instead of petri dish covers, reusable microscope slides were prepared by defining margins on them with a PAP pen, so that, the water was kept on the sample. For one fly, one drop of 2% low melt agarose was poured onto the slide and subsequent steps were kept the same.

The reporter line Rh1-GFP was used to visualize the outer PRs at 488 nm wavelength under the confocal microscope and allowed us to evaluate ommatidial rotation and chirality phenotypes. Image processing was performed using ImageJ and Adobe Photoshop CS6 programs.

3.4.2. Clonal Analysis

Since homozygous mutants of *fas* are lethal, whole eye homozygous mutants were generated in heterozygous flies by using FLP/FRT technique. Additionally, mosaic clones of *seven-up* mutants were generated for epistasis analysis.

3.4.2.1. Generation of *fas* Mutant Lines Recombined to an FRT Site. As a first step, mutant alleles were recombined to an FRT site. For this purpose, flies carrying one *fas*^l or *fas*⁰⁵⁴⁸⁸ mutant allele balanced with CyO were crossed with FRT42D bearing flies. From the F1 generation, virgin females were collected by selecting against the CyO marker and crossed with the balancer line carrying sp and CyO on the 2nd chromosome, and TM2 and TM6B on the 3rd chromosome. Then, from the offspring, the putative recombinant males carrying CyO were selected, while the ones with the sp marker were eliminated. Every single male fly was re-crossed with virgin females of the balancer line to generate a stock of recombinants. Since there were no markers indicating the presence of the FRT site or the mutant alleles, two approaches were followed to control the genotype of the putative recombinant lines.

One of them was tracking the presence of non-CyO lines in the offspring. The absence of CyO balancer means that the line only carries an FRT site, not the mutant allele recombined to it. In case of a successful recombination event, only balanced flies would

arise in the new generation because of the lethality of homozygous mutants. Thus, CyO balanced flies were collected and further analysed for presence of the FRT site.

In order to determine if the selected CyO balanced flies also carry an FRT site, they were crossed with virgin females carrying *ey-FLP* and FRT42D, *GMR-hid*. In the presence of the *GMR-hid* allele, the apoptotic gene *head involution defective (hid)* is expressed specifically in PR cells resulting in the death of PRs, which in turn causes loss of the eye (Grether *et al.*, 1995). *ey-FLP* is used to induce mitotic recombination between the homologous alleles carrying the same FRT sites. In the presence of an FRT site, the eyes would be rescued in the offspring.

3.4.2.2. Generation of Whole Eye Mutants. After generating the lines with a mutant allele recombined to an FRT site, these were crossed with flies carrying Rh1-GFP in order to examine PCP phenotypes after the mutants were generated. Therefore, flies carrying FRT42D, *fas** on the 2nd chromosome and Rh1-GFP on the 3rd chromosome were selected and this step was followed by crossing with *ey-FLP* and FRT42D, *GMR-hid* carrying flies. In the progeny, eyes were expected to be homozygous mutant for *fas*.

3.4.2.3. Generation of Mitotic Clones for Epistasis Analysis. In order to investigate if *fas* and *svp* genes are epistatic, mosaic null mutant clones of *svp* were generated in the 3rd instar larval eye disc. To be able to detect *fas* expression via antibody staining in mutant and wild type areas of the mosaic eye, LacZ inserted hypomorphic allele *fas*⁰⁵⁴⁸⁸ was used (Lekven *et al.*, 1998). For this purpose flies carrying the *fas*⁰⁵⁴⁸⁸ allele on the 2nd chromosome and FRT82B, *svp*^{E22} on 3rd chromosome were generated. Then, males from this line were crossed with the virgin females of *ey-FLP*;FRT82B,*GMR-myrGFP* line to induce mitotic recombination between FRT82B sites by *ey-FLP*. Figure 3.3 shows all steps of the crosses to generate mitotic clones.

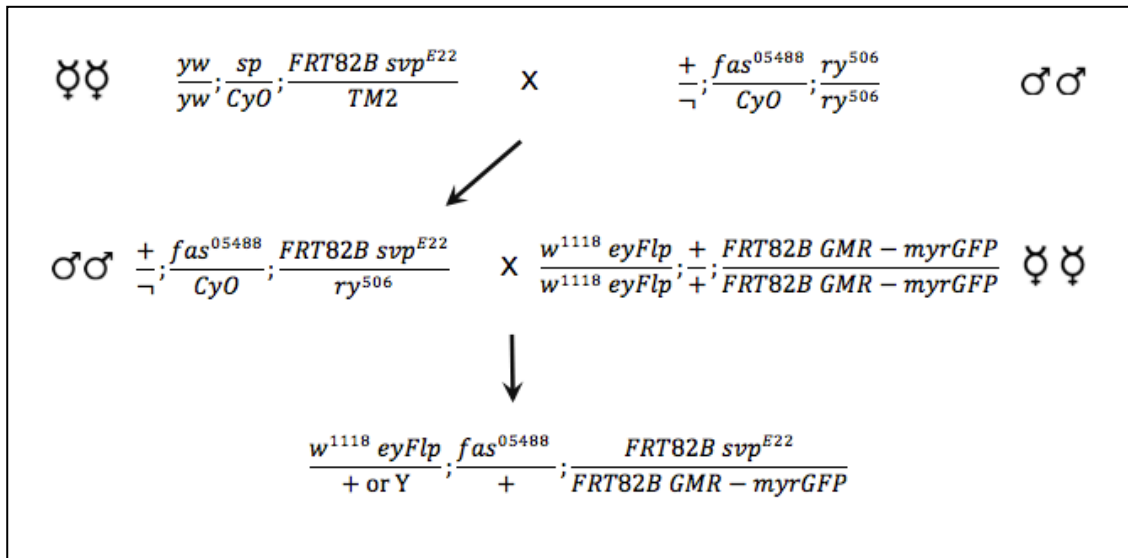


Figure 3.3. Crosses for generating mitotic clones of *svp* for the epistasis analysis.

3.5. Histological Methods

3.5.1. Immunohistochemistry

3.5.1.1. Preparation of Larval Eye Imaginal Discs. Wandering 3rd instar larvae were collected in PBS. Eye discs were dissected as attached to the mouth hook and brain, and collected in PBS in a 1.5 ml test tube.

3.5.1.2. Antibody Staining of Larval Eye Imaginal Discs. All the steps were performed at room temperature and on a shaker at 200 rpm unless stated otherwise. Fixation of the dissected tissues was done by replacing PBS with formaldehyde solution (4% in PBS) and incubating tissues in it for 20 minutes. Then, tissues were washed for three times with PBX3 for 10 min. For blocking, tissues were incubated in PaxDG solution for 2 hours. After blocking, a primary antibody staining solution was prepared in PaxDG and the tissues were incubated overnight at 4°C. After that, the primary antibody mix was removed and kept at 4°C for further use (up to three times). Tissues were washed with PBX3 for 3 times and incubated with secondary antibodies prepared in PaxDG for 2 hours in the dark. After 3 washes with PBX3 for 10 min, eye discs were separated from brains and mouth hooks. Finally, eye discs were mounted on a slide with Vectashield.

3.5.2. Visualization and Image Processing

Mounted eye discs were visualized under a fluorescent microscope to check if the staining worked before confocal microscopy was performed to identify expression patterns of the candidate genes. Image processing was done with ImageJ, Fiji and Adobe Photoshop CS6.

3.6. Selection of R3/R4 Specific Lines for RNA Sequencing

This part of the project mostly focuses on the specification of R3 and R4 PRs since their proper specification is necessary to obtain the regular arrangement of ommatidia through the *Drosophila* eye by adopting correct ommatidial chirality and rotation (Domingos *et al.*, 2004). To enlighten this process, we aimed to identify differentially expressed (DE) genes in R3/R4 PR pair through cell sorting, RNA sequencing, and bioinformatic analysis. The overall methodology is shown in Figure 3.4.

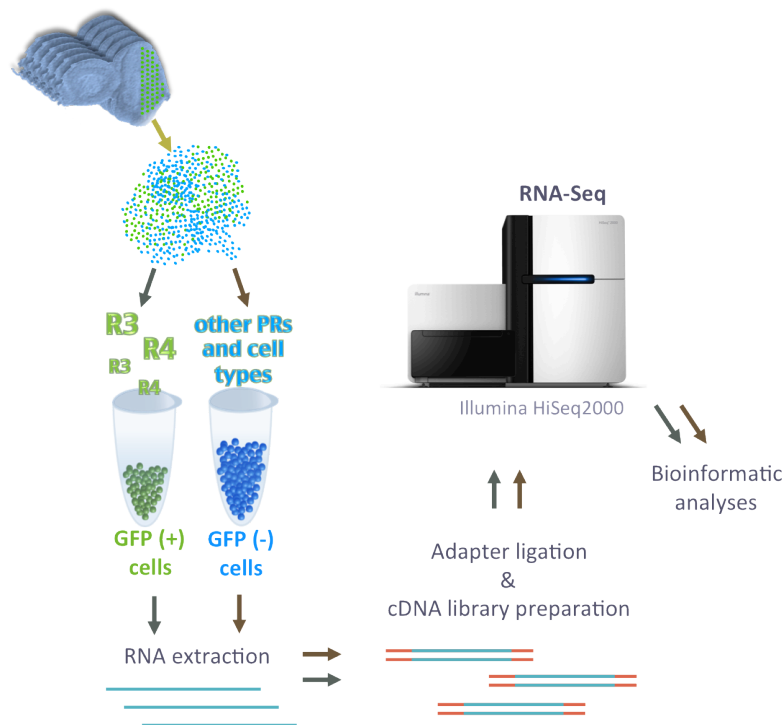


Figure 3.4. General workflow for the RNA-Seq experiment.

To obtain a population of R3/R4 cells for RNA sequencing, first step was to investigate lines that specifically label R3 and R4 cells. Since the enhancer Gal4 lines were not in our hands anymore, the FlyLight Gal4 Line database, which is known for labelling subset of cells better than enhancer trap lines, was examined. As previously mentioned, these lines carry on average 3 kb length of genomic DNA fragments that drive Gal4 expression, which can be observed using a UAS-reporter construct (Pfeiffer *et al.*, 2008). From the FlyLight database (<http://flweb.janelia.org/cgi-bin/flew.cgi>), 346 lines having expression patterns posterior to the morphogenetic furrow were investigated. The ones showing a R3/R4 PR-specific expression while not having an expression in the antennal disc were selected. In order to confirm their expression patterns, antibody stainings were performed with specific PR markers as described in Section 3.5.1. Figure 3.5 shows the crossing scheme that was set up for the antibody stainings.

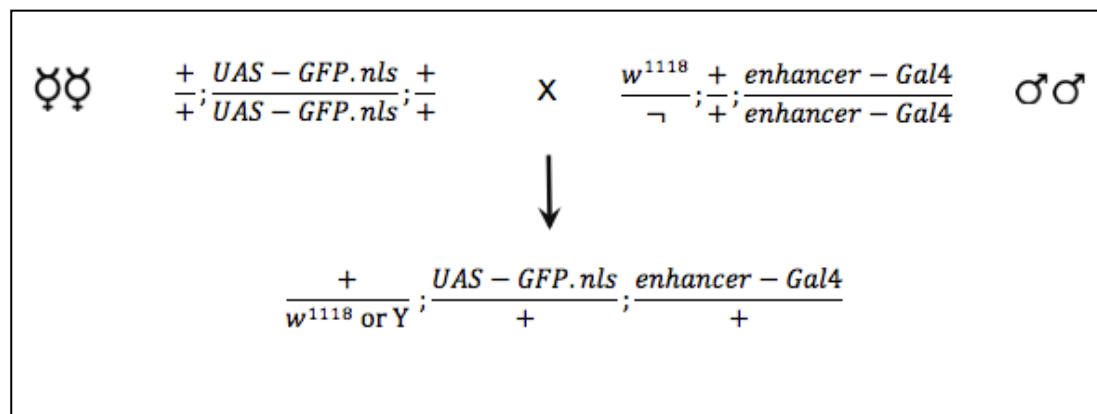


Figure 3.5. Crossing scheme to screen FlyLight lines.

3.7. Sorting of Cells from the Eye-Antennal Discs

Lines expressing nuclear GFP under the control of Gal4 binding sites were crossed to the selected Gal4 expressing lines. Thus, in the progeny, GFP expression reflected the activity of the enhancer, which drives Gal4 expression (see Figure 3.5 for the crossing scheme).

3.7.1. Preparation of Larval Eye-Antennal Discs for Cell Sorting

Wandering 3rd instar larvae were collected in PBS. Eye-antennal imaginal discs were dissected in 1X PBS as clean and as fast as possible. Any other tissue was removed and 50-120 eye-antennal discs were put into a 1.5 ml test tube covered with aluminum foil containing 200 µl of Sf-900 II SFM medium.

3.7.2. Dissociation of the Cells

In order to gather R3/R4 cells, cells in the dissected imaginal discs were dissociated. For this purpose, eye-antennal discs in Sf-900 II SFM medium were centrifuged for 5 minutes at 800 rpm. Then, the medium was removed and 200 µl of trypsin solution was added. Tissues were incubated for 1 hour on a shaking incubator at 37°C. After centrifugation for 5 minutes at 800 rpm the trypsin solution was removed. After addition of 200 µl of Sf-900 II SFM medium tubes were rotated for 3 minutes and then centrifuged for 5 minutes at 800 rpm. Then, the supernatant was removed and cells were resuspended gently in Sf-900 II SFM medium. Samples were kept on ice and in the dark.

3.7.3. Sorting of the Cells by the Fluorescent Activity

GFP-labelled cells were sorted from the dissociated cell mixture using BD FACSAria™ III cell sorter with 85 µm nozzle size and under 44 psi pressure. The sorted cells were collected in test tubes and kept on ice.

3.8. Molecular Biological Techniques

3.8.1. Isolation of RNA

After cell sorting was performed, sorted samples were centrifuged for 5 minutes at 800 rpm and the medium was replaced with lysis solution to perform RNA extraction. RNA was isolated with RNAqueous®-Micro Kit by applying the manufacturer's

instructions. RNA quality was checked by using Agilent Bioanalyzer with the Agilent Series II RNA 6000 Pico kit.

3.8.2. Preparation of cDNA Libraries

In order to prepare cDNA libraries from the isolated RNA, SMARTer™ Ultra Low RNA Kit for Illumina Sequencing was used according to the manufacturer's instructions.

3.9. RNA Sequencing and Data Analysis

Single-end RNA sequencing was performed through Illumina HiSeq 2000 system. Sequencing was performed on cDNA libraries generated from GFP-positive samples.

The bioinformatic analysis to acquire DE genes in R3 and R4 PR cells and gene regulatory network analyses were done by Delphine Potier from the Laboratory of Computational Biology at KU Leuven. Then we have performed subsequent gene ontology (GO), motif discovery analyses and validation experiments.

3.9.1. Pre-processing the Data

Raw data generated from RNA sequencing were obtained in FASTQ format. The data were processed by clipping the adapter sequences using the FASTQ Clipper tool. Then, quality control of the clipped reads was done by using FastQC. Reads were mapped to the reference *Drosophila melanogaster* genome (FlyBase dm3 r5.45) by using TopHat2 (Trapnell *et al.*, 2009). Samtools (Li *et al.*, 2009) was used to pass bam files into bai to visualize them in the genome viewer program IGV (J. T. Robinson *et al.*, 2011).

3.9.2. Measuring Gene Expression

Counts per genes were obtained by using HTSeq-count. The annotation file dm3 r5.45 from FlyBase was used, as it is the same with the genome file used for mapping.

Normalization and differential expression analysis were done in R environment by using the edgeR (M. D. Robinson *et al.*, 2010) and DESeq (Anders and Huber, 2010) packages of Bioconductor. The data were filtered to eliminate the genes with low counts (less than 1 read per million, RPM, in 1 sample).

3.9.3. GO Analysis

In order to detect enriched GO terms in the ranked list of differentially expressed genes, web-based gene ontology enrichment analysis tool GOrilla (Eden *et al.*, 2009) was used. The ranked DE gene list (from up-regulated to down-regulated) was given as input and all *Drosophila* genes were used as background. The output was taken as directed acyclic graphs and tables showing enriched GO terms related to biological process and molecular function.

For the other gene ontology analyses, web-based application GeneCodis was used as it provides pie charts of the classified genes according to the associated GO terms representing their biological process, molecular function and cellular compartment (Carmona-Saez *et al.*, 2007; Nogales-Cadenas *et al.*, 2009; Tabas-Madrid *et al.*, 2012).

3.9.4. Motif Discovery and Transcription Factor Prediction

In order to find enriched TF binding motifs we used i-cisTarget tool (Herrmann *et al.*, 2012). As an input we used differentially expressed genes in R3/R4 as three different sets: up-regulated ones, down-regulated ones and all DE genes. As i-cisTarget predicts TFs associated with the motifs, we aimed to find transcription factors that can regulate R3/R4 specification. Normalized E-score threshold was set to 2.5.

Moreover, we included different sets of RNA-Seq data to have more accurate results about the expression profiles of the genes related with 3rd instar larval eye disc. Our aim was to examine if the co-expressed genes were also regulated by the same transcription factors.

The different sets of data were coming from 72 RNA-Seq experiments. The experiments include RNA sequencing of wild type tissues, sorted cells, and perturbations for several genes encoding transcription factors (Table 3.7).

Table 3.7. Summary of 72 RNA-Seq experiments of wild type and perturbed tissues of 3rd instar larvae. Developing eye-antennal discs were used unless stated otherwise.

Wild types (20)		Perturbations (52)	
Dissected tissues	Sorted cells	Mutants	LOF/GOF
Eye-antennal discs Wing discs Brains	PRs and other cells	aop dfd E(spl)	ato lab CG12071 Lim3
	R8 PRs and other cells	gl	dac lz
	<i>chp</i> expressing cells and others	Kr	dan mam
	<i>eya</i> expressing cells and others	lz	Danr nerfin-1
		m	Dfd oc
Eye-antennal disc	peb	Dip3 Optix	
	ro	eya peb	
	sv	gl repo	
		gsb-n retn	

Initial steps consisting of raw data processing, mapping, getting counts per genes, and acquisition of differentially expressed genes were done by using the FastX/TopHat2/HTSeq/DESeq pipeline.

So far, 753 transcription factors have been identified in *Drosophila* and catalogued in FlyTF database (Adryan and Teichmann, 2006). The expression levels of the genes encoding these 753 TFs were examined through the 72 RNA-Seq experiments and the ones with 1rpm in 5/72 samples were kept (692 TFs). To obtain the clusters of genes which are co-expressed or anti-expressed with these 692 TFs, the GENIE3 tool (Huynh-Thu *et al.*, 2010) and PTM (correlation/anti-correlation) (Pavlidis and Noble, 2001) were used.

Therefore, for a requested TF, co-expressed and anti-expressed genes were extracted and searched for enriched transcription factor binding motifs among their 5 kb upstream and intronic regions. This was carried out by using the Cytoscape plug-in iRegulon, which uses Motif2TF algorithm to associate similar sequences to an enriched

motif and to calculate orthology of the related TFs. Thus, the enriched motifs and associated TFs (according to databases consist of evidence about motif-TF interactions) are listed. Conservation levels of motifs and TF are directly proportional to their rankings (Janky *et al.*, n.d.). Through this analysis, subsets of genes were identified as being enriched for particular TF binding motifs in their 5 kb upstream or intronic regions. Resulting TF targetomes were clustered as their relation with biological processes by using Clust & See plug-in of Cytoscape (Spinelli *et al.*, 2013). Then, a targetome was selected and the target genes were examined through the list of the DE genes in R3/R4 PRs and ranked according to their expression levels. The ones that are not observed as differentially expressed in R3/R4 PRs were eliminated and several candidate genes were selected for *in vivo* validation experiments.

3.9.5. Validation Experiments for the Candidate Genes

In order to validate the predicted TF-candidate gene network, we generated null mutant mosaic clones for the gene encoding the predicted TF. Clones were generated in the 3rd instar larval eye disc by inducing mitotic recombination with *ey*-FLP. Immunostainings were performed with antibodies against the candidate genes as described in section 3.5.

4. RESULTS

4.1. Confirmation of the Expression Patterns of Putative R3/R4-Specific Genes

The enhancer-trap lines were identified in a previous study and were predicted to be expressed in R3/R4 cells by visual inspection (see Appendix A, Öztürk, 2010). In order to confirm the R3/R4-specific expression patterns of these lines in 3rd instar larval eye discs, we performed immunostainings using antibodies that allow us to identify R3 and R4 PRs unequivocally. There are two R3/R4 specific markers that can be used: Svp and Salm. Thus, we used both of them interchangeably to identify R3 and R4 cells, although in addition to R3/R4 Svp is also expressed in R1 and R6 PRs and Salm is also expressed in inner PRs and cone cells after row seven. The expression of the Gal4 lines were monitored by crossing them to *UAS-nuclearGFP* lines, where GFP localizes to the nucleus, so that colocalization with the nuclear Svp and Salm antibodies can be assessed.

The expression pattern of the *CG33259*-Gal4 enhancer trap line, as visualized by the GFP reporter signal, was observed to colocalize with Seven-up at the position of R3/R4 PRs (Figure 4.1). By comparison with the expression pattern of Elav, which allows the visualization of differentiating PRs starting right after the morphogenetic furrow, we inferred that *CG33259*-Gal4 expression starts in early-born R3/R4 PRs. Although, in general, expression was detected both in R3 and R4 PR cells, in some ommatidia it was only observed in R3 or R4. Overall, *CG33259* was considered as a prominent candidate because of its R3/R4 specific expression pattern.

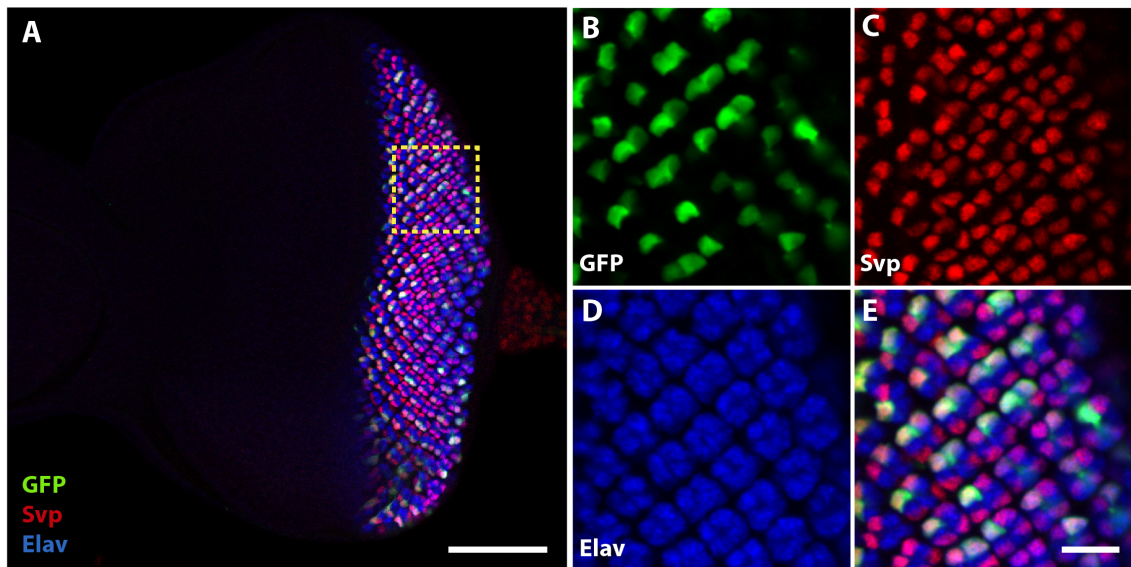


Figure 4.1. *CG33259*-Gal4 enhancer trap line displays a R3/R4-specific expression pattern in the 3rd instar larval eye-antennal disc. Immunostaining was performed with antibodies against GFP (B), Seven-up (C), and Elav (D). Magnified view of the region inside the yellow square (B-E). GFP expression driven by *CG33259*-Gal4 (B), R3/R4, R1/R6 marker Svp (C), and neuronal marker Elav (D) colocalize in R3/R4 PR cells (E).

Unfortunately, it was not possible to perform similar immunostainings for the other enhancer-trap Gal4 lines since these lines were lost in an incubator breakdown. However, we obtained tools from public stock centers for some of them to help reveal the expression patterns of our genes of interest.

We used an antibody against *headcase* (*hdc*) and analyzed its colocalization with Salm. *salm* is expressed in R3/R4 PRs from row 3 to 7 and then starts to be expressed by inner PRs, while it gradually fades away in R3/R4 (Domingos *et al.*, 2004). As can be seen in Figure 4.2, Hdc displays a cytoplasmic localization, and therefore, does not colocalize with the transcription factor Salm. Additionally, it is neither expressed specifically nor appears to be enriched in R3/R4 PR cells. Therefore, we eliminated this gene from the candidate list of possible PCP regulators.

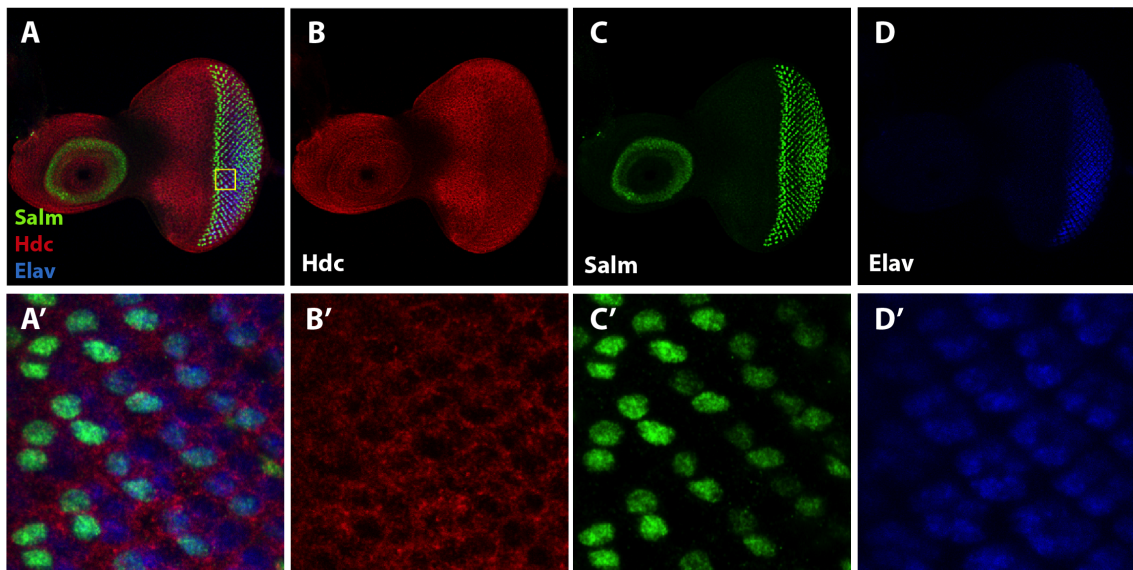


Figure 4.2. *Headcase* expression is not specific to R3/R4 in 3rd instar larval eye disc. Immunostainings were performed with antibodies against Hdc (B), Salm (C), and Elav (D). Magnified view of the region inside the yellow square (A'-D'). Salm localizes to R3/R4 cell nuclei from row three to eleven (C, C'), Elav localizes to the nuclei of all PR cells (D, D'). Hdc seemed to be localized in cytosol of all PRs (A, A').

For the candidate gene *faint sausage* (*fas*) we used a LacZ reporter line. This line was generated by Karpen and Spradling and represents a LacZ-bearing P element insertion into the upstream region of the *fas* gene (1992). In addition to showing *fas* expression, this insertion resulted in reduced Faint sausage expression levels (Lekven *et al.*, 1998) and thus represents a hypomorphic allele. As can be observed in Figure 4.3, β -gal expression is detected at low levels (Figure 4.3B, B') (low levels are probably caused by the hypomorphic trait of the line). Elav is localized in the nuclei of all PRs. By considering the organization of PRs in ommatidia, we concluded that β -gal colocalizes with Elav in R3 and R4 PR cells. On the other hand, there were additional signals not localizing to the nuclei. Since the overall signal was very weak and the background staining was high, we were not sure if this additional signal exactly reflects Fas localization or is just background noise. To better understand the *fas* expression pattern, the immunostaining procedure for this line has to be optimized further. Taking our previous results and the interesting molecular function of Fas (Ig-like domain containing extracellular membrane protein) into account, we considered *fas* as another prominent candidate that might have role in planar cell polarization in the *Drosophila* eye.

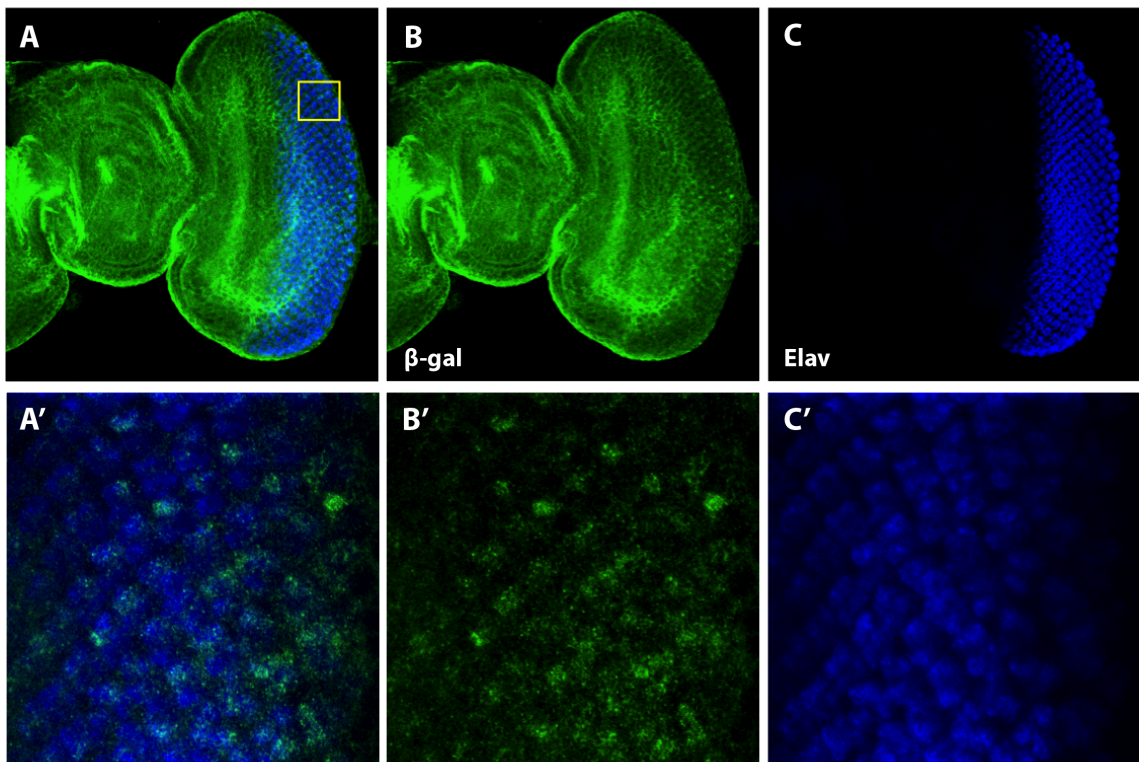


Figure 4.3. R3/R4 specific expression of *faint sausage* was confirmed in 3rd instar larval eye discs. Immunostainings were performed on the *fas-lacZ* line *fas*⁰⁵⁴⁸⁸. β -gal represents *fas* expression (B, B'), Elav localizes to PR nuclei (C, C'). Fas and Elav colocalization was observed at the position of R3/R4 cells (A, A'). Magnified view of the region inside the yellow square (A'-C').

4.2. Observed PCP Phenotypes After Down-regulating the Candidate Genes

In order to understand if the selected candidate genes play a role in planar cell polarity establishment in the *Drosophila* eye, we performed loss of function analyses. We performed a screen by down-regulating the candidate genes and examining the phenotypic changes on adult eye PR organization.

In the *Drosophila* eye, planar cell polarization starts at the 3rd instar larval eye disc after R3/R4 PRs adopt their cell fates. To establish polarization, each PR cluster has to exhibit a clockwise 90-degree rotation in the dorsal half and a counter-clockwise rotation in the ventral half of the eye. In the final pattern, rhabdomeres are organized as trapezoids in two chiral forms, pointing to opposite polar sites in both halves. In case of loss of

molecules that are important in this process, PRs adopt several PCP defect phenotypes, such as misrotation and wrong chirality. In some cases, R3 and R4 PRs cannot be specified properly and one adopts the other's cell fate. In this situation, R3/R3 or R4/R4 symmetric PR clusters are formed instead of the asymmetric ones with R3/R4 PRs.

As PCP defects can be tracked by examining phenotypic changes in the organization of rhabdomeres, we directly visualized the adult eye under a confocal microscope after down-regulating the candidate genes. Since outer rhabdomeres, organized as trapezoidal structures, express only the visual pigment Rhodopsin 1, we used a GFP-tagged version of Rh1 to be able to visualize rhabdomere organization under the fluorescence microscope.

As Figure 4.4A shows, we successfully visualized the eyes of Rh1-GFP flies by applying the cornea neutralization technique (Pichaud and Desplan, 2001). The Rh1-GFP line was used to show the correct pattern of the adult eye in which planar cell polarity was already established. In this arrangement, the rhabdomere located at the top of the trapezoid always belongs to R3 and points to different directions in dorsal and ventral halves of the retina, which in turn generates mirror symmetry across the equator (Figure 4.4A).

There are two genes encoding transcription factors, which are crucial for R3/R4 specification: *seven-up* (*svp*) and *spalt* (*sal*). Mutants of these genes reveal chirality and ommatidial rotation phenotypes related with misspecification of R3/R4 cells and misinterpretation of Fz/Dsh signalling (Domingos *et al.*, 2004; Fanto *et al.*, 1998). In order to confirm our system's reliability, we down-regulated those genes specifically in the eye and checked whether we observe similar PCP defective phenotypes.

Additionally, we used *flamingo* (*fmi*), which encodes an atypical cadherin and localizes asymmetrically through R3/R4 cell membranes and plays a major role in the Fz/Dsh signalling pathway. Since we did not knock out the genes, we expected to observe less severe phenotypes in our controls. However, the general distribution of PCP defective PRs through the eye was very similar as will be described in detail (Figure 4.4B, C, D).

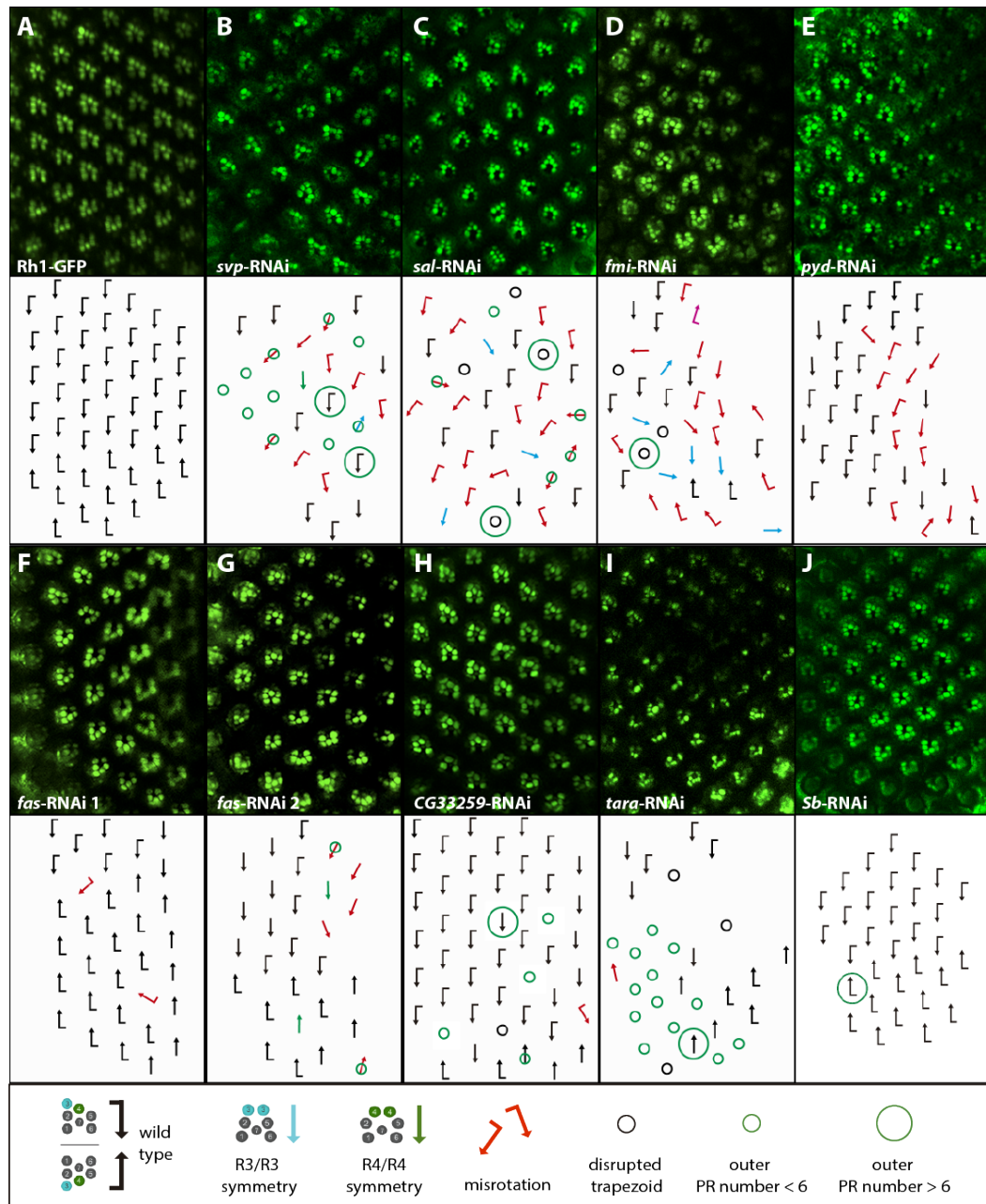


Figure 4.4. PCP defective phenotypes in adult eyes. Rh1-GFP expressing flies were used as they allow visualizing rhabdomeres by cornea neutralization with water. PCP is established by trapezoid organization of PRs and mirror symmetrical arrangement along the equator (A). Downregulation of known PCP genes (B-D) and candidate genes (E-J) revealed several defects in PCP such as symmetric ommatidia and misrotated ommatidia.

Downregulation of *svp* resulted in misrotated ommatidia and PR clusters having less than 6 outer PR rhabdomeres (Figure 4.4B). Since it was known that Svp prevents PRs from adopting an inner PR cell fate, this phenotype was expected. In some of the

ommatidia, extra Rh1-GFP expressing PR cells were observed; however, the rhabdomere sizes were smaller than outer PR rhabdomeres. Therefore, this could be either an ectopic expression of Rh1 in inner PR rhabdomeres or a technical artifact. Moreover, chirality defects were observed with symmetric rhabdomere organization within the ommatidium. Since *Svp* is required for proper specification of R3/R4, this phenotype was expected and consistent with the literature (Domingos *et al.*, 2004; Fanto *et al.*, 1998).

In the adult eye, where *sal* is downregulated, most of the ommatidia exhibited rotational defects (Figure 4.4C). Additionally, there was a decrease in the number of outer PR rhabdomeres. It was thought that in these PRs, Spalt could not induce *svp* expression and therefore, those cells could not adopt an outer PR cell fate. Moreover, some of the PR clusters showed extra Rh1-GFP expressing cells, which can be interpreted as inner PRs adopting an outer cell fate. Furthermore, it was observed that some of the R4 cells choose the R3 fate, which results in R4/R4 symmetrical ommatidia. Except the latter, all of these phenotypes were previously reported in *spalt* mutant eyes (Domingos *et al.*, 2004).

The third positive control was *fmi*. RNA interference for flamingo gave rise to chirality defects and misrotation in the ommatidia (Figure 4.4.D). It was thought that misinterpretation of Fz signalling results in failure of R3 cell fate choice, therefore, R4/R4 symmetric ommatidia were observed. Additionally, some of the ommatidia lacked PRs. These phenotypes were consistent with previously documented phenotypes (Das *et al.*, 2002).

The first candidate to be examined for planar cell polarity establishment was *polychaetoid* (*pyd*). Downregulation of *pyd* in the eye resulted in misrotation and lack of chirality since the number of outer PR cells was less than normal in some of the PR clusters (Figure 4.4E). Therefore, *pyd* was considered a promising candidate.

For the other candidate *faint sausage*, downregulation caused misrotated ommatidia. Additionally, R4/R4 symmetric ommatidia phenotypes were obviously seen (Figure 4.4F, G). In addition, considering that the ommatidia had less than 6 outer PRs, it was thought that this gene may be affecting outer cell fate choice and specifically, it plays

a role in correct interpretation of Fz/Dsh signalling. Therefore, *fas* was considered as a prominent candidate.

Generally, the most obvious phenotype that we have encountered was misrotated ommatidia; however, in adult eyes where *CG33259*, *taranis* or *Stubble* were down-regulated, this phenotype was not obvious (*CG33259*, *tara*, Figure 4.4.H, I) or was not observed at all (*Sb*, Figure 4.4.J). Therefore, we concluded that these genes either do not play a major role in ommatidial rotation or the RNAi lines work with a low efficiency.

In the adult eye in which *CG33259* was down-regulated several PR clusters revealed an abnormal number of rhabdomeres visualized by Rh1-GFP (Figure 4.4.H). This phenotype might result from inner PR cells adopting an outer cell fate or vice versa. Therefore, this gene might have a role in outer-inner cell fate choice. However, wrong chirality generated by the abnormal number of outer PRs did not result in misrotation. Therefore, it was thought that outer PR cells might have adopted the correct fate; however, could not express Rhodopsin 1.

Downregulation of *taranis* (*tara*) also revealed an abnormal number of outer PRs expressing Rh1-GFP (Figure 4.4.I). However, these PR clusters were generally not proper to evaluate the rotation since the trapezoidal structure was not formed. Therefore, it is likely that *tara* has a role in cell fate choice. It is also possible that *tara* affects Rhodopsin 1 expression.

Downregulation of *Stubble* (*Sb*) did not result in planar cell polarity defective phenotypes (Figure 4.4.J). Therefore, we concluded that this gene is not related to PCP establishment in the eye. However, it should be noted that the RNAi line might not be working efficiently enough to reflect the paucity of *Sb*.

The last candidate gene was *cropped* (*crp*). *Cropped* could not be examined in terms of PCP establishment since its downregulation disrupted the hexagonal structure of ommatidia and additionally resulted in smaller eyes with an abnormal shape and thus it was not possible to connect misrotation to the ommatidial rotation process (Figure 4.5B). For all other candidates that were examined, the general eye morphology was observed to

be similar to wild type (Figure 4.5A). Thus, we did not consider *crp* as a possible player of PCP establishment in the eye.

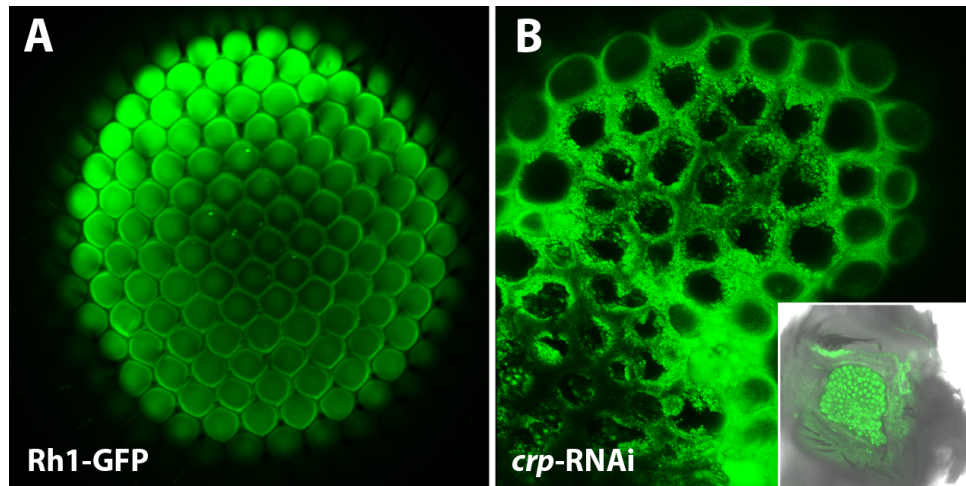


Figure 4.5. Eye structure was abnormal in *crp* down-regulated flies. Precise alignment of ommatidia as hexagons in wild type (A). Disrupted hexagonal structure (B) and eye shape (B, inset) after down-regulation of *crp*.

In summary, from the genes that were screened, *pyd* and *fas*, remained as candidates. Previously, *pyd* has been associated with pupal disc patterning and shown that its loss results in the accumulation of E-cadherin in the adherens junctions (Seppa *et al.*, 2008). In the eyes where *pyd* is down-regulated, rotation defects were observed, which might be the effect of the regulation of cadherin dynamics. On the other hand, in the eyes where *Fas* levels are reduced, we observed both R4/R4 symmetry and rotation defects, indicating that this gene might be involved in R3/R4 cell fate choice, which would affect PCP establishment. Due to the time constraints in this study, we focused on *fas* because of its novelty in eye development.

4.3. Mutant Analyses of the Selected Candidate *faint sausage*

The *fas* gene encodes an immunoglobulin superfamily member protein, which has structural similarities with extracellular proteins. It was associated with the *Drosophila* salivary gland shaping (Myat and Andrew, 2000), heart development (Haag *et al.*, 1999) and axonal pathfinding processes (Lekven *et al.*, 1998).

In order to understand its effect in PCP, we used two *fas* mutant alleles: *fas*^l and *fas*⁰⁵⁴⁸⁸. The *fas*^l allele was generated by ethylmethane sulfonate treatment and genetically behaves as a null allele (Nüsslein-Volhard *et al.*, 1984). On the other hand, the *fas*⁰⁵⁴⁸⁸ allele was generated by P element insertion into the upstream of the *fas* gene (Karpen and Spradling, 1992), which resulted in decrement in Fas levels in homozygous *fas*⁰⁵⁴⁸⁸ mutants (Lekven *et al.*, 1998).

The cornea neutralization technique was applied on *fas* mutant eyes and the resulting phenotypes were examined. However, it was not possible to use homozygous flies carrying both copies of the *fas* mutant alleles since this causes lethality. One way to overcome the lethality is to generate mutant clones in the tissue of interest using the FLP/FRT system.

Before going into a long process of whole mutant eye generation, we first examined heterozygous mutants by following the same methodology as was used for the RNAi screen. Since we expected a reduction in levels of *fas* expression with one copy of the mutant allele, we expected phenotypes similar to the ones observed in the RNAi screen.

As Figure 4.6A shows, in heterozygous mutants carrying one copy of the null mutant allele *fas*^l, ommatidial rotation defects similar to the *fas* RNAi results were observed, although they seemed less severe. Occasionally, R4/R4 symmetric ommatidia were also encountered.

Heterozygous mutants carrying the hypomorphic allele *fas*⁰⁵⁴⁸⁸ displayed ommatidial rotation defects. Additionally, there were chirality-defective PR clusters that consisted of five outer PRs (Figure 4.6.B). Occasionally, a GFP signal was detected in rhabdomeres residing in the core of the ommatidia. Since these rhabdomeres were smaller than the other ones, they could be inner rhabdomeres expressing Rh1-GFP, representing an outer PR that may have chosen an inner cell fate. If so, *fas* could also be affecting Rhodopsin 1 expression. However, it is necessary to make sure if this is a real phenotype or only an artifact. For this purpose an alternative technique was optimized to visualize rhabdomeres (Phalloidin staining) and monitor Rh1 expression (Rh1 antibody staining).

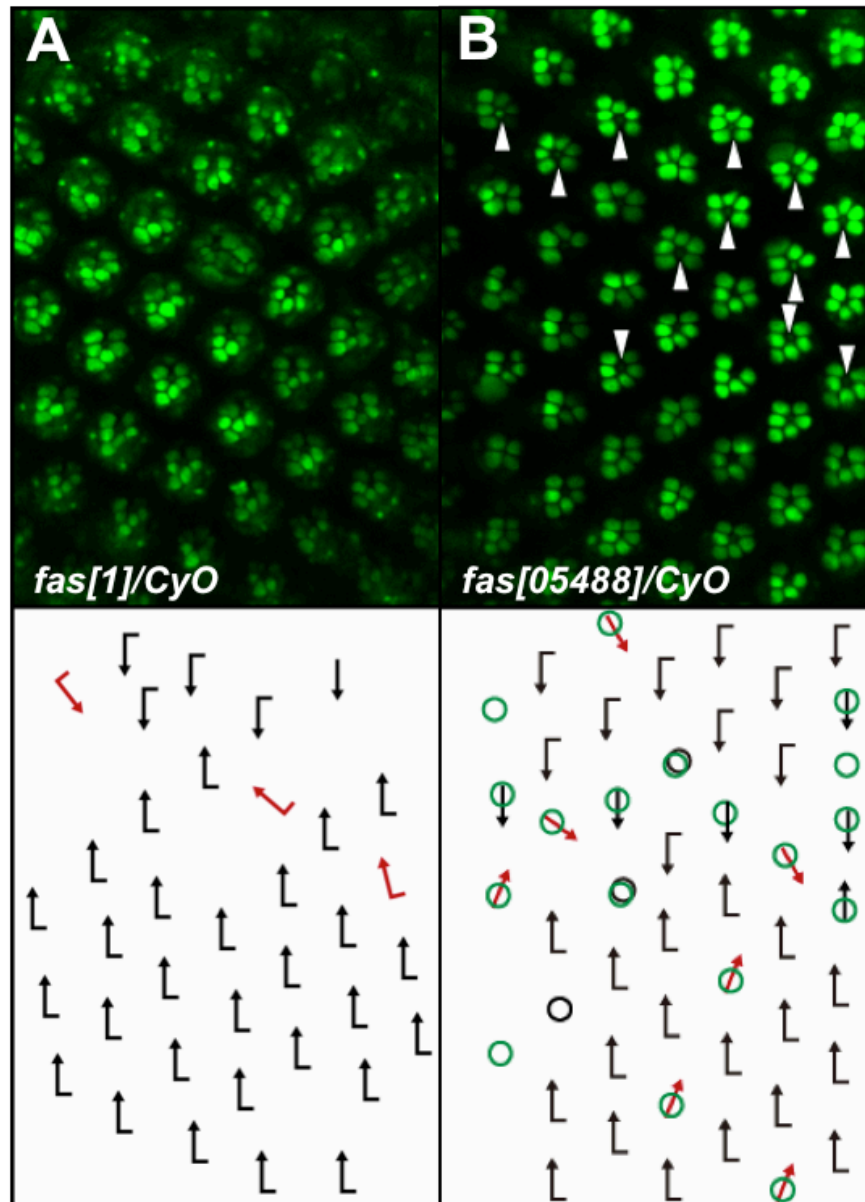


Figure 4.6. PCP defective phenotypes in the eyes of heterozygous *fas* mutants. Rh1-GFP expressing rhabdomeres were visualized using cornea neutralization with water. Observed phenotypes were similar to the RNAi phenotypes of *fas*. Dorsal is up.

All in all, heterozygous mutants reveal similar phenotypes with the knock-down experiments. As an addition, Rh1-GFP expression was seen at inner rhabdomeres in *fas*⁰⁵⁴⁸⁸ eyes.

4.4. Generation of Whole Eye Mutants for *faint sausage*

In order to generate homozygous mutant eyes of *fas*¹ and *fas*⁰⁵⁴⁸⁸, we aimed to use the FLP/FRT technique to circumvent lethality. To make use of this technique, the mutation has to be located on the same allele and in particular on the same chromosome arm as the FRT site. Since such an allele has not been available we had to recombine the mutant alleles with an FRT bearing chromosome. *FRT42D* is an FRT site that lies upstream of the *fas* gene and thus the *fas* mutations. The problem is to follow the mutation, which is not marked by any marker and to judge if recombination has happened. We reasoned that the mutation could be followed by lethality in the homozygous state and the presence of the FRT site by the ability of generating whole mutant eye clones.

To initiate the recombination, we first set up crosses to generate female flies carrying one copy of the mutant *fas* allele and one copy of the *FRT42D* allele (Figure 4.7). Then, we took advantage of meiotic recombination, which occurs only in females, and set another cross that gives rise to recombinant and non-recombinant flies. From them, we selected possible recombinant male flies to avoid any further meiotic recombination. More than a hundred males were separately crossed with the balancer stock to generate a stock of recombinants.

After generating stocks from each single male flies, we tracked them if they can survive without the *CyO* allele, which is used to balance the recombinant allele. We detected many stocks in which non-*CyO* bearing flies emerged in the F1 generation. This indicates that they do not carry the mutant allele. On the other hand, the presence of the *FRT42D* site was assessed using the apoptotic effect of the *hid* gene in PRs. This was achieved by crossing the possible recombinants with *FRT42D*, *GMR-hid* line and inducing mitotic recombination between two *FRT42D* regions in the eye. A detailed explanation of the genotypes and phenotypes of the emerging flies is given in Figure 4.7. If the putative recombinant line carries an *FRT42D* region, the eye will be rescued in the emerging flies.

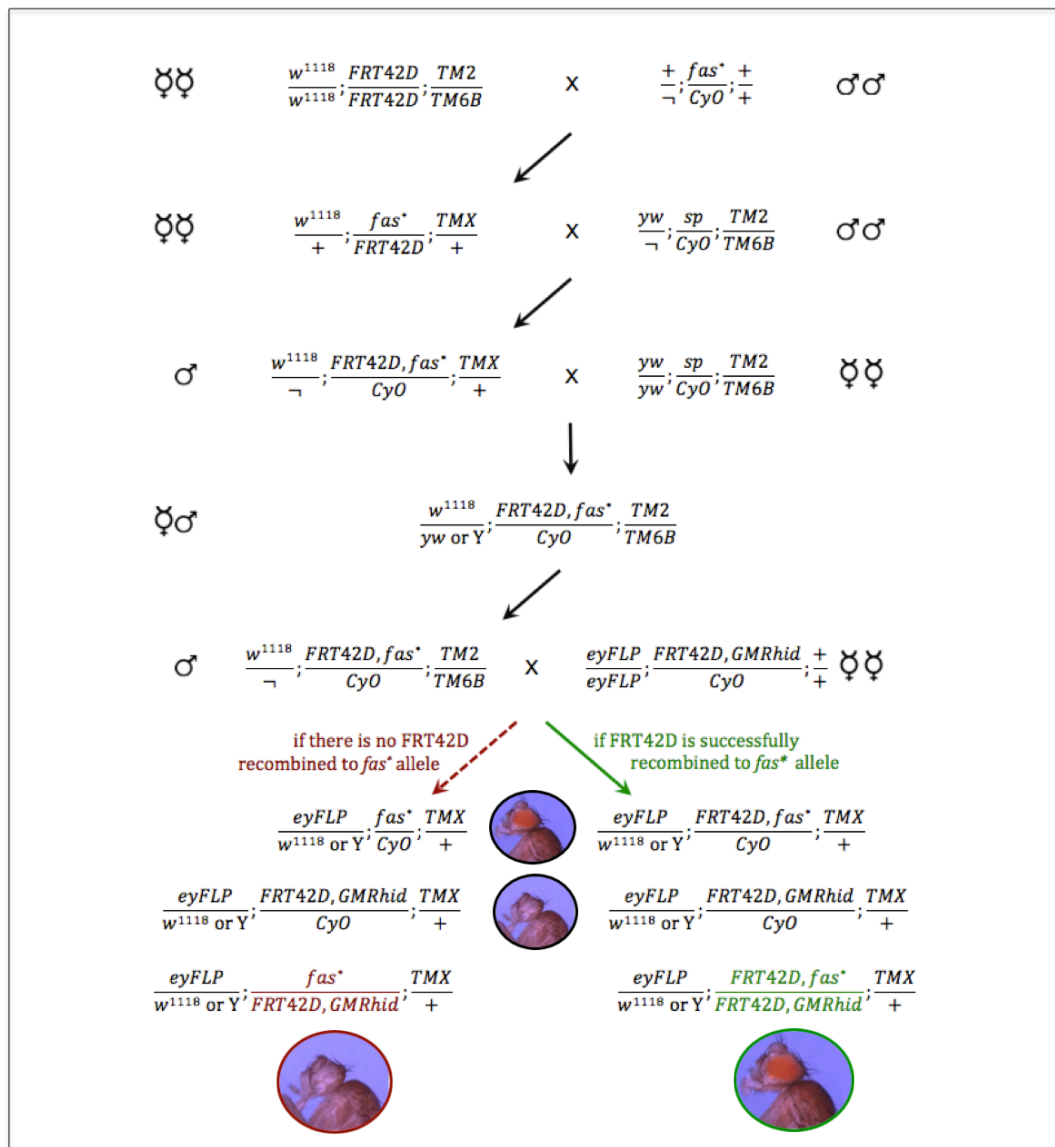


Figure 4.7. Generation of whole *fas* mutant eyes in heterozygous flies. The first two crosses aim to recombine FRT42D and *fas** alleles via meiotic recombination. Then, possible recombinants are selected, amplified and crossed with FRT42D GMR-*hid* line. The fourth cross both provides control for the presence of the FRT allele and generates the whole mutant eyes. Red and green arrows show the possibilities in the progeny.

From the stocks that were screened by these approaches, one stock could pass all the tests. Therefore, we concluded that these lines have the *fas*^l mutant allele recombined on the *FRT42D* chromosome, which makes it appropriate to use for further experiments.

Although PCP defects could not be examined by using this line in the time course of this study, experiments are being continued to add the *Rh1-GFP* allele to prepare them

for visualization. Therefore, we will be able to evaluate the phenotypes in whole mutant eyes. Alternatively, whole mutant eyes will be stained with Rh1 antibodies and phalloidin to visualize the rhabdomeres.

4.5. Interaction Between *fas* and *svp*

Svp is a transcription factor that has an important role in R3/R4 specification by regulating *salm* expression in this PR pair (Domingos *et al.*, 2004). In order to understand if there is any direct or indirect interaction between *fas* and *svp* we generated *svp* null mutant clones in the eye disc and compared the expression levels of *fas* in the mutant and wild type regions. To be able to detect R3/R4 cells, we used an antibody against Salm that enables identification of R3/R4 cells starting from row three to eleven. However, after row seven, *Svp* repression causes a decrease in Salm levels and makes it disappear gradually in R3/R4 PRs. This interaction also allows us to control the area, which is mutant for *svp* by observing Salm expression even after row seven (Figure 4.8).

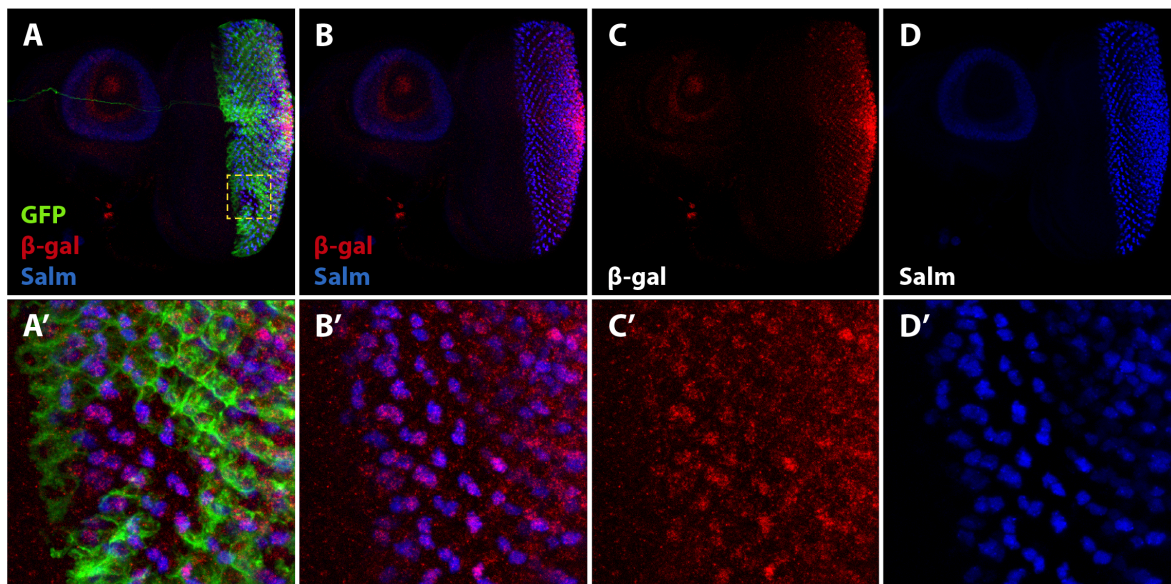


Figure 4.8. *Svp* might be repressing *fas* in R3/R4 PRs. *svp* null mutant clones were generated in the 3rd instar larval eye discs and marked by the absence of GFP.

Immunostainings were performed with antibodies against GFP (green; A, A'), β -gal to mark Fas (C, C'), and Salm (D, D'). Fas expression appeared as increased in R3/R4 PRs in the clones compared to the wild-type region (B'-D').

To detect *fas* expression, we used the hypomorphic *fas* allele that has a LacZ insertion and an antibody against β -gal for its detection. As can be evaluated from Figure 4.8, in the *syp* null mutant area (marked by loss of GFP expression) *fas* expression was observed as similar with *salm*, which continues to be expressed in R3/R4 after row seven. Outside the clonal area, levels of *fas* expression seemed lower than in the clones. While this result appears to be promising this experiment needs to be repeated in order to be more confident with this result.

4.6. Transcriptome Analysis of the R3/R4 PR Pair

As previous studies suggest, planar cell polarity establishment in the *Drosophila* eye is directly connected to the specification of the R3 and R4 PR pair. Asymmetric specification of this pair is crucial to obtain correct ommatidial chirality, which is one of the main aspects of planar polarization in the eye. Moreover, the other aspect, ommatidial rotation, is also linked with the chirality as it affects direction of rotation (Domingos *et al.*, 2004; Fanto and Mlodzik, 1999; A. Tomlinson and Struhl, 1999; Wolff and Rubin, 1998; Zheng *et al.*, 1995). Even though it is known that several pathways have a role in PCP establishment, we still lack the information of all players involved in this process.

In the light of previous studies, we hypothesized that the genes, which have a role in establishment of PCP through R3/R4 specification as well as ommatidial rotation, might be expressed differentially in the R3/R4 PR pair. In order to find these possible candidate genes, we aimed to obtain the R3/R4 transcriptome. For this purpose we specifically labelled R3/R4 PR cells and through fluorescence-activated cell sorting collected fluorescently labelled R3/R4 PR cells. RNA extraction and cDNA synthesis were followed by RNA sequencing and bioinformatic analysis.

Through bioinformatic analyses, we also examined if there is enrichment for some motifs that can be bound by particular transcription factors. Therefore, we aimed to find major regulatory TFs and their targetome to be able to enlighten the gene regulatory network of differentiating R3/R4 PR cells, which in turn, provides better understanding of R3/R4 PR specification. Moreover, since Svp TF might be targeting genes playing role in

R3/R4 specification and PCP establishment, we intended to validate predicted targetome of Svp, which is obtained from a gene regulatory network analysis performed by Delphine Potier from Aerts lab.

4.6.1. FlyLight Database Screen to Select R3/R4-Specific Lines

Prior to fluorescent-activated cell sorting, it was necessary to find a line, which has a specific expression in R3/R4 cells. The *CG33259-Gal4* line, which is the only R3/R4 specific enhancer trap line we have, was not covering all R3/R4 PRs in the eye disc. Therefore, we thought that we could find a line to label all R3/R4 cells to increase our starting material. For this purpose, we made use of the lines from the FlyLight database. This database, with the aim to find all enhancers of the *Drosophila* genome, was generated by cloning of 3 kb genomic fragments into a Gal4 vector and establishing transgenic fly lines. The expression patterns were determined and images showing the expression patterns in different tissues were posted on the FlyLight database. The images in this database were screened by visual inspection. As a first step, the image data were filtered for lines that show expression posterior to the morphogenetic furrow where the differentiating PRs reside. This approach decreased the number of lines to be examined to 346. These were screened further to identify lines that show subset-specific expression. Out of the 346 lines 12 were selected to potentially label R3/R4 PRs specifically. In order to confirm the observed expression patterns, first, the selected Gal4 lines were crossed with UAS-GFP.nls reporter lines to visualize the expression pattern of the enhancer line, then, 3rd instar eye discs were dissected and stained with antibodies against cell-type specific transcription factors. Since the reporter line has GFP with a nuclear localization sequence, we expected the GFP signal to colocalize with the cell-type specific markers, especially with Svp. Even though its expression levels in R3/R4 PRs are low, Rough was also used in some instances as R3/R4 PR marker; however, it is also expressed in R2/R5 PRs, where it's expression is usually more obvious than in R3/R4. Additionally, an antibody against Prospero was also used in some stainings to label R7 PRs, and an antibody against the neuronal marker Elav to visualize all PRs. After confocal microscopy, the images were examined and the observed expression patterns were summarized in Figure 4.9. Strength of

the GFP signal was considered as a display of expression levels and was represented in different intensities of the green color.

As can be observed from the chart, most of the lines label more than one pair of the PR cells. However, three of them, *CG30143*-Gal4, *ro*-Gal4, and *sNPF*-Gal4 lines displayed R3/R4 PR-specific expression patterns. It was also important to select the ones that do not have any expression in the antenna to avoid false positive results at the following steps. Luckily, none of the selected lines showed expression in the antennal disc (Figures 4.10, 11, 12, and see AppendixB).

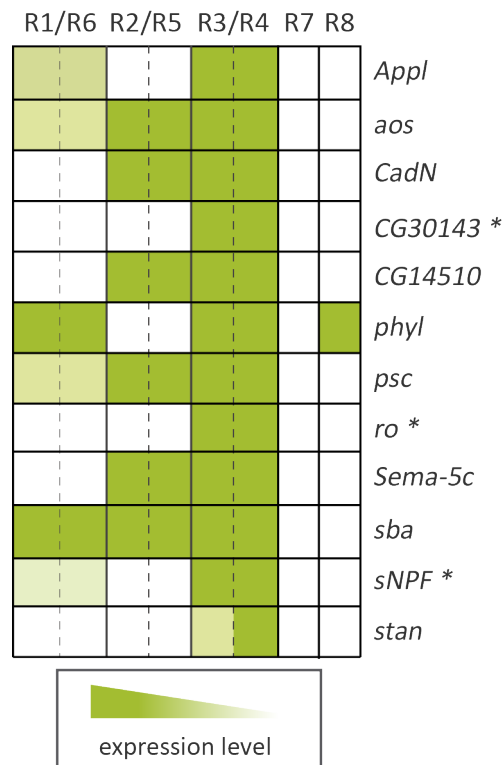


Figure 4.9. Expression patterns of the screened FlyLight Gal4 lines. Subtypes of the PRs are shown at the top and the genes related to the Gal4 lines are shown on the right side of the chart. Intensity of the green color indicates the expression level inferred from the strength of the GFP signal. Asterisks show the candidate lines with specific expression in R3/R4 PRs.

The expression pattern of the FlyLight line *CG30143*-Gal4 can be observed in Figure 4.10 and shows expression in a pair of cells (GFP signal), which are colocalizing with the neuronal marker, *Elav*, at the position of R3/R4 PR cells (Figure 4.10C, E). In

order to confirm this location, a second staining was performed with anti-Svp and anti-Ro antibodies (Figure 4.10B). With this immunostaining, it was expected to visualize all outer PRs; anti-Svp staining PRs R1/R6, R3/R4 and anti-Ro staining R2/R5; therefore, it would be possible to define the PR subtype from which the GFP signal comes. However, anti-Ro did not work well and made it difficult to identify ommatidial clusters as well as PR pairs. Nevertheless, the position of the cells in which GFP and Svp colocalize are specified before the other Svp expressing PR pair, reflecting R3/R4 specification. Thus, we inferred that this line has a R3/R4 specific expression pattern (Figure 4.10H). To be convinced, it would be better to perform an immunostaining by using antibodies against Elav, Svp and GFP.

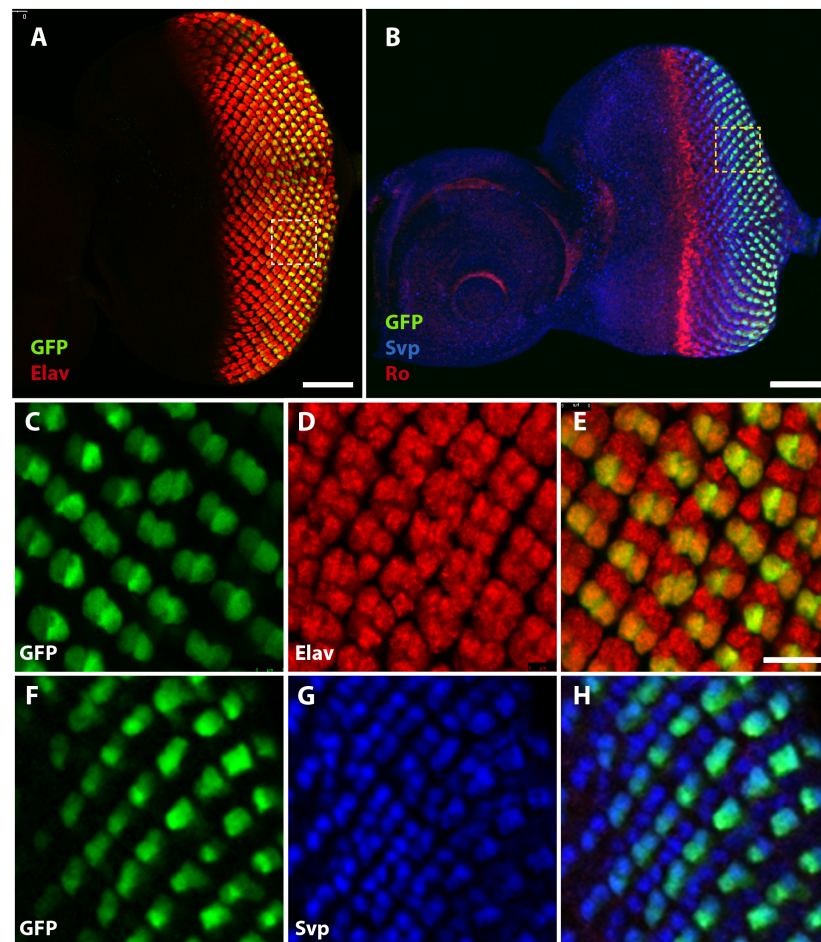


Figure 4.10. *CG30143-Gal4* FlyLight line displays a R3/R4-specific expression pattern in the 3rd instar larval eye-antennal disc. Immunostaining was performed with antibodies against GFP and Elav (A), and antibodies against GFP, Seven-up, and Rough (B). Magnified view (C-E) and inside the yellow square (F-H). GFP expression (C, F) colocalizes with neuronal marker Elav (E) or with the R3/R4 and R1/R6 marker Svp (H).

The GFP signal displayed by the other candidate FlyLight line, *ro-Gal4*, was determined to be R3/R4 specific (Figure 4.11). Even though Ro staining did not work well (Figure 4.11C), the expression pattern still can be identified by colocalization of GFP and Elav at the position that R3 and R4 PRs should reside (Figure 4.11E).

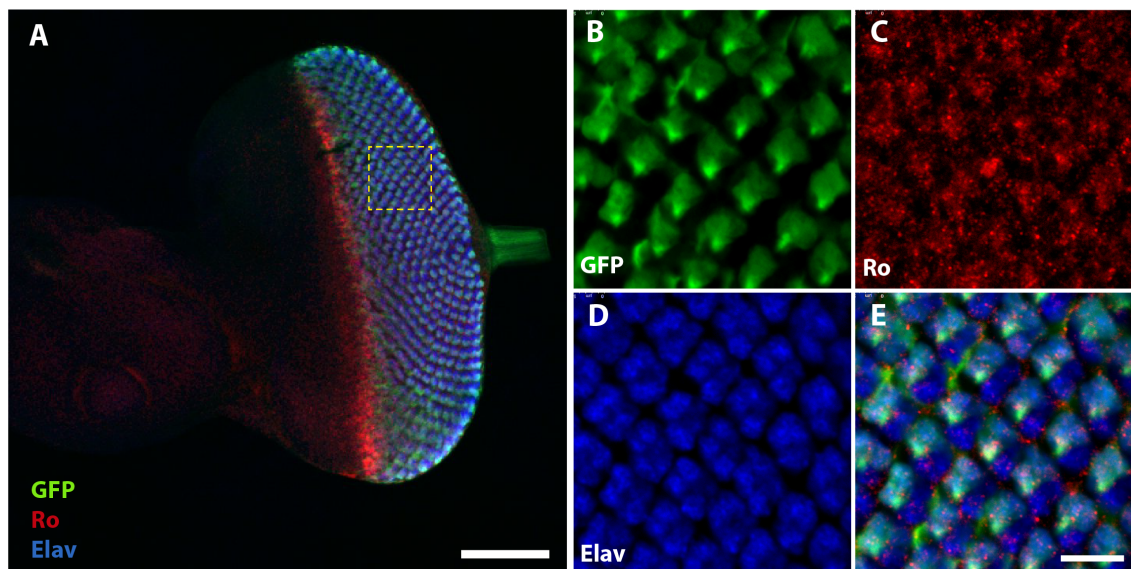


Figure 4.11. *ro-Gal4* FlyLight line has R3/R4 specific expression pattern in the 3rd instar larval eye-antennal disc. Immunostaining was performed with antibodies against GFP (B), Rough (C), and Elav (D). Magnified view of the region inside the yellow square (B-E). GFP expression driven by *ro-Gal4* (B) and neuronal marker Elav (D) colocalize at the position of R3/R4 PRs (E). R2/R5 marker Ro did not work well (C).

The third candidate, *sNPF-Gal4* FlyLight line, shows a strong GFP signal at the position of R3 and R4 PRs, which colocalize with Svp (Figure 4.12). Additionally, a weak GFP signal was observed in R1/R6 PRs that also colocalizes with Svp. These cells have a low possibility to be detected and collected via fluorescent-activated cell sorting and even if they were sorted, their amount would be very small among the sorted R3/R4 cells; therefore, our cells of interest would still be enriched in the sorted cell population. Thus, the rare signal was ignored, as it would not present a problem for the differential expression analysis based on enrichment.

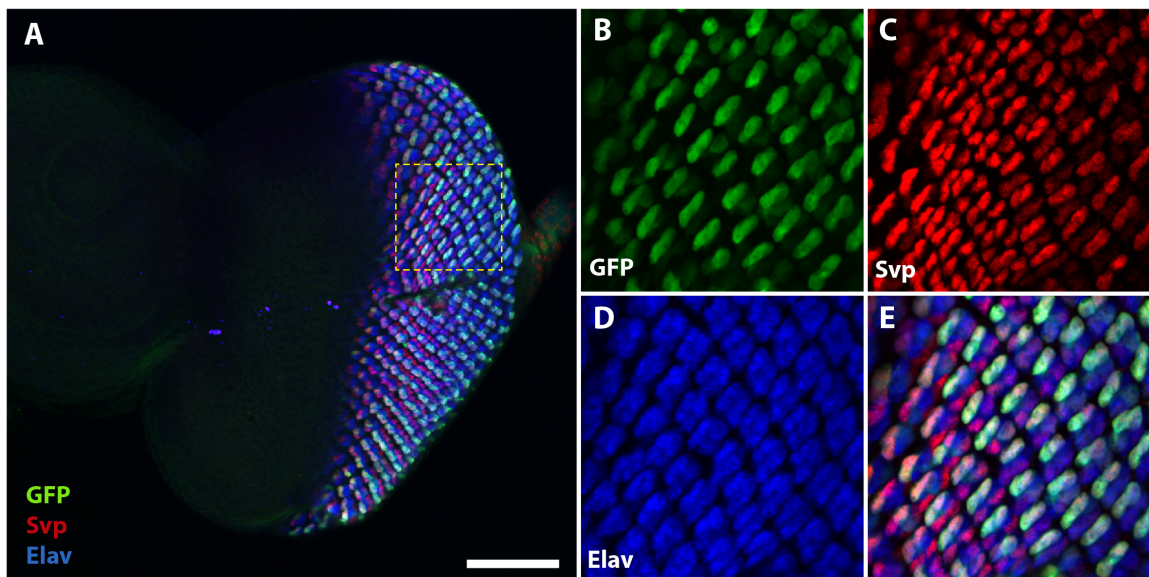


Figure 4.12. *sNPF*-Gal4 FlyLight line has R3/R4 specific expression pattern in the 3rd instar larval eye-antennal disc. Immunostaining was performed with antibodies against GFP (B), Seven-up (C), and Elav (D). Magnified view of the region inside the yellow square (B-E). GFP expression driven by *sNPF*-Gal4 (B), R3/R4, R1/R6 marker Svp (C), and neuronal marker Elav (D) colocalize at the position of R3/R4 PRs (E).

All in all, *sNPF*-Gal4 FlyLight line was the most prominent candidate as its R3/R4 specific expression pattern was confirmed with Svp staining. Therefore, it was selected to label R3/R4 PRs and FACS sorting.

4.6.2. Sorting of R3/R4 PR Cells

As we aimed to pick R3/R4 PRs from the population of dissociated cells of the eye-antennal imaginal disc, we performed fluorescent-activated cell sorting. FACS works through directing laser beams to cell droplets which are flowing out of a nozzle and sorts the cells according to their fluorescent signal (Tomlinson *et al.*, 2013). We used GFP as a fluorescent marker to sort the cells of interest.

In order to drive GFP expression in R3/R4 PRs, the *sNPF*-Gal4 line was crossed with an UAS-GFP.nls reporter line. From the first generation coming out of this cross, 3rd

instar larval eye-antennal discs were dissected and collected in Eppendorf tubes. In total, approximately 660 eye-antennal discs were dissected (Table 4.1).

Table 4.1. Number of sorted cells from the dissected eye-antennal (EA) discs.

Tube ID	Number of cells		GFP positive fraction (R3/R4)	GFP negative fraction (other cell types and PRs)
	Number of EA discs			
#1	160		1.605	207.427
#2	130		3.265	487.592
#3	110		1.592	204.812
#4	100		1.486	208.397
#5	80		1.046	168.115
#6	80		728	101.886
Total	660		9.722	1.387.951

To be able to sort single cells, first, a dissociated cell population was obtained by trypsinization and centrifugation and then cells were sorted by FACS according to their fluorescent marker. At the sorting stage, the parameters for collecting the cells of interest were defined and gates (border lines) were set by examining dot plots (Figure 4.13). The dots in the graphs represent cells, which were detected by photodiodes while passing through the laser beam. The gates were selected by considering fluorescence level, cell volume, and cell complexity. The side-scattered light (SSC) value is determined by the amount of light that a cell reflects and refracts according to its granularity, while the forward-scattered light (FSC) value is determined by the diffracted light and represents the volume of a cell (Marti *et al.*, 2001). Since dead cells become less granular as they lose their content and may get fragmented, we expected them to be closer to the origin of the SSC versus FSC graph. Therefore, the gate was set to avoid collecting those cells (see the first graphs of each sample in Figure 4.13) and approximately 40% of the cell population was eliminated. Selected cells were then gated for FITC value, which represents the fluorescence intensity (see the second graphs of each sample in Figure 4.13).

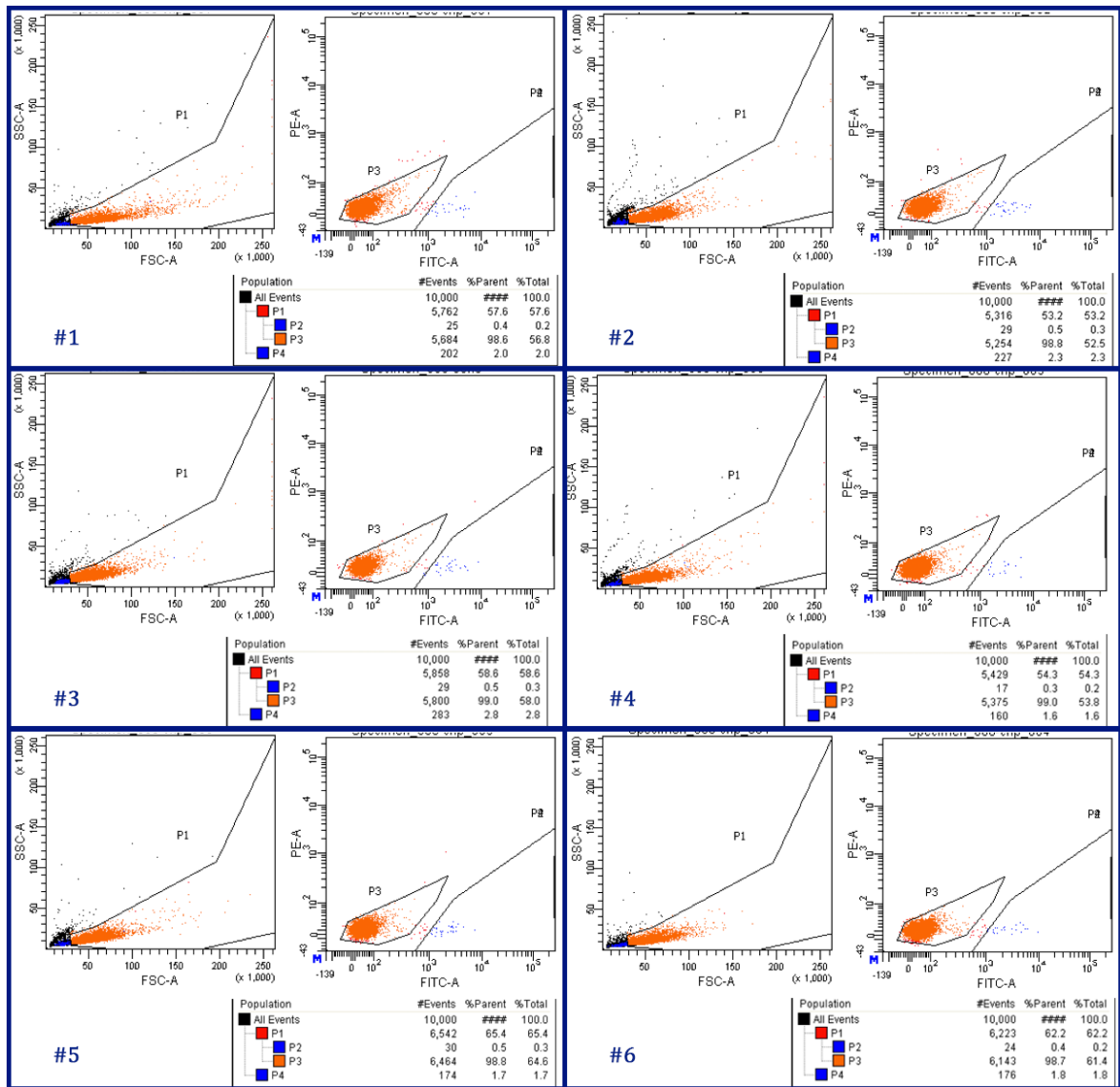


Figure 4.13. FACS dot plots of R3/R4 cell sorting. P1 gate was set to collect cells at higher complexity and bigger size. The cells in P3 were deemed to consist of non-fluorescently labelled cells while the P2 gate was determined to collect GFP-positive cells. The IDs of the tubes from which the cells were sorted are shown at the left corners of each rectangle containing related dot plots.

The approximate number of ommatidia in the *Drosophila* eye is ~ 800 and thus the expected number of R3 and R4 cells is 1600 for one disc, which amounts to 1,056,000 cells for 660 eye-antennal imaginal discs. Comparing this expected number to the numbers obtained after sorting the cells as shown in Table 4.1, we were able to sort $\sim 0.9\%$ of the expected R3/R4 PR cells. It is very likely that some of the cells were lost because of

physical disruptions or enzymatic degradations; thus, to make a more accurate comparison we compared the GFP-positive and -negative cell numbers. The percentage of the collected R3/R4 cells among all sorted cells was calculated as $\sim 1\%$. Comparing this to the number of R3/R4 cells in one eye-antennal disc (1600), approximately 3,6% of ~ 44.000 cells comprising the eye-antennal disc (Kumar, 2011) are supposed to be R3 and R4 cells. This means that we could recover almost 25% of the R3/R4 cells that can be used for further analysis. GFP-positive cells were used to extract RNA and generate a cDNA library using the SMART™ approach. This kit is adapted for use for small amounts of RNA.

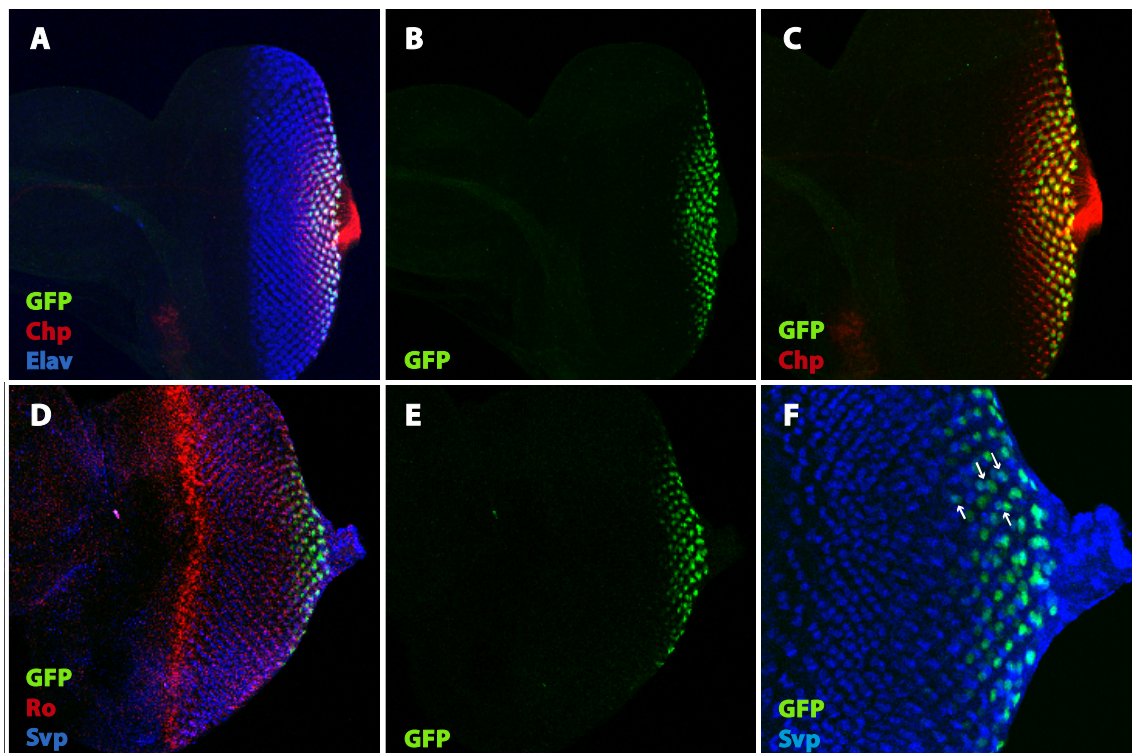


Figure 4.14. Chp-GFP expression is limited to approximately five rows at the posterior margin of the 3rd instar eye disc. Immunostainings of a 3rd instar larval eye-antennal disc. Anti-GFP shows Chp-GFP expression (B, E) which starts after endogenous Chp (C). Elav shows nuclei of all PR cells (A). Antibody against Svp shows R3/R4 and R1/R6 PRs and Ro is supposed to show R2/R5 PRs (D).

Instead of generating a cDNA library and performing RNA-Seq for the GFP negative fraction out of this experiment, already available RNA-Seq data generated from the GFP-negative fraction of FACS sorted *chaoptin (chp)*-GFP line were used. The same procedure was followed for obtaining the RNA-Seq data from this line starting from

dissection step to data analysis. The reason to use this line's negative fraction is that it is almost like a wild-type eye-antennal disc (Figure 4.14). It shows very late expression, so GFP expression is observed in a small number of rows at the posterior margin of the eye disc. Immunostainings using antibodies against cell type-specific markers (data not shown) show that *chp*-GFP is expressed in several PR subtypes containing a low percentage of R3/R4 PRs (Figure 4.14F). Therefore, sorted GFP-negative PRs from this line contain all types of PRs and any of the subtypes is expected to be enriched considerably in this cell population as in a wild type eye-antennal disc.

4.6.3. Quality of the Extracted RNA

RNA extraction from the sorted cells was followed by assessment of the quality of the RNA. For this purpose, a Bioanalyzer was used, which by looking at the state of rRNAs gives an assessment about the RNA integrity and quality. The RNA integrity number (RIN) indicates the level of integrity. Higher RIN number represents better quality.

In detail, the Bioanalyzer separates RNAs according to their size through capillary electrophoresis that takes place in micro wells loaded with a sieving polymer matrix and an intercalating fluorescent dye. This dye allows to detect the amount and speed of RNAs passing through the polymer matrix (Krupp, 2005).

Prior to electrophoresis, it exposes the RNA to high temperatures for a couple of minutes in order to dissociate weakly bound fragmented RNA. For insect RNA, this procedure results in separation of the 28S rRNA into two fragments, which are at similar sizes with 18S rRNA, approximately 2000 nucleotides in length (Winnebeck *et al.*, 2010). Therefore, we expected to see two peaks at the position of 2000 nt, one belonging to 18S rRNA and the other belonging to fragmented 28S rRNA. As electropherograms show (Figure 4.15), both *sNPF*-GFP-positive and *chp*-GFP-negative samples have two sharp peaks at around the 18S region. Peaks at around 25 nt were thought to represent 5S and other small rRNAs. Overall, there are no additional significant peaks at different regions, which would reflect RNA degradation. This profile is supported by two clear bands observed in gel-like images (Figure 4.15 right panel).

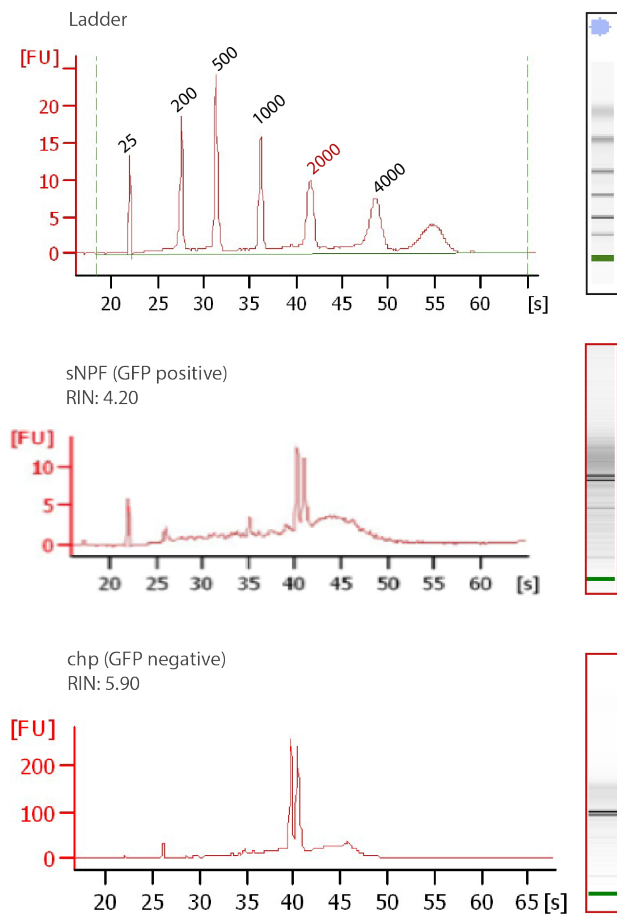


Figure 4.15. rRNA measurements for sNPF GFP-positive and chp GFP-negative fractions. Electropherograms show two peaks at ~2000 nt. Two distinct bands are seen in the gel-like images (right). Ladder is shown at top.

RIN values are directly proportional to RNA quality and vary among species, tissues, and RNA isolation methodologies (Krupp, 2005). In general, values higher than seven are considered to be good; however, there is not a reported minimum RIN value that should be obtained to perform RNA sequencing in *Drosophila*. In addition to other parameters, the RIN algorithm calculates RNA integrity by considering 28S/18S ratio and height of the 28S peak (Schroeder *et al.*, 2006). In our case, since the system had been programmed for detection of non-degraded 28S rRNA it misrecognized 28S rRNA peak and took the small values associated to the 45th second on the electropherogram (where normally a high peak of non-degraded 28S rRNA is observed). Therefore, the algorithm should have miscalculated the RIN, which resulted in a lower value than it is supposed to

be. Considering other experiments done by the same procedure in the Aerts lab where these experiments were performed, which yielded similar RIN values (data not shown) and the clear peaks at desired positions in our experiment, we reasoned that our RNA samples have mostly intact 18S and 28S rRNAs, and thus a good quality mRNAs as well.

SMART™ technology allowed us to generate a cDNA library from the low number of sorted cells (less than 10.000). This approach was preferred not only as it allows cDNA synthesis even from picogram amount of RNA, but also since it provides full-length transcript generation. It uses a modified oligo(dT) primer and takes advantage of the terminal transferase activity of Moloney murine leukemia virus reverse transcriptase for cDNA synthesis (Zhu *et al.*, 2001).

Table 4.2. RNA-Seq analyses for sNPF GFP-positive and chp GFP-negative fractions.

		sNPF GFP positive	chp GFP negative
	reads in initial FASTQ	24.751.453	10.748.471
	cleaning with multiplex primer	23.591.501	9.590.360
Discarded reads	too short reads	1.095.340	1.076.730
	adapter only reads	64.612	81.381
	second cleaning	9.691.883	8.808.839
Discarded reads	too short reads	5.362.270	724.647
	adapter only reads	8.537.348	56.874
	% of remaining reads	39%	82%
QC passed + QC failed	unmapped reads	1.427.080 + 6566	326.622 + 352
	mapped reads	31.622.236 + 0	29.541.855+ 0
	unique alignment	8.258.237	8.481.865
	% of mapping (after cleaning)	85.21%	96.29%
	% of mapping (regarding all reads)	33.36%	78.91%
	HTSeq library (accepted hits)	36.618.807	35.356.036

The prepared cDNA libraries were sequenced and the data was processed. After cleaning, a quality-check yielded ~ 30 million high quality reads for each sample. Finally, 85.21% of the reads from the *sNPF*-GFP-positive fraction and 96.29% of the reads from *chp*-GFP-negative fraction were mapped to the *Drosophila* genome. Detailed information about data analyses is shown in Table 4.2.

After counting the reads per genes, a differential expression analysis was performed. Comparing the normalized gene expression levels in R3/R4 versus almost all PRs revealed that 80 genes were up-regulated and 72 genes were down-regulated with an

at least 2-fold change ($pval < 0.05$). The first 40 genes from the ranked list of up-regulated and down-regulated genes in R3/R4 PRs are shown in Table 4.3.

As expected, the R3/R4 and R1/R6-specific gene *seven-up* (Mlodzik *et al.*, 1990) was detected as up-regulated (11.96 FC, $pval = 0.02$), while the R7-specific gene *prospero* (Kauffmann *et al.*, 1996) was down-regulated (22.77 FC, $pval = 0.003$) in R3/R4 PRs. Additionally, the expression level of the *rough* gene was also examined, since it is known to be expressed in several PR precursors throughout the morphogenetic furrow and later on specifically in R2/R5 and R3/R4 PRs (Kimmel *et al.*, 1990). As can be presumed, the expression level of *ro* was detected as up-regulated in R3/R4 PRs with a 2.5 fold change; however, this result was not highly significant ($p = 0.1$). Similarly, detection of the R8-specific gene *senseless* yielded low significance level ($p = 0.7$), yet its expression level showed a less than 2-fold change as expected. We reasoned that the high p values for some of the genes, which normally are expected to have a higher read number could be due to a low number of reads at the beginning. Unfortunately, we do not have replicates for this experiment. However, controlling the differential expression levels of these known genes gave confidential results. Therefore, we concluded that this dataset was appropriate to use for further analyses.

Table 4.3. The top 40 differentially expressed genes in R3/R4 PRs.

Up-regulated Genes			Down-regulated Genes		
Name	Fold change	p value	Name	Fold change	p value
Him	127.69	5.20E-05	CG12239	-162.96	5.02E-05
CR40469	80.44	1.61E-04	Eig71Ee	-146.59	7.71E-04
Tektin-C	214.20	3.28E-04	eater	-101.15	1.14E-03
m6	33.91	1.14E-03	mGluRA	-81.17	1.36E-03
Act57B	24.21	3.23E-03	CG34296	-26.69	2.76E-03
Akh	23.68	5.85E-03	pros	-22.77	2.98E-03
CR34335	16.81	6.29E-03	FucTA	-47.54	3.02E-03
CG14075	22.43	8.60E-03	Ilp3	-150.26	3.97E-03
CG17738	62.30	8.90E-03	CG11317	-31.42	4.17E-03
HLHm7	13.90	1.01E-02	Sgs3	-45.08	4.46E-03
CG14567	22.81	1.12E-02	Mec2	-65.72	4.65E-03
CG4702	19.15	1.17E-02	CG13248	-28.00	5.79E-03
obst-F	28.38	1.21E-02	CG15831	-27.07	6.37E-03
m2	12.09	1.47E-02	Lin29	-18.21	6.37E-03

Table 4.3. The top 40 differentially expressed genes in R3/R4 PRs (cont.).

BicC	22.71	1.49E-02	igl	-30.38	6.38E-03
CG9975	17.84	1.49E-02	alrm	-129.00	6.55E-03
CG9691	11.99	1.60E-02	CG8193	-42.36	7.19E-03
E(spl)	11.51	1.65E-02	yellow-f	-47.46	7.46E-03
malpha	11.21	1.71E-02	fd102C	-42.88	1.01E-02
CG42565	32.52	1.75E-02	Gad1	-17.25	1.06E-02
CG15373	27.80	1.76E-02	Eaat2	-14.49	1.30E-02
side	13.24	1.77E-02	rho-5	-15.36	1.37E-02
mt:lrRNA	11.57	1.78E-02	CG33465	-17.34	1.47E-02
svp	11.96	2.03E-02	CG32017	-13.51	1.51E-02
CG3546	15.83	2.18E-02	mei-9	-23.16	1.53E-02
CG17224	13.85	2.18E-02	CG2993	-13.19	1.59E-02
bond	15.58	2.19E-02	nAcRbeta-96A	-14.46	1.64E-02
CG9452	17.74	2.20E-02	Sgs4	-36.28	1.65E-02
CG15909	32.74	2.31E-02	TepIV	-11.24	1.71E-02
CG15522	11.86	2.32E-02	Hml	-15.91	1.78E-02
CG8492	18.56	2.37E-02	CG1607	-11.94	2.00E-02
CG15353	19.00	2.41E-02	mthl6	-53.14	2.00E-02
w	14.14	2.50E-02	scro	-11.19	2.00E-02
HLHmbeta	9.41	2.51E-02	CG10253	-15.39	2.07E-02
CG2663	14.16	2.56E-02	HPS1	-24.29	2.13E-02
peb	9.80	2.65E-02	Ef1alpha100E	-9.99	2.17E-02
Lip1	23.71	2.72E-02	Fer1	-32.25	2.29E-02
Rh6	14.24	2.85E-02	CG8032	-28.15	2.33E-02
Cpr62Bc	55.26	2.91E-02	kek2	-16.31	2.35E-02
Vha36-3	27.06	2.91E-02	CG14989	-10.08	2.45E-02

4.6.4. Enriched Gene Ontology Terms and Possible Candidates

After obtaining the list of differentially expressed genes we aimed to control the accuracy of this data by examining enriched GO terms among the ranked list of DE genes. For this purpose, we used the gene ontology enrichment analysis tool GOrilla (Eden *et al.*, 2009) and searched for GO terms related to molecular function and biological process (FDR<0.05).

Concerning the known mechanisms of R3/R4 specification and planar cell polarization, we expected to find terms related to signalling pathways, gene regulation, and PR development. The results were promising because of statistically significant enrichment

of compound eye development under sensory organ development term and G-protein coupled and Notch signalling pathways under cell surface receptor signalling pathway term. The GO term, negative regulation of gene expression also yielded several TFs, which may have a role in R3/R4 specification through repressing the expression of genes specific to other PR subtypes (Figure 4.16 and Table 4.4). In summary, we were able to cover a set of genes involved in biological processes that may lead to R3/R4 specification and PCP establishment in the eye.

Additionally, the significantly enriched GO terms related with molecular function were coherent with the enriched biological function terms. It is very likely that sequence-specific DNA binding molecules and RNA polymerase II transcription factor activity regulators play a role in R3/R4 specification as well as signalling receptors (Figure 4.17 and Table 4.5).

The other goal in performing GO analysis was to pick up some candidate genes to further examine their roles. There might be possible candidates among the genes that are grouped in enriched GO terms related with processes of our interest and also have not been studied yet for their role in R3/R4 specification and planar cell polarization. In that respect, *edl* (*ETS-domain lacking*) was determined as a candidate with its role in gene regulation through sequence-specific DNA binding function and in sensory organ development (Table 4.4 and 4.5). Also, by considering its significant 7.79-fold up-regulation in R3/R4 PRs (pval=0.04), we regarded *edl* as a prominent candidate.

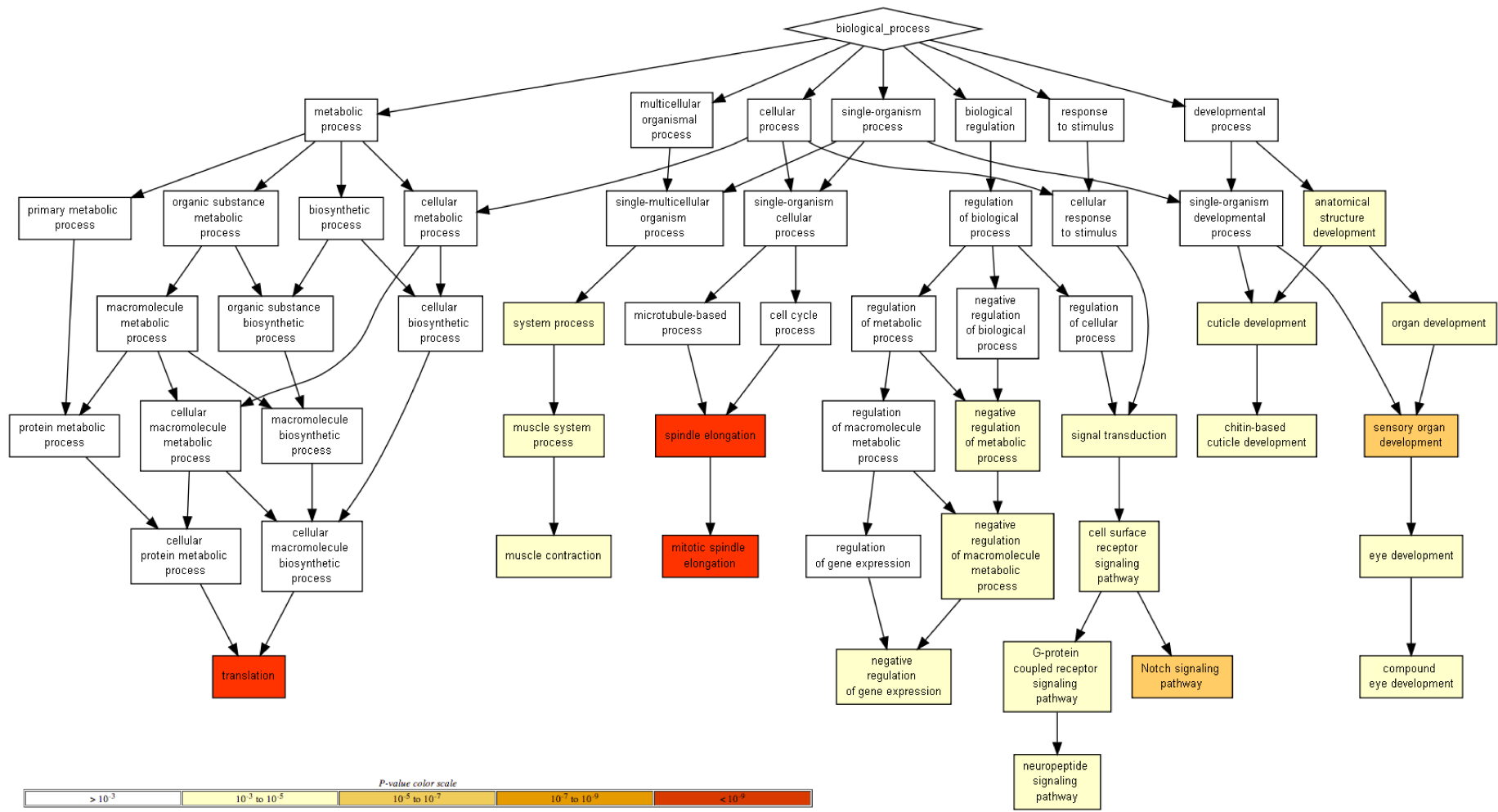


Figure 4.16. Hierarchical graphs of enriched GO terms related to biological processes among DE genes in R3/R4.

Table 4.4. Significantly enriched biological process related GO terms among DE genes in R3/R4 (FDR<0.05).

GO Term	Description	P-value	FDR q-value	Enrichment	Related Genes
GO:0006412	translation	6.73E-15	3.7E-11	2.84	Rp gene family members, CG12413
GO:0000022	mitotic spindle elongation	3.32E-10	9.12E-7	3.6	Rp gene family members
GO:0051231	spindle elongation	7.41E-10	1.36E-6	3.51	Rp gene family members
GO:0007219	Notch signalling pathway	4.22E-6	5.79E-3	32.01	E(spl)m3-HLH, E(spl)m2-BFM, E(spl)malpha-BFM, E(spl)mbeta-HLH, E(spl)m8-HLH
GO:0007423	sensory organ development	7.16E-6	7.87E-3	7.21	futsch, E(spl)m3-HLH, svp, E(spl)m2-BFM, E(spl)malpha-BFM, Sobp, E(spl)mbeta-HLH, E(spl)m7-HLH, edl, E(spl)m8-HLH
GO:0003012	muscle system process	1.62E-5	1.48E-2	5.19	Arc1, Mlc2, Mhc, fln, KCNQ, CG2121, Neurochondrin, Rya-r44F, Mlc1, Chd64
GO:0048749	compound eye development	1.97E-5	1.55E-2	4.13	futsch, mam, E(spl)m3-HLH, ro, svp, E(spl)mbeta-HLH, E(spl)mgamma-HLH, E(spl)mdelta-HLH, so, boss, Abl, lz, toe, Sobp, E(spl)m7-HLH, E(spl)m8-HLH
GO:0007186	G-protein coupled receptor signalling pathway	2.15E-5	1.48E-2	3.67	Akh, itp, TrissinR, inaC, Pk1r, 5-HT7, boss, CG32547, DmsR-2, Rh6, CG43795, AR-2, Ast-C, Ast, GRHRII, Pdfr
GO:0040003	chitin-based cuticle development	4.13E-5	2.52E-2	2.36	Cpr35B, Cpr78Ca, Cpr78Cc, TwdlW, Twdlalpha, grh, dib, Cpr51A, TwdlM, mgl, TwdlY, Lcp65Ad, Cpr65Eb, Ccp84Ad, drd, CG34461, Cpr97Eb, Cpr76Bc, Cpr76Bb, Cpr65Ea, TwdlE, Cpr47Ec, Cpr30F, Cpr62Bc, Cpr31A, Cpr64Ac, Cpr62Bb, sec23, Cpr49Ae
GO:0001654	eye development	4.9E-5	2.69E-2	3.87	futsch, mam, E(spl)m3-HLH, ro, svp, E(spl)mbeta-HLH, E(spl)mgamma-HLH, E(spl)mdelta-HLH, so, boss, Abl, lz, toe, Sobp, E(spl)m7-HLH, E(spl)m8-HLH
GO:0007218	neuropeptide signalling pathway	7.9E-5	3.95E-2	6.48	Akh, AR-2, itp, Ast-C, Ast, GR, Pk1r, Pdfr, DmsR-2
GO:0006936	muscle contraction	8.43E-5	3.86E-2	6.72	fln, KCNQ, Rya-r44F, Mlc1, Chd64
GO:0010629	negative regulation of gene expression	8.44E-5	3.57E-2	4.97	E(spl)m3-HLH, retn, twi, E(spl)mbeta-HLH, E(spl)m7-HLH, edl, E(spl)m8-HLH, bin, scrt, blanks, Rh6

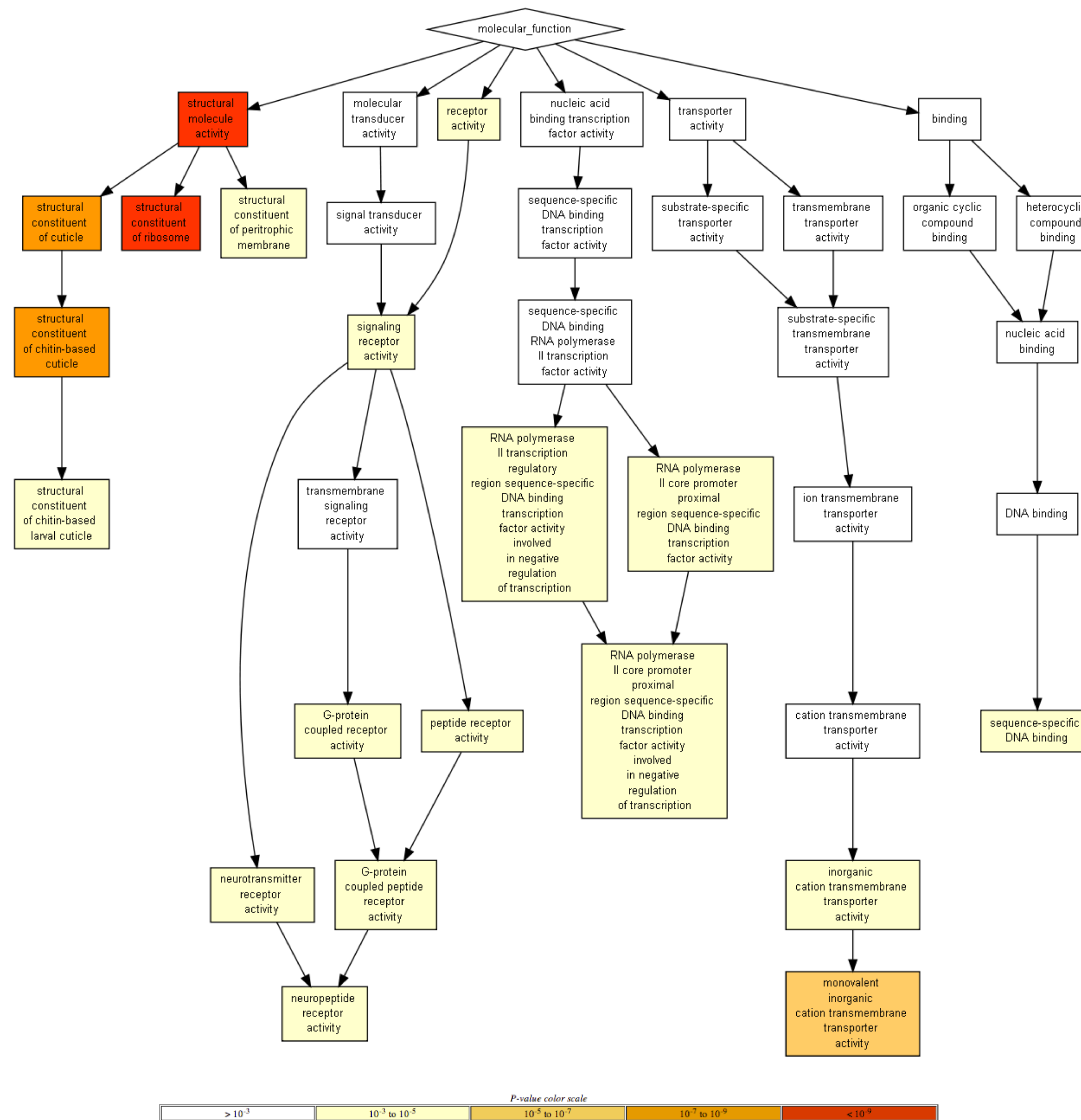


Figure 4.17. Hierarchical graphs of enriched GO terms related to molecular function among DE genes in R3/R4.

Table 4.5. Significantly enriched molecular function related GO terms among DE genes in R3/R4 (FDR<0.05).

GO Term	Description	P-value	FDR q-value	Enrichment	Related Genes
GO:0005198	structural molecule activity	2.92E-26	7.05E-23	2.65	obst. CG1368, CG43896, vkg, sls, CG5897, Act57B, mRpL42, Prm, Yp1, betaTub60D, Ppn, TwdlM, TwdlY, Strn-Mlck, Cg25C, Muc4B, obst-E, Ccp84Ad, CG15754, TwdlE, RpS7, CG7298, obst-F, CG7794, Gasp, dy, CG8543, Act79B, CG8541, Cp38, CG10154, TwdlW, LamC, Twdlalpha, Cpr51A, Jupiter, CG34461, Peritrophin-A, CG10625, Muc11A, Act87E, zormin, CG2955, Rp family members
GO:0003735	structural constituent of ribosome	5.18E-19	6.24E-16	3.31	Rp gene family members
GO:0042302	structural constituent of cuticle	6.36E-9	5.11E-6	3.16	Cpr35B, Cpr78Ca, Cpr78Cc, TwdlW, Twdlalpha, Cpr51A, TwdlM, Lcp65Ad, TwdlY, dy, Ccp84Ad, Cpr65Eb, CG34461, Cpr97Eb, dy1, Cpr76Bc, Cpr76Bb, Cpr65Ea, CG15754, TwdlE, CG10625, Cpr47Ec, Cpr30F - cuticular protein 30f, Cpr47Ed, Cpr62Bc, CG8543, Cpr31A, Cpr64Ac, Cpr62Bb, CG8541, Cpr49Ae
GO:0015077	monovalent inorganic cation transmembrane transporter activity	6.61E-6	3.19E-3	2.00	CoVIb, ppk19, KCNQ, CG2003, CG1698, CG4476, CG9657, CG34396, ATPsyn-b, Ndae1, CG15096, ppk16, slo, ppk11, CG17167, sun, List, CG33296, CG42594, CG7580, CG13794, CG13793, CG15719, CG3321, l(2)06225, CoVIIc, VhaAC39-2, eag, CG15555 Shawl CG8850 CoVb, Vha36-2, Vha36-3, elk, Vha100-5, cype, CG9903, CG14239, lh, CG18809, salt, ox, Rh50, CG7091, CG4692, ATPsyn-Cf6
GO:0016490	structural constituent of peritrophic membrane	1.07E-5	4.3E-3	14.74	Cpr65Eb, Ccp84Ad, Cpr97Eb, CG34461, Cpr35B, Cpr65Ea, Cpr47Ed, Cpr30F, Cpr62Bc, Cpr62Bb, Cpr51A, Lcp65Ad, Cpr49Ae
GO:0030594	neurotransmitter receptor activity	1.46E-5	5.02E-3	6.14	AR-2, CG33639, TrissinR, nAcRalpha-7E, GRHRII, Pk1r, 5-HT7, Pdfr, ETHR, CG32547, DmsR-2
GO:0001078	RNA polymerase II core promoter proximal region sequence-specific DNA binding transcription factor activity involved in negative regulation of transcription	2.05E-5	6.19E-3	100.02	svp, E(spl)m7-HLH, E(spl)m8-HLH,
GO:0043565	sequence-specific DNA binding	8.3E-5	1.82E-2	2.00	B-H2, B-H1, retn, E(spl)m3-HLH, svp, ro, Atf3, knrl, E(spl)mbeta-HLH, oc, E(spl)mgamma-HLH, Bsg25A, E(spl)mdelta-HLH, Clk, prd, lz, run, dmrt11E, dar1, vnd, Pdp1, gm, Hr96, abd-, Hmx, so, Dfd, CG32006, bin, Ptx1, eyg, croc, toe, dys, Lim3, otp, CG18619, E(spl)m7-HLH, edl, E(spl)m8-HLH, zfh1
GO:0008188	neuropeptide receptor activity	8.31E-5	1.67E-2	7.39	AR-2, CG33639, TrissinR, GRHRII, Pk1r, Pdfr CG32547, DmsR-2
GO:0008528	G-protein coupled peptide receptor activity	8.31E-5	1.54E-2	7.39	AR-2, CG33639, TrissinR, GRHRII, Pk1r, Pdfr CG32547, DmsR-2
GO:0001653	peptide receptor activity	9.99E-5	1.72E-2	7.20	AR-2, CG33639, TrissinR, GRHRII, Pk1r, Pdfr CG32547, DmsR-2

4.6.5. Enriched Motifs and Possible Regulators of R3/R4 PR Specification

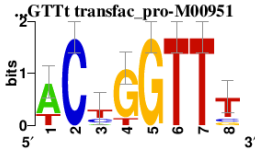
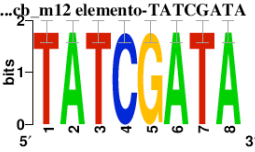
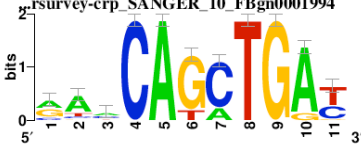
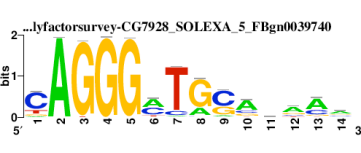
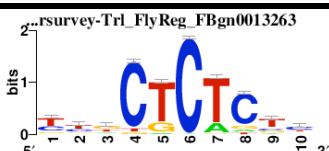
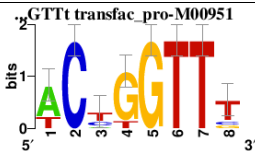
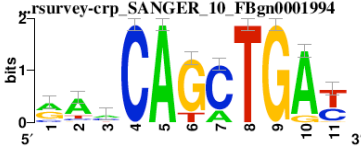
Choosing one cell fate over another and being specified into a particular cell type is usually a process regulated by several transcription factors. In that respect, we aimed to understand if our gene-set shares common *cis*-regulatory sequences that a particular TF can bind. For this purpose, we used three gene sets consisting of up-regulated genes, down-regulated genes and all of the DE genes to search for over-represented motifs through 5 kb upstream and intronic regions by using the program i-cisTarget. This tool uses various databases of transcription factor binding motifs, such as TRANSFAC, Fly Factor Survey, and JASPAR and allows cross-species search for motifs. The output contains clusters of predicted motifs that are ranked according to a normalized enrichment score (NES). As suggested (Herrmann *et al.*, 2012), we set the threshold for NES as greater than 2.5.

This motif search yielded various motif clusters including several position weight matrices (PWMs) with similar sequences, derived from different motif databases. For each motif, i-cisTarget reveals predicted transcription factors. The first three motifs from each gene-set and predicted TFs are shown in Table 4.6. The confidence level of a predicted motif and its related putative transcription factor is directly proportional to direct interaction of the TF with the motif and conservation level of the region (Herrmann *et al.*, 2012).

Table 4.6. Enriched motifs among DE genes in R3/R4 PRs and putative TFs that bind them.

Gene Set	Motif Cluster	PWM Ranking	TF	NES	PWM ID	PWM Logo
Up-regulated genes	1	2	Trl	5.035	flyfactorsurvey- Trl_FlyReg_FBgn0013263	
	2	11	Jim	4.028	flyfactorsurvey- jim_SANGER_2.5_FBgn0027339	

Table 4.6. Enriched motifs among DE genes in R3/R4 PRs and putative TFs that bind them (cont.)

Up-regulated genes	3		Grh	3.430	transfac_pro-M00951	
Down-regulated genes	2	2	Dref	6.452	elemento-TATCGATA	
	3	10	Crp	4.827	flyfactorsurvey-crp_SANGER_10_FBgn0001994	
	4	135	CG7928	2.573	flyfactorsurvey-CG7928_SOLEXA_5_FBgn0039740	
All differentially expressed genes	1	1	Trl	5.074	flyfactorsurvey-Trl_FlyReg_FBgn0013263	
	2	11	Grh	4.283	transfac_pro-M00951	
	3	22	Crp	3.416	flyfactorsurvey-crp_SANGER_10_FBgn0001994	

The predicted TFs Trithorax-like (Trl), Jim, Grainy head (Grh) and DNA replication-related element-binding, are known to be involved in gene regulation processes during *Drosophila* eye development (Dos-Santos *et al.*, 2008; Farkas *et al.*, 1994; Gambis *et al.*, 2011; Hirose *et al.*, 2001; Matsukage, 1995; Mukherjee *et al.*, 2006). Additionally, in the enhancer-trap screen that was performed in our lab, the expression pattern of Cropped in R3/R4 PRs was shown. The only TF we do not have any information about its expression

in the *Drosophila* eye is CG7928. Overall, these predicted TFs were considered as promising candidates that may be regulating the transcription of DE genes in R3/R4.

4.6.6. Enlightening the Transcription Factor-Targetome Network of R3/R4

In order to get a better understanding of genetic regulatory networks (GRN) involved in R3/R4 specification, we used GRN prediction data, based on 72 RNA-Seq experiments including *sNPF*-positive versus *chp*-negative differential expression analysis.

The GRN predictions were done for eye development in 3rd instar larvae by using network interference challenges and analyzing *cis*-regulatory regions. In this way, the expression profile of each given gene is predicted according to the profiles of other input genes by applying tree-based ensemble methods. As a result, co-expressed and anti-expressed gene clusters were obtained and further analyzed to find co-regulated groups among them. For this purpose, iRegulon was used to check if there are over-represented *cis*-regulatory sequences and putative regulators for subgroups of genes. As a result, 241 TFs with 5667 putative target genes were identified and among these the Glass-binding motif was ranked first with a high enrichment score (NES=6.3). As mentioned before, *glass* is one of the early expressed master regulators of eye development and regulates the development of PR cells. Moreover, the TFs related with other high ranked motifs, Pointed and Lozenge, are well known for having a role in eye development. All the evidence suggests that the data are robust and appropriate to study interactions between predicted TFs and their target genes.

In order to select a TF targetome of interest, clustering was performed for the predictions and this resulted in 9 sub-networks of several regulatory mechanisms including PR differentiation posterior to the morphogenetic furrow. From this sub-network, we selected the Svp targetome, since it is known to be necessary for R3/R4 specification as well as R1/R6 specification. The enriched motif that iRegulon predicted as Svp-binding region was from the JASPAR database (Figure 4.18).

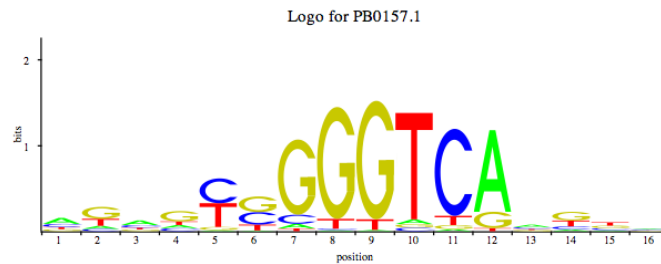


Figure 4.18. Enriched TF binding motif associated with Svp. Motif ID: jaspar-PB0157.1, NES=2.91.

Moreover, the predicted Svp target genes were grouped according to their biological meanings. This allowed us to deduce the significance level of the predictions. Fortunately, we captured many GO terms related with eye development, including establishment of ommatidial planar polarity, R3/R4 cell fate commitment, homophilic and heterophilic cell-cell adhesion terms (Figure 4.19A). The GO terms associated with molecular function were also interesting as they refer to TF activity, cytoskeletal and cell adhesion molecule binding (Figure 4.19B). Consistently, the cellular compartments that were detected in the GO analyses were nucleus, plasma membrane, apical cortex, and adherens junctions (Figure 4.19C).

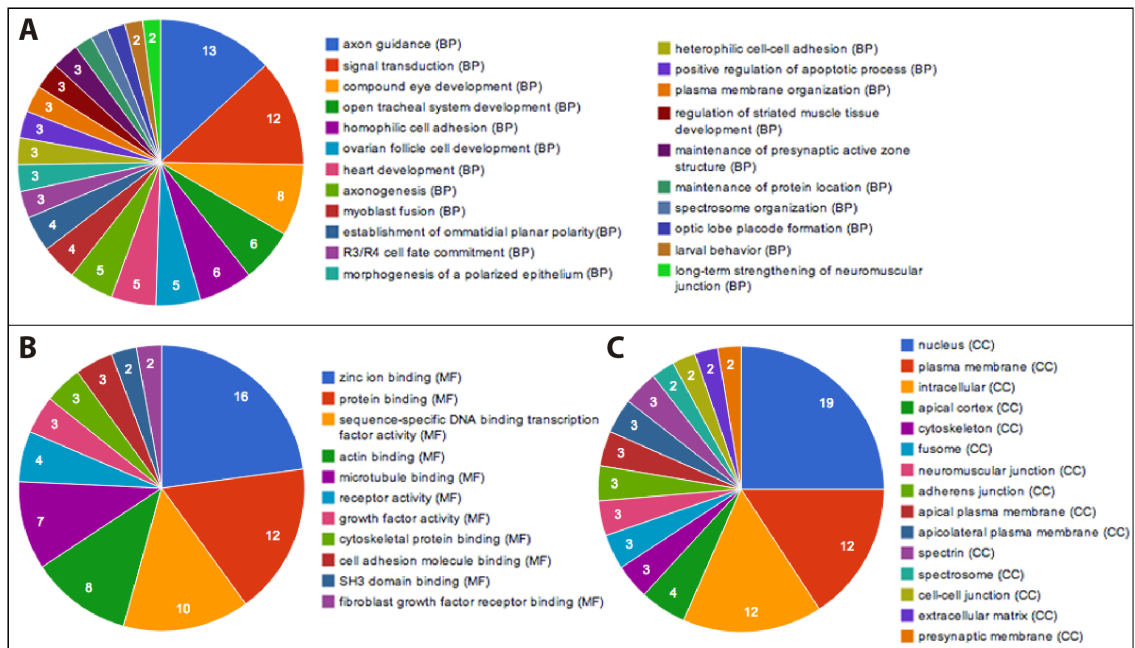


Figure 4.19. GO analyses of the Svp predicted target genes. Number of genes per GO term associated with biological process (A), molecular function (B), and cellular compartment (C) are color-coded (adjusted p value ≤ 0.05).

4.6.7. Validation of the Predicted Target Genes of Svp

From the Svp targetome, we selected several candidate genes by eliminating the ones for which antibodies are not available. Therefore, *couch potato (cpo)*, *futsch*, *bruchpilot (brp)*, and *pebbled (peb, a.k.a hindsight/hnt)* were selected. In order to validate the interaction between Svp and its putative target genes, we generated *svp* null mutant clones in the 3rd instar larval eye disc and examined the expression levels in mutant and wild type areas through antibody stainings.

At first, we analyzed the expression level changes of *salm*, which is one of the known Svp target genes, in *svp*⁻ mosaic eye discs. Since the interaction between *svp* and *salm* was already shown (Domingos *et al.*, 2004), our aim was to control if we can successfully generate mosaic eyes and are able to recapitulate these published results in our hands. In wild type eyes, Spalt expression starts around the third row and induces *svp* expression in R3/R4 PRs. This results in repression of *salm* by Svp in this cell pair, starting from row seven (Domingos *et al.*, 2004). Therefore, lack of Svp results in de-repression of Salm. Consistently, Figure 4.21 shows that Salm expression is not down-regulated after row seven in *svp* mutant clones. This experiment showed that we were able to generate *svp*⁻ mosaics in the eye discs.

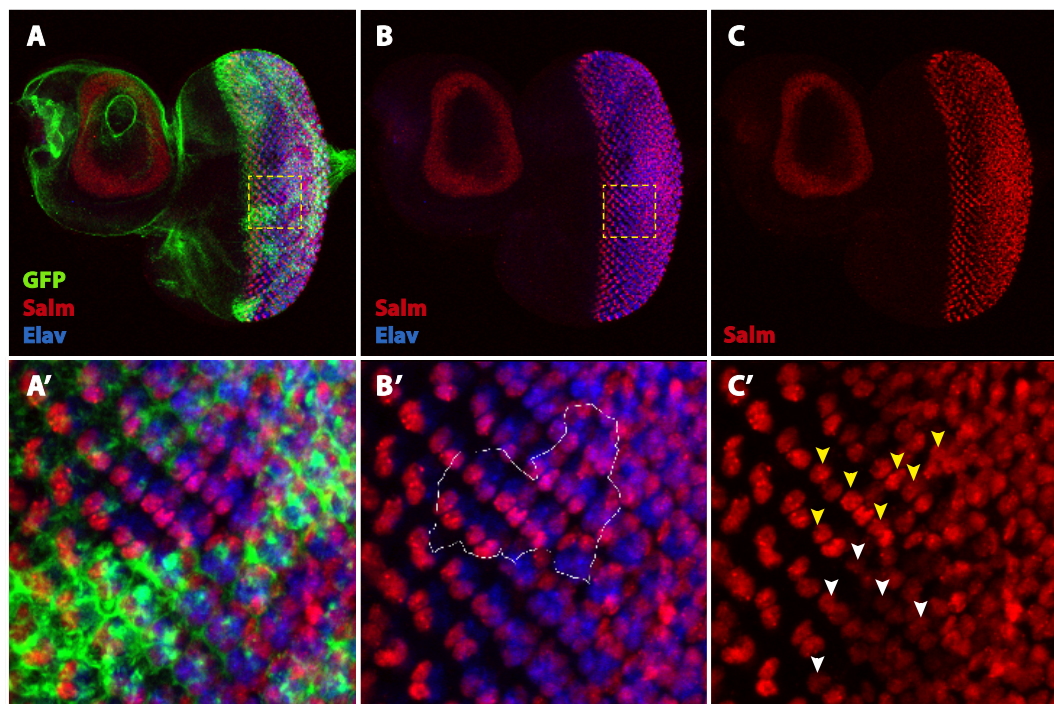


Figure 4.21. The Svp -Salm interaction in R3/R4 PRs was recapitulated. *svp* null mutant clones were generated in the 3rd instar larval eye discs and marked by the absence of GFP. Immunostainings were performed with antibodies against GFP (green; A, A'), Salm (C, C'), and Elav (blue). In the wt area (B') Salm levels decrease after row seven (C'), whereas in *svp* null mutant clones (inside the white lines in B') Salm does not fade away (C').

4.6.7.1. Selected candidate: *couch potato*. One of the predicted targets of Svp is couch potato. According to the sequence similarity Cpo is predicted to be a mRNA binding protein and in the embryonic stage, it localizes to the nuclei of neural precursor cells (Bellen *et al.*, 1992). A role in eye development has not been reported so far; however, its expression posterior to the MF in the 3rd instar larval eye disc was previously shown by LacZ staining (Bellen *et al.*, 1992).

As shown in Figure 4.22, Cpo localizes to the nuclei of PR cells in the 3rd instar larval eye disc. Its expression pattern appears to be quite homogenous through the eye disc posterior to the MF.

Since it was predicted as a Svp target gene, we expected a difference in its expression level in R3/R4 cells in the *svp* mutant clones compared to wild type PRs. However, no change in expression level was observed in Svp mutant clones (Figure 4.23).

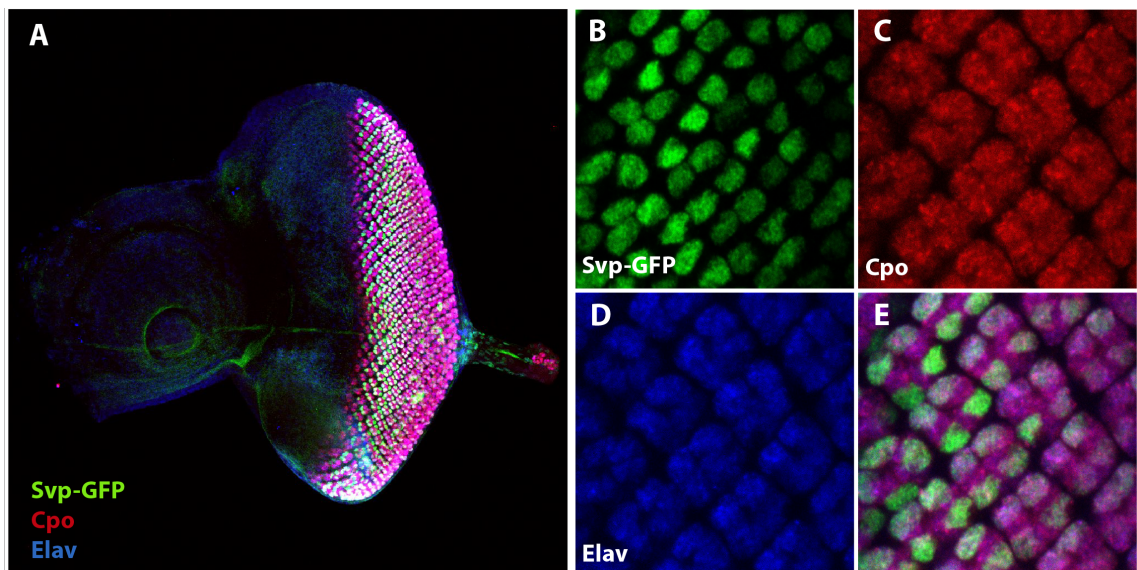


Figure 4.22. Cpo displays a homogenous expression pattern through all PRs in the 3rd instar larval eye disc. Immunostainings were performed on Svp-GFP line with antibodies against GFP (B), Cpo (C), and Elav (D). Magnified view of the dorsal part (B-E). GFP expression driven by *svp*, represents R1/R6 and R3/R4 PRs (B). Cpo (C), and neuronal marker Elav (D) colocalize in all PRs, not specifically in R3/R4 (E).

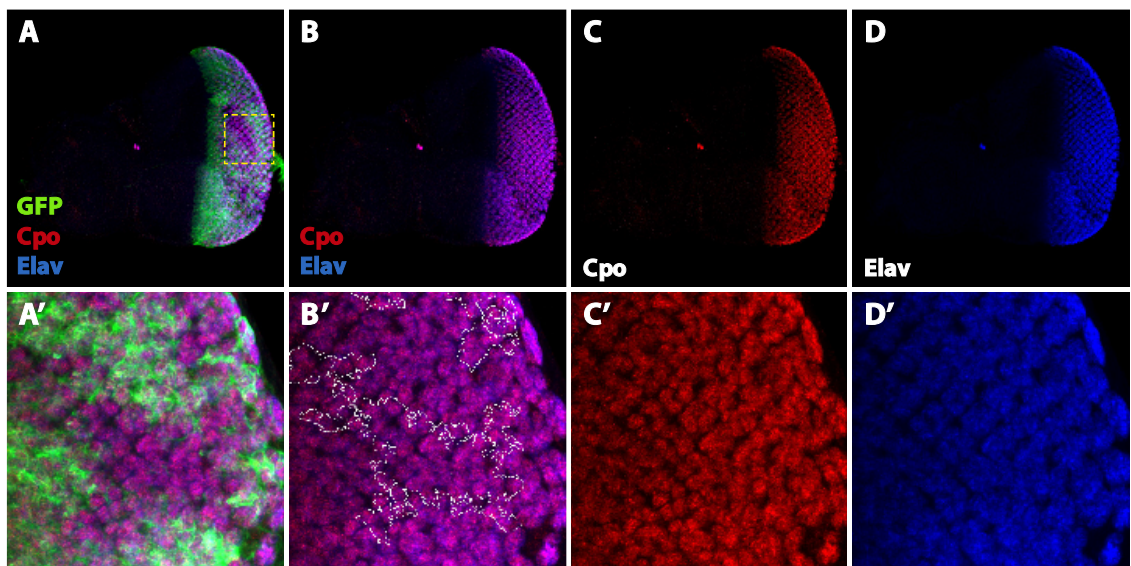


Figure 4.23. Svp does not affect the expression of Cpo. *svp* null mutant clones were generated in the 3rd instar larval eye discs and marked by the absence of GFP. Immunostainings were performed with antibodies against GFP (green; A, A'), Cpo (C, C'), and Elav (D, D'). Cpo levels do not change in *svp* clones (inside the white lines) compared to the wild-type area (B').

4.6.7.2. Selected candidate: *futsch*. The second candidate gene to be validated was a microtubule-associated protein encoding the gene *futsch*. It is known to have a role in axonal and dendritic growth processes (Hummel *et al.*, 2000). Futsch was localized to the developing axons throughout the eye disc and additionally, around the nuclei of PRs (Figure 4.24). This localization was expected to be difficult to evaluate visually, unless a very significant change would be encountered.

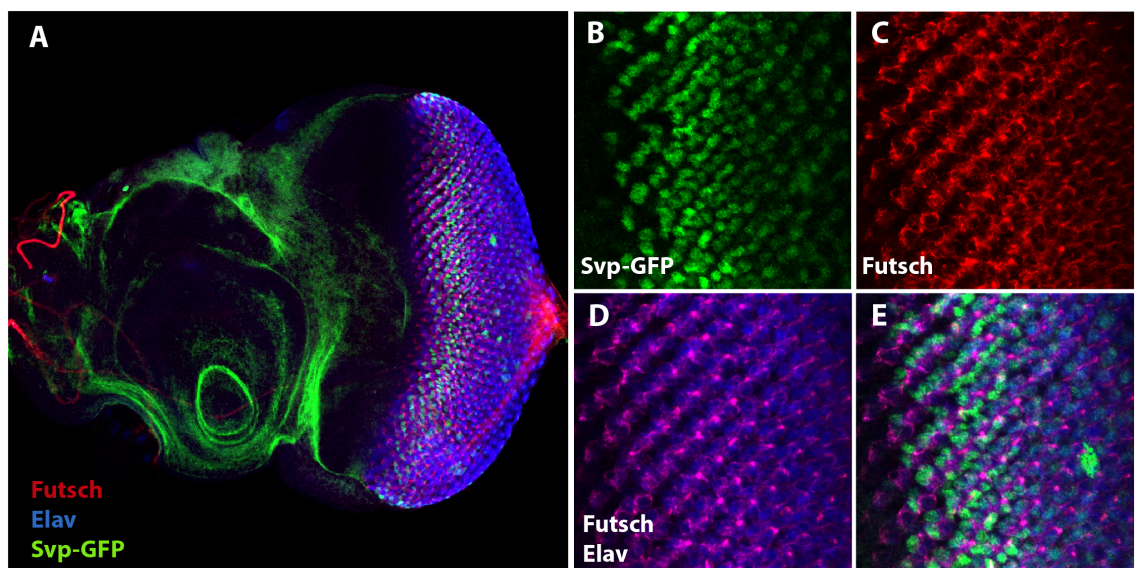


Figure 4.24. Futsch localizes to the developing axons and around the nuclei of PRs in the 3rd instar larval eye disc. Immunostainings were performed on Svp-GFP line with antibodies against GFP (B), Futsch (C), and Elav. Magnified view taken from the dorsal part (B-E). GFP expression driven by *svp*, represents R1/R6 and R3/R4 PRs (B). *futsch* might be expressed in all PRs (D), not specifically in R3/R4 (D).

As can be seen in anti-Futsch stainings in *svp* mutant clones, no change in Futsch levels was observed in the clonal area when compared to the wild type region (Figure 4.25). As expected from the wild-type staining the evaluation was difficult and a slight change in expression level cannot be excluded for sure.

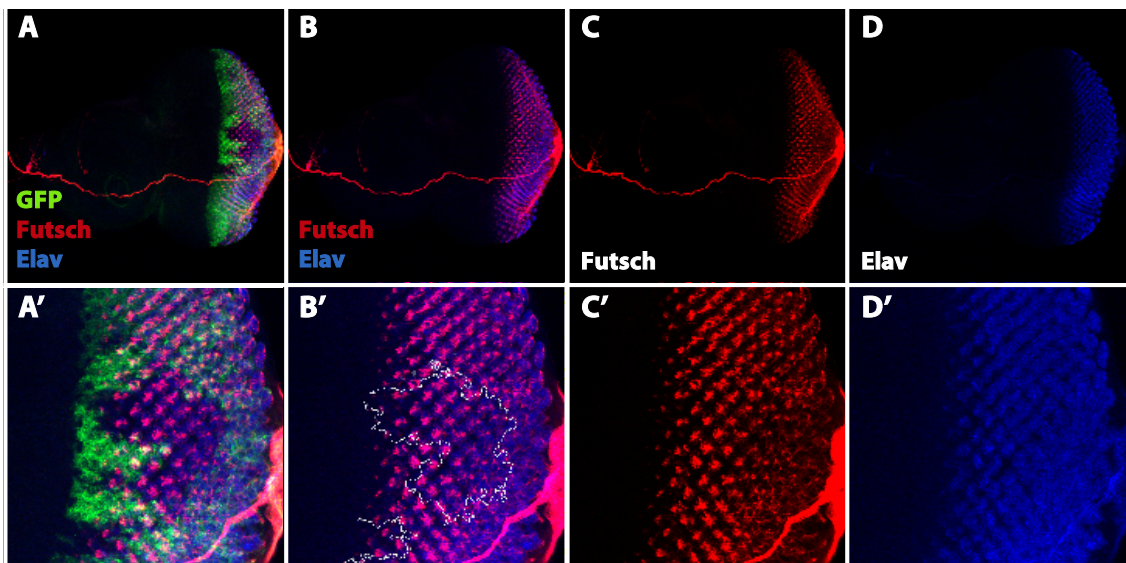


Figure 4.25. Svp does not affect the expression of Futsch. *svp* null mutant clones were generated in 3rd instar larval eye discs and marked by the absence of GFP.

Immunostainings were performed with antibodies against GFP (green; A, A'), Futsch (C, C'), and Elav (D, D'). Futsch levels do not change in *svp* clones (inside the white lines) compared to the wild-type area (B').

4.6.7.3. Selected candidate: *bruchpilot*. Another predicted candidate Svp to target gene was *bruchpilot*, which has been reported to have a role in synaptic transmission. Besides its localization at presynaptic active zones, it is thought to be involved in cytoskeletal organization as it has structural similarities with cytoskeletal proteins (Wagh *et al.*, 2006).

The localization of Brp was analyzed in 3rd instar larval eye discs using an antibody against Brp. As can be observed in Figure 4.26, it colocalizes with Elav in the nuclei of all PRs. We did not observe any difference in R3/R4 PRs in terms of Brp expression.

In *svp* mutant mosaic eye discs, the localization and level of expression of Brp did not appear as changed when compared to the wild type areas (Figure 4.27). Therefore, it seemed not to be affected by the *svp* mutation in the eye.

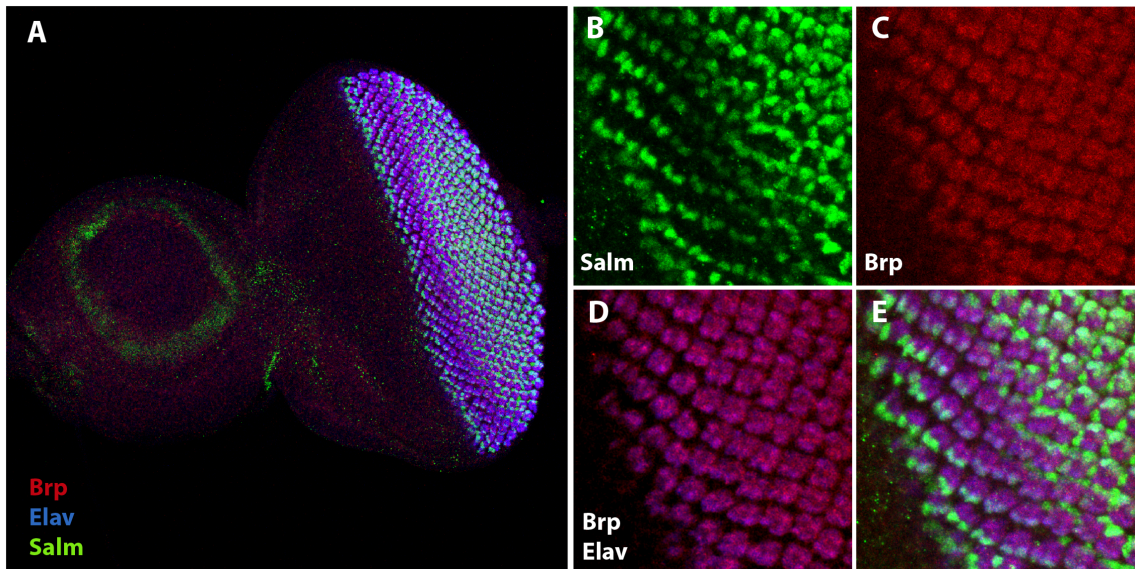


Figure 4.26. Brp displays a homogenous expression pattern through all PRs in the 3rd instar larval eye disc. Immunostainings were performed on wild-type eye-antennal discs with antibodies against Salm (B), Brp (C), and Elav. Magnified view taken from the ventral part (B-E). Salm marks only R3/R4 PRs in first seven rows (B). Brp (C), and neuronal marker Elav colocalize in all PRs (D) not specifically in R3/R4 (E).

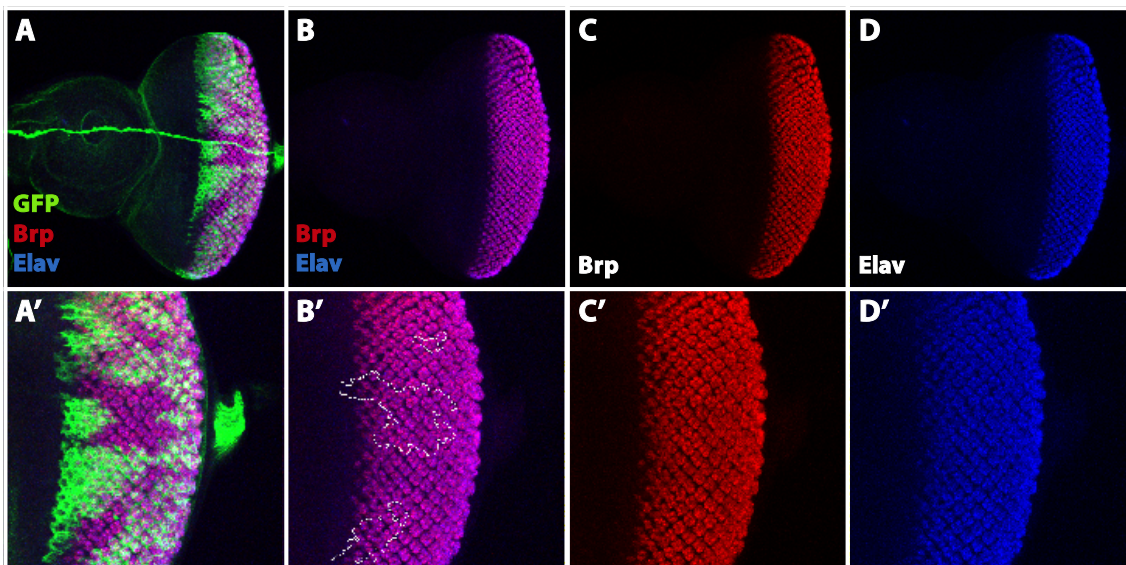


Figure 4.27. *Svp* does not affect the expression of Brp. *svp* null mutant clones were generated in the 3rd instar larval eye discs and marked by the absence of GFP. Immunostainings were performed with antibodies against GFP (green; A, A'), Brp (C, C'), and Elav (D, D'). Brp levels do not change in *svp* clones (inside the white lines) compared to the wild-type area (B'). Magnified view of the clones (A'-D').

4.6.7.4. Selected candidate: *pebbled*. The last candidate we examined was *pebbled* (a.k.a *hindsight*). Its expression in all PRs has been previously reported; it is also known that Peb levels are slightly higher in R3/R4 cells from row two to six (Pickup *et al.*, 2002). We also detected higher Peb expression in R3/R4 PRs (Figure 4.28C, D).

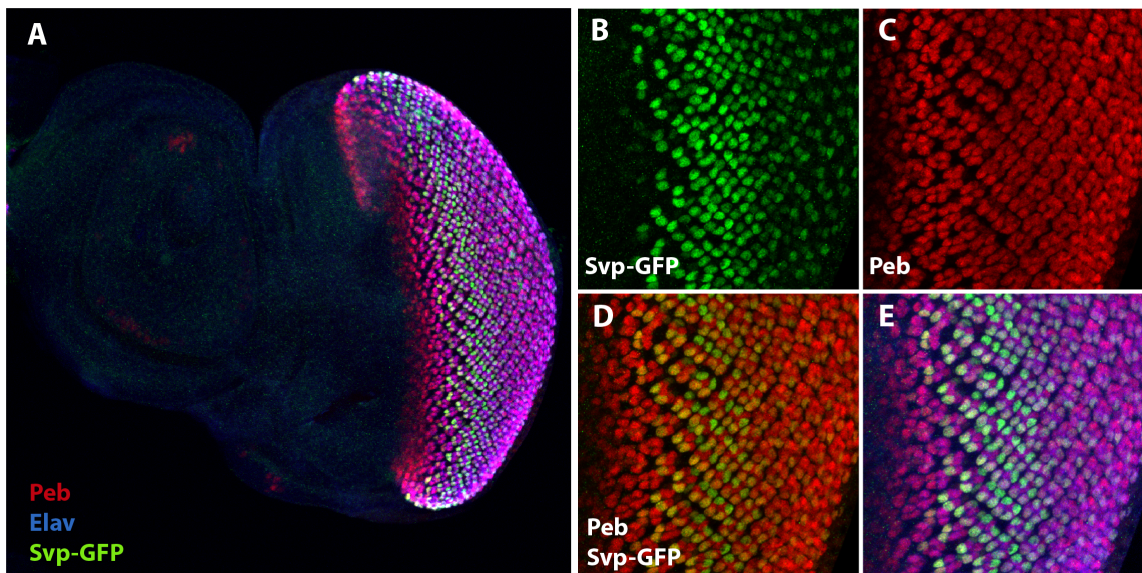


Figure 4.28. Peb is expressed in all PRs in the 3rd instar larval eye disc. Immunostainings were performed on Svp-GFP line with antibodies against GFP (B), Peb (C), and Elav. Magnified view taken from the ventral part (B-E). GFP driven by *svp*, represents R1/R6 and R3/R4 PRs (B). Peb (C) expression slightly increases in R3/R4 from around row two to six (D). Peb and neuronal marker Elav colocalize in all PRs (E).

In *svp* mutant PRs, *peb* expression levels did not change drastically; however, in the mutant area, a slight decrease in R3/R4 cells was apparent (Figure 4.29). Thus, we aimed to examine the expression levels of Peb in *svp* mutant and wild type R3/R4 cells by detecting R3/R4 with anti-Salm (Figure 4.30).

However, it was difficult to analyse the expression pattern because of the small sizes of the clones and disruptions in ommatidial preclusters. Thus, to be more confident with this result the number of clones and immunostainings has to be increased.

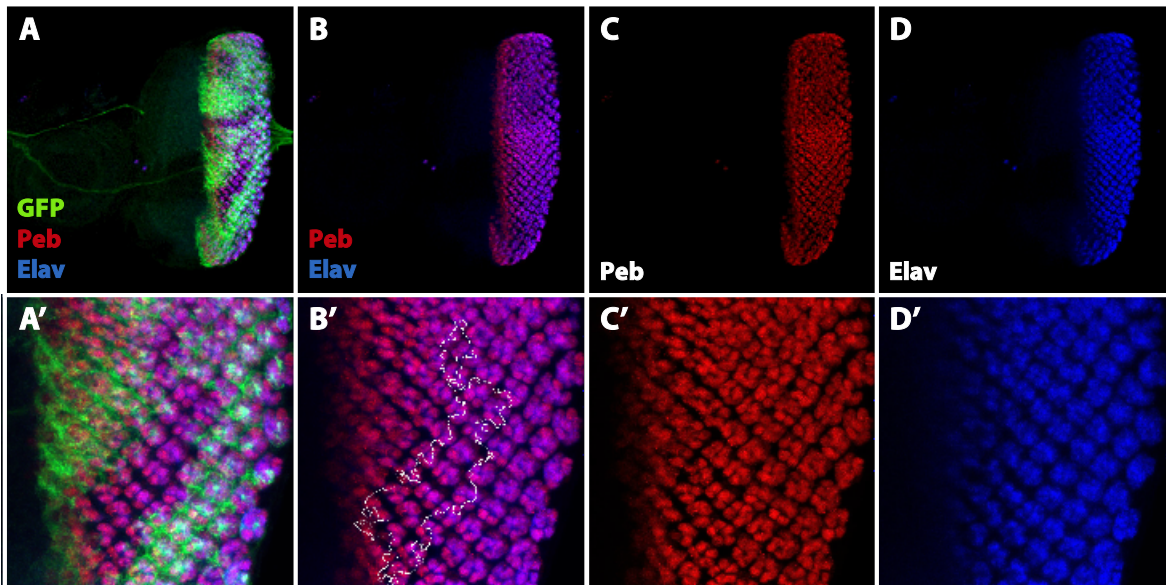


Figure 4.29. *Svp* might be affecting the expression of *Peb*. *svp* null mutant clones were generated in the 3rd instar larval eye discs and marked by the absence of GFP. Immunostainings were performed with antibodies against GFP (green; A, A'), *Peb* (C, C'), and *Elav* (D, D'). Normally, from row two to six *Peb* levels are higher in R3/R4 compared to the other PRs, which is not observed in the *svp* mutant clones (B').

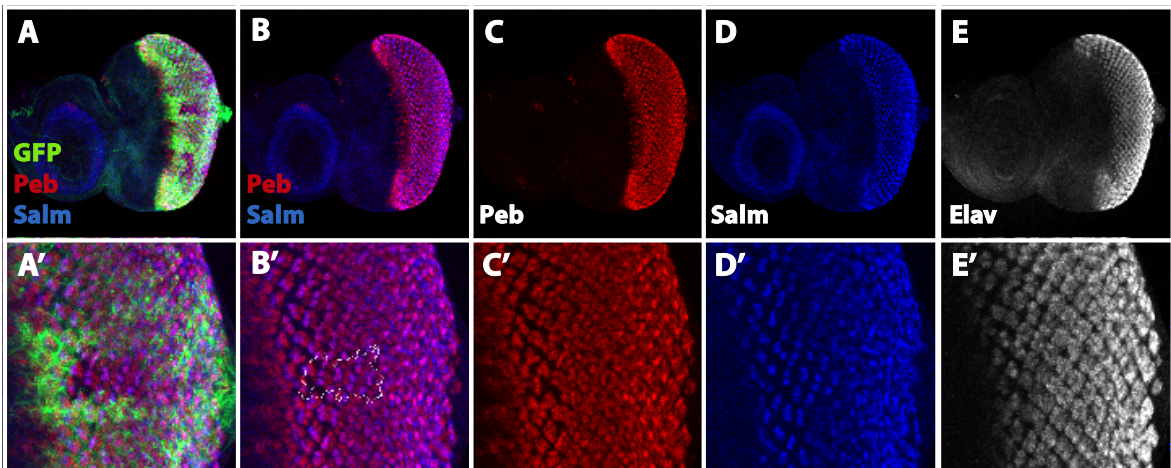


Figure 4.30. Examination of *Peb* expression in mosaic eye disc by quadruple staining. *svp* null mutant clones were generated in the 3rd instar larval eye discs and marked by the absence of GFP. Immunostainings were performed with antibodies against GFP (green; A, A'), *Peb* (C, C'), *Salm* (D, D') and *Elav* (E, E'). Small-sized clones did not allow evaluating a slight change in R3/R4 (inside the white lines, B').

5. DISCUSSION

Understanding of the mechanisms through which cells align in a precise polarized pattern along tissues is an intriguing topic in developmental biology. So far, several signalling pathways and genes have been associated with this type of cellular organization, namely planar cell polarization. However, we still do not know the whole repertoire of players whose identification will provide a complete understanding of the mechanisms involved as well as their interactions. The *Drosophila* eye represents an excellent model to study planar cell polarization as its ~800 ommatidia properly align through this mechanism.

PCP establishment in the fly eye is achieved by accomplishing two aspects: chirality establishment and rotation of PR clusters. The first one is directly linked to the specification of the R3/R4 PR pair and precedes the latter aspect, ommatidial rotation, and usually affects its direction. In R3/R4 precursors, asymmetric localization of particular membrane-bound receptors, cell-adhesion molecules, and cytoplasmic proteins enables cells to interpret polarization signals and direct adhesion dynamics between cells to establish planar cell polarity. The asymmetric localization is accompanied by specification of R3/R4 PRs, which is regulated by cell-type specific transcription factors (reviewed in Mlodzik, 2005). So far, only two TFs, Seven-up (Mlodzik *et al.*, 1990) and Spalt (Domingos *et al.*, 2004), are identified as regulators of this specification process; however, their direct targets and the subsequent regulatory mechanisms have not been elucidated yet.

Therefore, we aimed to expand the knowledge of PCP-associated genes by following two approaches considering the importance of R3/R4 PRs in planar cell polarization. In the first part, as a follow-up of a study performed in our lab we did loss of function analyses for genes that were identified as R3/R4-specific (Öztürk, 2010). In the second part, we took an unbiased approach and performed RNA-Seq on R3/R4 cells to find DE genes, which might be associated with PCP establishment in the eye. We used this dataset to predict transcription factors that might be regulating the expression of the DE genes in R3/R4 PRs. Additionally, we utilized the data of the predicted targetome of Svp TF. Since

Svp might be targeting genes involved in PCP, we tried to validate the relationship between Svp and its putative target genes.

5.1. Correlating R3/R4 Specific Genes to Planar Cell Polarity Establishment

A previously performed enhancer-trap screen has yielded several lines with R3/R4-specific expression. However, since enhancer-trap lines might not be representing the exact expression pattern of the genes in which they are inserted, we looked for antibodies against them to confirm the R3/R4-specific expression patterns. Unfortunately, the only candidate having a commercially available antibody against it was Headcase. After immunostainings, it turned out that *headcase* is expressed in R3/R4; however, is not specifically expressed in this cell pair. These discrepancies in expression might be due to disruption of possible proximal enhancers of *headcase* or because the minimal promoter only captures a partial enhancer.. Another explanation could be that the enhancer regulates another gene, eg. *CG18404*, located upstream of *hdc*, and the expression pattern that we observe corresponds to this gene.

In the other enhancer trap lines *piggyBac* element insertions were in the genes encoding cell-adhesion molecules, an endopeptidase, transcription factors or unknown molecules. Thus, they could be involved in different steps of planar cell polarization.

In order to investigate if these candidate genes have a role in PCP establishment, we down-regulated these by RNAi and examined possible PCP defects. Since chirality establishment is evident in mature ommatidia, we analyzed chirality and consequent ommatidial rotation in the adult eye. The analyses revealed two genes as possible candidates of PCP establishment: *polychaetoid* and *faint sausage*. Although we focused on the latter because of its novelty, *pyd* is also a promising candidate.

Pyd is the homologue of mammalian Zona occludens 1 (ZO-1) protein and localizes at adherens junctions. It has been shown that this protein could interact with Canoe, which is the *Drosophila* homologue of the mammalian adaptor protein Afadin (AF6). As a

component of the Jun N-terminal kinase (JNK) signalling pathway, this complex might be regulating actin dynamics in cells (Takahashi *et al.*, 1998). Furthermore, in the pupal retina, Pyd functions in cell-cell adhesions to acquire the precise pattern of cone cells and interommatidial cells (Seppa *et al.*, 2008). Since reduced levels of Pyd resulted in ommatidial misrotation while not affecting chirality, we concluded that Pyd is not affecting R3/R4 cell fate choice; however, it is likely that it contributes to ommatidial rotation by regulating cell-cell adhesion dynamics and cytoskeletal arrangements. Alternatively, we thought that, Pyd might not be a major regulator of cell adhesion dynamics in the larval stage; however, its absence in the pupal stage might disrupt PCP, which has already been correctly determined in the larval stage, because of the misalignments of the supporting cells. To examine the validity of this hypothesis, firstly, one should show the expression pattern of *pyd* in the 3rd instar larval eye discs by performing immunostainings with cell-type specific markers, such as Svp for R3/R4, m δ -LacZ for R4, and Elav for all PRs. Then, performing similar immunostainings on the *pyd* mutant eye discs would help to understand if R3/R4 specification and ommatidial rotation can be achieved correctly in the larval stage. If so, the hypothesis could still be valid and additional stainings on tangential sections of *pyd* mutant adult eyes can help to understand whether rotation-defective ommatidia have also abnormally organized accessory cells or not.

The other promising candidate gene was *faint sausage*, which encodes a cell-adhesion protein of the immunoglobulin superfamily (IgSF). Predictions of its structure have shown that Fas has five Ig domains and a glycosylphosphatidylinositol (GPI) anchor (Lekven *et al.*, 1998; Vogel *et al.*, 2003) or a transmembrane helix (TMH) (Özkan *et al.*, 2013). In addition to these predictions, we checked the aminoacid sequence using the MisPred tool, which has been developed to detect conflicts in predictions and decrease the number of mispredicted proteins in the literature (Nagy *et al.*, 2008; Nagy and Patthy, 2013). It revealed one GPI and one TMH domain without any conflict. Moreover, in the study of Lekven *et al.*, it was claimed that results of PIPLC treatments to cleave GPI sites support the idea that Fas has a GPI anchor. Additionally, they show that Fas localizes to the membranes of neural cells (1998). Considering all of this information, we concluded that the extracellular protein Fas might be anchored to the membrane in two different ways according to its function in the cell that it exists. In both forms it might be establishing homophilic or heterophilic interactions between cells and thus, contributing to pattern

formation in several tissues including the eye. This is consistent with its role in embryonic nervous system development of *Drosophila* as it participates in nerve cell migration and axonal pathfinding (Lekven *et al.*, 1998) as well as heart development of *Drosophila* where it provides proper cardioblast alignment by arranging cell adhesion dynamics (Haag *et al.*, 1999).

In our experiments, downregulation of *fas* in the *Drosophila* eye resulted in two important planar cell polarity defects: misrotated ommatidia with correct or wrong chirality (R4/R4 symmetry). Ommatidial rotation defects have also been observed in heterozygous mutants of *fas*¹, and *fas*⁰⁵⁴⁸⁸. In flies in which *fas* was downregulated by RNAi, the degree of rotation was more than 90, while it was variable in flies having one copy of the null allele. Therefore, we suspected a dose-sensitive effect of *fas* on ommatidial rotation. To test this hypothesis, in different backgrounds (*fas* overexpression and heterozygous mutant backgrounds) a dominant negative construct of *fas* can be overexpressed by using an appropriate driver, such as *sevenless* or *seven-up*. This commonly used approach can provide a better understanding of the dosage-sensitive effect of *fas* in the ommatidial rotation process. However, this hypothesis could not be tested in the framework of this thesis since an overexpression construct for *fas* was not available.

The way Fas affects ommatidial rotation is possibly related with its cell adhesive property. As a supportive example, cell adhesion molecules DE- and DN-cadherins are known to be involved in the ommatidial rotation process in the *Drosophila* eye by arranging the rate of PR cell movement. Their localization at the membranes of PR precursors complements each other and the balance between the adhesive forces that they generate determines the degree of rotation (Mirkovic and Mlodzik, 2006). Therefore, Fas might be a part of cell adhesion dynamics by localizing to the cell membranes and providing interactions with neighboring cells. Inferring from the RNAi downregulation results, its effect might be restricted to rotation. Expression patterns generated by the enhancer-trap line and LacZ line support an expression of *fas* to R3 and R4 PRs; however, this idea is open to speculations until expression is verified with anti-Fas antibody (unavailable) stainings or *fas in situ* hybridization.

Homology analysis provided us to gain an evolutionary insight into the function of Fas. According to the DRSC integrative ortholog prediction tool, *fas* might be orthologous to human Nectin-3 encoding *poliovirus receptor related 3 (PVRL3)* gene. Loss of *PVRL3* in humans was reported as a possible reason for human ocular defects, since it results in disturbed adherens junctions between lens-forming epithelial cells (Lachke *et al.*, 2012). Nectins are cell adhesion molecules that can establish homophilic and heterophilic interactions. They interact with Afadin adaptor proteins, which link them to the actin cytoskeleton. So far, there is no nectin homologue reported in *Drosophila*; however, there is an afadin orthologous protein, Canoe, which interacts with the transmembrane protein Echinoid. We thought that Fas might be a protein that functions like nectins, which are also reported as being involved in PCP establishment. For instance, in the mouse inner ear, sensory hair cells and supporting cells are aligned in a checkerboard-like pattern to establish planar cell polarity (Sipe *et al.*, 2013). This pattern formation, which is necessary for normal hearing, is assessed via nectin-mediated adherens junctions between sensory hair cells and supporting cells (Togashi *et al.*, 2011).

Additionally, reduced levels of Fas resulted in a symmetric ommatidia phenotype (R4/R4). This phenotype could be caused by failure of cells to adopt the R3 fate and their specification as R4. Since Fz/PCP pathway is known to be necessary for this cell fate choice (Zheng *et al.*, 1995), we suspected that Fas might be participating in this signalling pathway either by interacting with one of the components or facilitating signal propagation by keeping cells close to each other.

To be able to decipher the function of Fas, it is important to understand if it interacts homophilically with another Fas protein or heterophilically with other molecules. In a recent study to identify the interactome of extracellular Ig, FnIII, and LRR family proteins, Fas has not been reported to establish any homophilic or heterophilic interactions with the proteins in that study (Özkan *et al.*, 2013). However, considering that this study has failed to detect several known interactions, the trustworthiness of this study has been questioned. Another possibility would be that Fas might be undergoing weak interactions with its partner. This prediction would be consistent with the prediction of its orthologue, Nectin-3, which undergoes weaker interactions than cadherins (Rikitake *et al.*, 2012). The study did not include Fz, Fmi/Stan and Stbm/Vang, which are the transmembrane proteins

that have a role in PCP establishment in the eye. Therefore, they can be considered as candidates for Fas interaction. Elucidation of such an interaction would help to elucidate the Fas signalling pathway.

Considering the predicted structure of the Fas protein, which lacks an intracellular domain, we thought that its contribution to a signalling pathway might be through interaction with a membrane bound receptor as a ligand. Such an interaction between Fz and Stbm/Vang in PCP establishment has been shown in the *Drosophila* eye (Wu and Mlodzik, 2008). The candidate membrane receptors of PCP signalling are the seven-pass TM protein Fz, the four-pass TM protein Stbm/Vang or the atypical cadherin Fmi/Stan. Another possibility is that Fas might be facilitating ligand binding to one of these receptors or increasing its stability on the membrane. For instance, during gastrulation in vertebrates, Fz/PCP signalling has a role in convergent extension and in zebrafish, the membrane-bound Knypek molecule mediates convergent extension by interacting with Fz and its ligand Wnt11. In this way, it facilitates receptor-ligand binding and thus signal transduction (Topczewski *et al.*, 2001). It is known that Fz/PCP signalling is also crucial for R3/R4 specification and PCP establishment in the *Drosophila* eye (Fanto *et al.*, 1998; Zheng *et al.*, 1995). Since Fz receptors have been associated with Wnt ligands, we thought that such an interaction could occur between Fz, Fas, and a possible Wnt ligand. Therefore, Fas might be facilitating Fz/PCP signalling in R3/R4 PR cells. Unfortunately, due to the lack of a Fas antibody such direct interactions could not be tested.

As mentioned before, in the heterozygous *fas*⁰⁵⁴⁸⁸ mutants, ommatidia had a lower number of outer PRs than the wild type. Some of these clusters were marked as misrotated; however, this might be a misinterpretation. Since the arrows to represent polarity have been drawn based on the location of the possible R3 PR, we might have been mistaken about showing the polarity when there is a Rh1 expression problem. By considering that there were ommatidia that adopted the correct polarity, while reflecting low Rh1-GFP signal in one of their rhabdomeres, we thought that in those presumptive PCP-defective five-cell clusters there might be a sixth PR (possibly R6), which is not able to express Rh1. In order to understand if there are missing outer PRs in those clusters and if there is an ommatidial rotation defect, plastic tangential sectioning of the adult eye should be performed. Moreover, not always in the ommatidia reflecting low Rh1-GFP signal, but in

some PR clusters we detected a GFP signal at the core of the ommatidia. It is also not clear if this is due to a technical problem or a PR expressing a low amount of Rh1. To be able to find an answer, Rh1 antibody stainings should be done for this mutant line.

In conclusion, our study lays the groundwork for further experiments; we came up with several ideas about the possible function of the cell-adhesion molecule Fas in PCP establishment in the fly eye and discussed the experiments that can be performed to test these hypotheses. Although the RNAi line that we used was reported as having no off-targets, a recent study revealed that even without using a driver, these lines might give phenotypes (Green *et al.*, 2014). Therefore, as a first step, whole eye mutants should be generated by using the prepared FRT recombined lines and eyes should be examined via plastic sectioning and anti-Rh1 and phalloidin immunostainings. Afterwards, *fas* expression pattern should be shown either by using an antibody against it or by tagging the protein to see its endogenous localization in all developmental stages. Additionally, in order to understand if it has an autonomous or non-autonomous effect, clonal analyses can be performed. Moreover, epistasis analyses should be expanded using several mutant lines of PCP signalling pathway components. Furthermore, performing binding assays like yeast two-hybrid screening or co-immunoprecipitation can be useful to identify its binding partners.

5.2. Transcriptome Analysis of R3/R4 Cells

It is known that PR clusters require accurately specified R3/R4 cells to adopt correct polarization. However, there are not many genes correlated with R3/R4 specification, therefore, we aimed to identify genes involved in this specification process, which are possibly expressed differentially in R3/R4 PRs. In order to acquire the set of DE genes in R3/R4 cells, we combined FACS with high throughput RNA sequencing.

5.2.1. Sorting of R3/R4 PRs by FACS

The demand to obtain cell type specific gene expression profiles by using high throughput methodologies generated a need to isolate specific cells in massive amounts.

FACS is one of the methodologies that allow scientists to extract particular cells from hundreds of dissociated cells from tissues. Although the use of FACS in the *Drosophila* studies is not as common as in the mammalian studies, it has been used to sort several *Drosophila* cells, such as wing imaginal disc cells (Neufeld *et al.*, 1998), hemocytes (Tirouvanziam *et al.*, 2004), neural stem cells (Berger *et al.*, 2012; Harzer *et al.*, 2013), and intestinal stem cells (Amcheslavsky *et al.*, 2011). We also made use of this powerful technique to isolate R3/R4 cells from the eye-antennal imaginal discs of third instar larvae.

Compared to the total number of the isolated cells, we could capture ~25% of the expected number of R3/R4 cells by FACS. The number of cells that we isolated (9.722) was enough to continue with; however, increasing the amount of the starting material would yield higher efficiency in the following experiments. Therefore, a better optimization of the cell sorting protocol is required.

In a successful cell sorting experiment, most of the cells should stay viable throughout the process. A low number of isolated cells might be caused by loss of cell viability. In order to avoid cell death, we have performed dissections as fast as possible and put the tissues in a special insect medium. Decreasing the time for this step by increasing the number of persons that dissect the tissues simultaneously might provide better results in the end. As an alternative to dissection, a recently published large-scale tissue isolation method, which is suitable to combine with FACS could be tried. This method requires a fluorescent label for the tissues of interest to separate them from the other imaginal discs. As a first step, larvae are collected and gently disrupted, then tissues are resolved by applying density gradient centrifugation on a Ficoll[®] gradient. Finally, the fluorescently-labelled tissues are separated from the other components by FACS (Marty *et al.*, 2014).

The step after tissue dissection is also very important as it requires fine-tuning of enzymatic exposure to avoid cell death as well as clustered cell populations. High exposure of the enzymes disrupts cells while under exposure results in clustered cell populations, which interfere with single cell isolation. In order to optimize this step, we can perform cell viability assays through Propidium Iodide (PI), Ethidium monoazide (EMA), or Hoechst staining (Dutta *et al.*, 2013; Perfetto *et al.*, 2006). If most of the cells are detected as dead, a milder enzyme such as, elastase or collagenase or a combination of these

enzymes in different concentrations can be used instead of trypsin (Dutta *et al.*, 2013). Additionally, incubation time and temperature can be adjusted to obtain a population of viable dissociated cells. Optimal incubation times vary for different cell types and enzymes and need to be optimized. For instance, in a study to dissociate cells from larval brains, tissues are incubated in collagenase and papain for one hour (Harzer *et al.*, 2013), while in the one to dissociate cells from midgut, tissues are incubated in trypsin for 2.5 hours (Amcheslavsky *et al.*, 2011). Since there is no published study about cell sorting from the *Drosophila* eye-antennal disc, it is necessary to optimize this methodology by controlling for clustering and cell viability after each modification step.

In addition to the effort to keep cells alive, it is important to remove dead cells during cell sorting to collect only R3/R4 cells. For this reason, we eliminated dead cells by considering forward and side scatter values. As a supportive assay to decrease the artifacts, viability dyes like PI can be used. Additionally, DAPI (4',6-diamidino-2-phenylindole) and antibodies against GFP, Elav, and Svp can be used to stain the sorted R3/R4 cells in order to control if they are living and still able to express the specific markers. Thereby, it would also be possible to calculate the efficiency of the FACS methodology to sort viable cells.

In recent years, several protocols have been developed to enhance cell type specific isolation from *Drosophila* tissues. Therefore, changing the cell isolation strategy may also help to increase the efficiency. One of the alternatives is magnetic bead isolation, which is reported as providing 95% viability among the captured ovary cells with beads (Wang *et al.*, 2008). In this method, cells of interest express mCD8-coupled fluorescent marker, which will localize on their cell surface and be captured by magnetic beads coated with antibody against mCD8 or the fluorescent marker (Safarik and Safariková, 1999; Wang *et al.*, 2008). However, this method has the same drawbacks with the FACS methodology in the cell dissociation step. In order to overcome those problems and obtain pure populations of R3/R4 cells, more advanced methods such as TU-tagging and TaDa can be used. These methods provide cell-type specific RNA isolation without any requirement of cell sorting (Miller *et al.*, 2009; Southall *et al.*, 2013). Moreover, it might be also possible to make use of laser microdissection in order to extract R3/R4 cells from different rows on the eye-antennal disc. In this way, comparative gene expression profile analyses can be performed for R3/R4 cells at different developmental stages. Since single cells can be cut from the

tissues by this method, R3 and R4 cells can be isolated separately to obtain their transcriptome (Iyer and Cox, 2010). Therefore, comparative expression profile analyses also can be done between R3 and R4 cells to better understand the asymmetric specification process. A possible drawback of this technique can be impurity of the population of isolated PR cells since they might be containing the cells from the peripodial membrane located under the PR cell layer (Gibson and Schubiger, 2001). Thus, individual isolation of R3 and R4 cells might be accomplished by combining TU-tagging or TaDa technique with laser microdissection.

5.2.2. Differential Expression Analyses

Bioinformatics analyses of R3/R4 transcriptome have revealed lots of DE genes in this cell pair. GO enrichment analysis have provided better interpretation of these data as it helps to find enriched GO terms among the list of DE genes. One of the highly ranked GO terms was Notch signalling pathway, which is expected since specification of R3/R4 PRs requires the activity of D1/N signalling. The other significant terms were related with eye development and included subsets of genes involved in this process, such as *svp* and *ro*. Additionally, the analyses revealed that genes involved in negative regulation of transcription were also enriched. Their expression levels in the R3/R4 cells were detected to be up-regulated more than seven fold. Therefore we thought that they might have important roles in R3/R4 specification through repressing the genes that lead to PR cell fate other than R3 and R4. Since *edl* was also involved in the sensory organ development process, we considered it as the most prominent candidate to study its function in R3/R4 specification and PCP establishment in the eye.

Edl is known to function in the EGFR signalling pathway by antagonizing the ETS domain TF Pointed P2 (Pnt-P2), which is activated upon phosphorylation by EGFR signalling (O'Neill *et al.*, 1994; Yamada, 2003). Pnt-P2 is known as a transcriptional activator while another ETS domain protein, Yan is a repressor of transcription. Opposite to Pnt-P2, Yan becomes inactive after phosphorylation (Rebay and Rubin, 1995). It has been shown that Fz/PCP pathway-dependent specification of R3/R4 cells requires phosphorylated Pnt-P2 in R4 cells and non-phosphorylated Yan in R3 cells (Weber *et al.*,

2008). Therefore, we thought that Edl might be required in R3 cells to antagonize Pnt-P2 and indirectly promote Yan function, which in turn allow cells to adopt an R3 fate.

5.2.3. Predicted TFs Involved in R3/R4 Specification and PCP Establishment

Since there are not many TFs known to be involved in R3/R4 specification, we aimed to find novel ones by performing a motif discovery throughout cis-regulatory regions of the DE genes in R3/R4. We thought that the predicted TFs may also have role in PCP establishment as they might provide correct specification of R3/R4 PRs and might activate genes that contribute to PCP establishment in the *Drosophila* eye.

For this purpose, i-cisTarget was used to identify over-represented TF binding motifs and obtain associated TFs. It was thought that a set of TF might have a role in activation of transcription of the up-regulated genes, whereas another set might be repressing transcription of the down-regulated genes in R3/R4 PRs. For this reason, we run the analysis for each gene in the list separately. As a result, Trl, Jim, and Grh TFs were predicted as candidates to regulate activity of the up-regulated genes while Dref, Crp, and CG7928 were predicted as regulators of the down-regulated genes in R3/R4 PRs. In order not to omit the ones that may have both activating and inhibiting roles in transcription, we also used the whole DE genes as an input. The results show that Trl, Grh, and Crp might be having a dual role in transcriptional regulation of the DE genes in R3/R4.

Trl, also known as GAGA TF, is a trithorax-group protein, which has a role in chromatin modifications in *Drosophila* (Bejarano and Busturia, 2004; Farkas *et al.*, 1994). Although Trl is usually involved in transcriptional activation, it may also function as a repressor (Bejarano and Busturia, 2004). Consistently, our findings attributed a possible dual role in regulation of the DE genes in R3/R4 PRs to Trl. Although no function for Trl in PR development and PCP establishment has been described, it has been shown that Trl mutants have rough eye phenotypes as it is required to achieve programmed cell death of excess interommatidial cells during the *Drosophila* eye morphogenesis (Dos-Santos *et al.*, 2008; Farkas *et al.*, 1994). On the other hand, our differential expression analyses revealed

that it is up-regulated in R3/R4 PRs with a 1.73 fold-change, which strengthens the possibility of Trl being involved in R3/R4 specification.

Grh was another TF predicted as a regulator of the DE genes in R3/R4 by activating and also repressing their expression. This result was consistent with its known function in transcriptional activation upon binding of several cofactors (Dynlacht *et al.*, 1991) and also in transcriptional repression through interacting with Trl (Liaw *et al.*, 1995). It has already been shown that ommatidium with *grh*-mutant R3 cells misrotates during planar cell polarization because of the failure of correct chirality formation, possibly as a result of misspecification of R3 into R4 PR cell (Gambis *et al.*, 2011). Considering the necessity of Grh in wing cells to assess Fz/PCP signalling (Lee and Adler, 2004), it was thought that Grh might be required for expression of Fz/PCP signalling pathway-related components. Although, its expression pattern has not been shown in the eye yet, it might be specifically expressed in R3/R4 PRs as we also found it as up-regulated in R3/R4 PRs with a 2.42 fold-change. Additionally, its interaction with Trl might be facilitated in R4 PRs to repress several targets, which remain expressed in R3 PRs through the activating effect of Grh. Further analyses of the direct targets of these two TFs is required to enlighten those possible interactions.

The basic helix-loop-helix TF Crp was also detected as a putative regulator of the DE genes in R3/R4 PRs. It was one of our candidates that was identified as R3/R4-specific gene in the enhancer-trap screen (Öztürk, 2010). It was predicted as directly targeting the genes up-regulated in the R3/R4 PRs. Considering its possible expression pattern, which is specific to R3/R4 PRs, it might be repressing the upregulated genes in this cell pair. Although its activating role upon binding to the TF Daughterless has been shown in *Drosophila* salivary glands (King-Jones *et al.*, 1999), it might also act as a repressor depending on spatiotemporal requirements.

The zinc finger TF Jim is known to be involved in regulation of chromatin silencing in the *Drosophila* eye; however, depending on the developmental stage, its activity may differ (Schneiderman *et al.*, 2010). Consistent with our prediction, its expression in the 3rd instar larval eye disc had been shown before (Mukherjee *et al.*, 2006). Therefore, performing loss

of function and gain of function analyses for Jim would enable us to understand if it affects R3/R4 specification and PCP establishment in the fly eye.

As a result of the motif discovery analysis for the up-regulated genes in PRs R3 and R4, one of the most common TFs, the DNA replication-related element-binding factor (DREF), was found at the top of the list. This was not a very surprising result since it regulates expression of more than a thousand *Drosophila* genes involved in cell proliferation and differentiation (Hirose *et al.*, 2001; Matsukage, 1995). DREF is highly expressed by the cells in and around the MF, additionally, low level of DREF expression has been observed in PRs posterior to the MF (Hirose *et al.*, 2001). Therefore, it seems possible for DREF to activate expression of several genes in R3/R4 PRs, which will activate signalling pathways and cause the expression of transcription factors leading to PR differentiation.

CG7928 was also predicted as activating the up-regulated genes in R3/R4 PRs. This TF belongs to the ZAD family of zinc-finger proteins, which are known to be involved in important processes during early developmental stages (Krystel and Ayyanathan, 2013). Although there is not much information about CG7928, it might be regulating critical genes for PR specification and signalling pathways participating in PCP establishment.

5.2.4. Validation of Svp Predicted Target Genes

In the meantime, a gene regulatory network analysis for the *Drosophila* eye disc has been performed by Delphine Potier from the Aerts Lab at KU Leuven, Belgium. Among the networks generated throughout the analyses, we aimed to select one related with R3/R4 PR specification. For this reason, we selected the predicted network of the Svp targetome. Since Svp is involved in R1/R6 and R3/R4 PR specification, generating a sub-network by only keeping the genes captured by *sNPF*-RNA-Seq experiment allowed us to eliminate R1/R6-specific targets.

In order to validate the putative target genes of Svp, we intended to examine expression level changes in the case of *svp* null mutation. Throughout the 3rd instar larval eye disc,

gene expression levels can be highly dynamic and can differ row by row. Therefore, it was important to choose a suitable approach allowing us to track these differences. For this reason, we did not perform qRT-PCR on mutant eye discs, instead, we generated *svp* null mutant clones in the 3rd instar larval eye disc and compared the expression level changes between mutant and wild type areas. We have determined the expression levels of the genes according to the signal they reflect by immunostaining. Since quality of immunostainings can be variable, comparing a mutant eye disc with a wild type eye disc would not yield trustable results. However, our methodology allowed us to overcome this difficulty as we could make comparisons within an eye disc.

To be able to perform the validation experiments, we have selected four putative target genes that have readily available antibodies against them: *cpo*, *futsch*, *brp*, and *peb*. The expression patterns of Cpo, Futsch, and Brp appeared as homogeneous through the wild type 3rd instar larval eye discs and did not change in the *svp*⁻ mosaic eye discs. Therefore, we thought that transcriptional activity of those genes might be regulated by a TF complex containing Svp TF. Since the expression levels appear as unchanged in the absence of Svp, there might be partial redundancy for the components of this transcription regulatory complex. In order to test this hypothesis, expression levels of the target genes can be examined in the eye discs both mutant for Svp and the putative components of a possible TF complex. On the other hand, loss of Svp might be causing little changes in the expression levels of these targets, which makes it very difficult to detect via immunostainings. It is also possible that bioinformatics analyses have revealed these target genes as false positives. Preferring more stringent thresholds might help to avoid such false positive results.

The analyses on Peb have revealed more interesting results. Normally its expression levels are high in R3/R4 PRs from row two to six; however, in the *svp* null mutant area its expression levels showed a slight decrease in R3/R4 PRs. We intended to recapitulate this pattern again in the *svp*⁻ mosaic eye discs by using a R3/R4-specific marker to confirm that the cells in which Peb expression is decreased are R3/R4. Although in the time course of this study, we could not encounter a proper mosaic eye disc to evaluate the expression level changes, experiments are being continued to achieve this aim.

6. CONCLUSION

From the first part of this study where we investigated roles of putative R3/R4-specific genes in PCP establishment in the *Drosophila* eye, we found *fas* as a promising candidate since its down-regulation resulted in ommatidial misrotation and R4/R4 symmetry. These phenotypes revealed that *fas* might be involved in PCP establishment via contributing to R3/R4 specification and ommatidial rotation. Further analysis with heterozygous *fas* mutants also yielded rotation and PR specification problems in the eye. Additionally, we generated lines that will enable us to make whole eye *fas* mutants to circumvent lethality of the alleles when they are in homozygous state. Thus, further experiments using these lines will provide better understanding of the role of *fas* in PCP establishment in the eye.

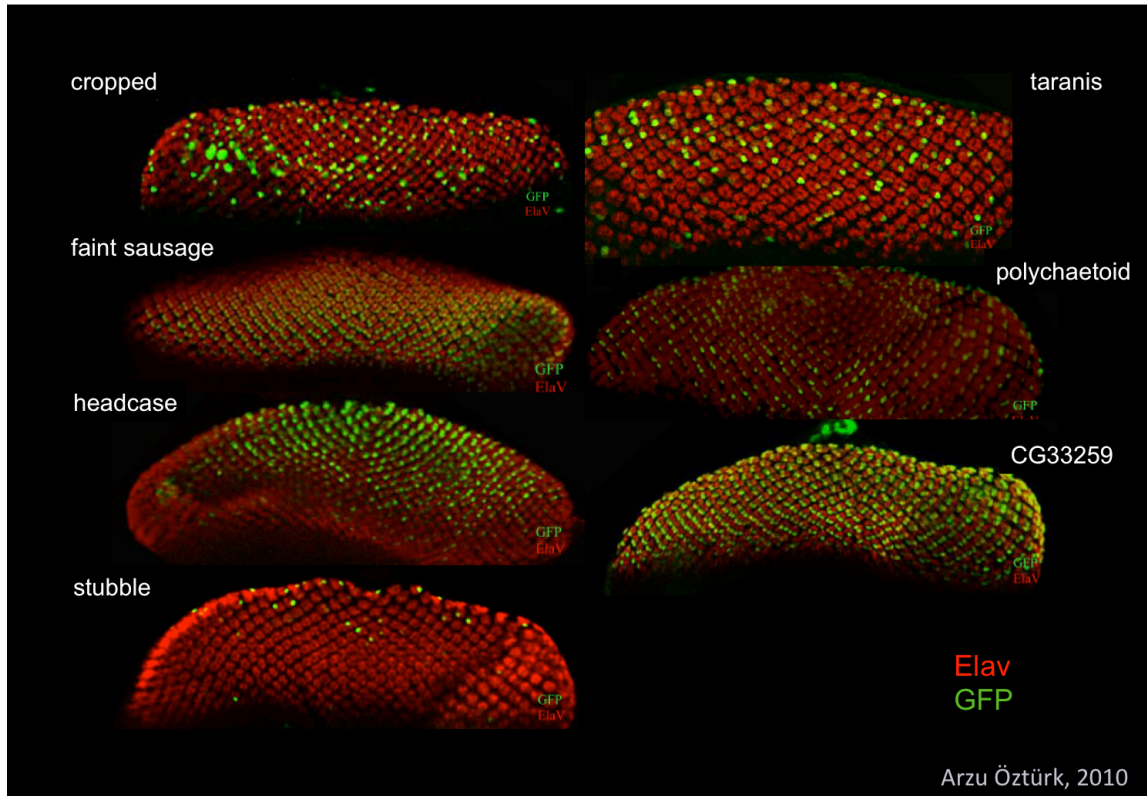
Moreover, we found that Fas levels increase in the absence of Svp. Thus, we concluded that Svp might be regulating the amount of Fas in R3/R4 cells through repressing its expression in a direct or indirect way.

From the second part of this study where we obtained DE genes in R3/R4 PRs, we identified Edl as a candidate that might be regulating R3/R4 cell fate choice through interacting with Yan and Pnt-P2. Further experiments will help to identify its role in R3/R4 specification and PCP establishment in the eye.

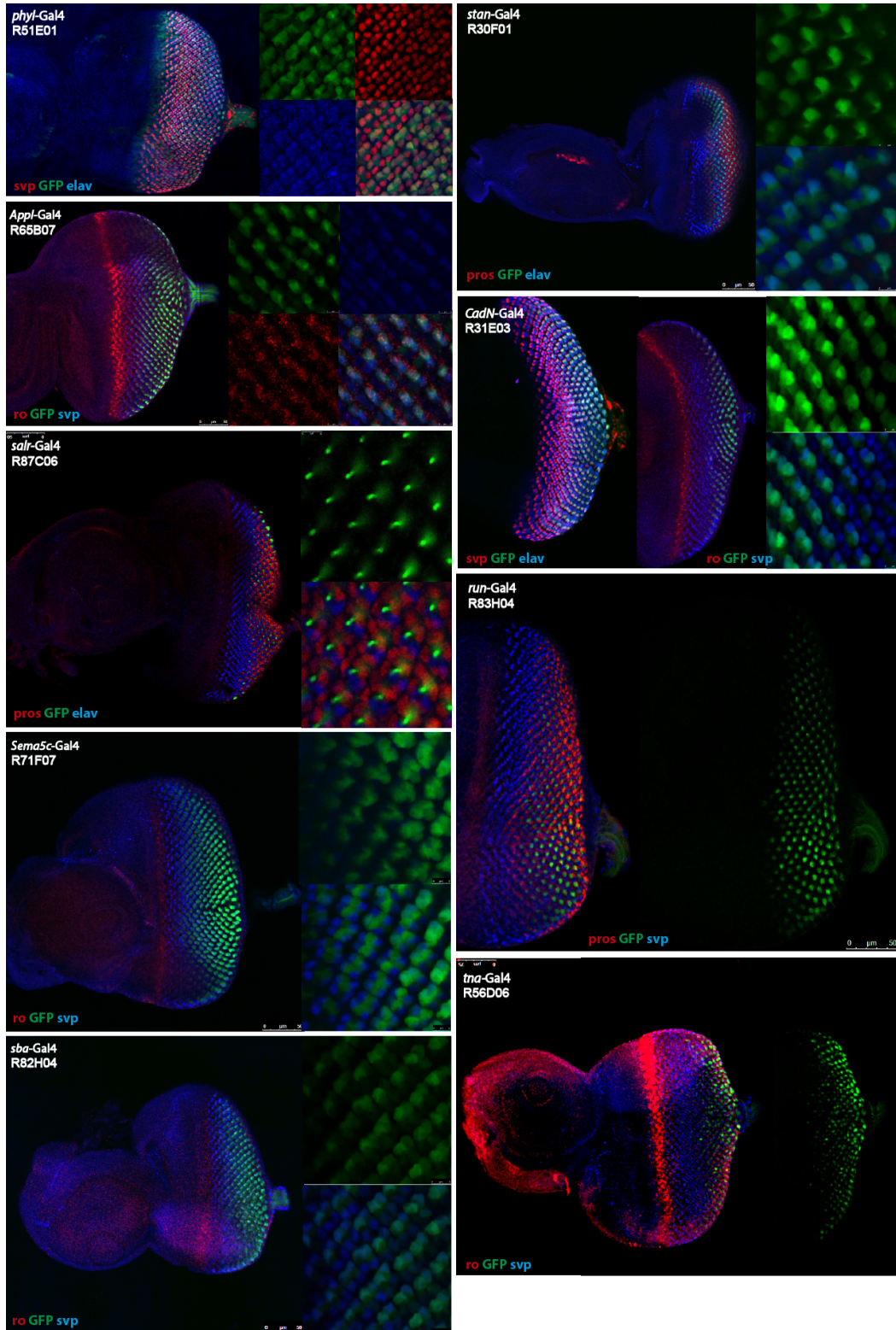
Additionally, motif enrichment analyses among DE genes yielded several TFs (Trl, Jim, Grh, Dref, Crp, CG7928) that might be involved in R3/R4 specification and PCP establishment. In order to understand if these TFs have an effect on these processes, further experiments have to be performed.

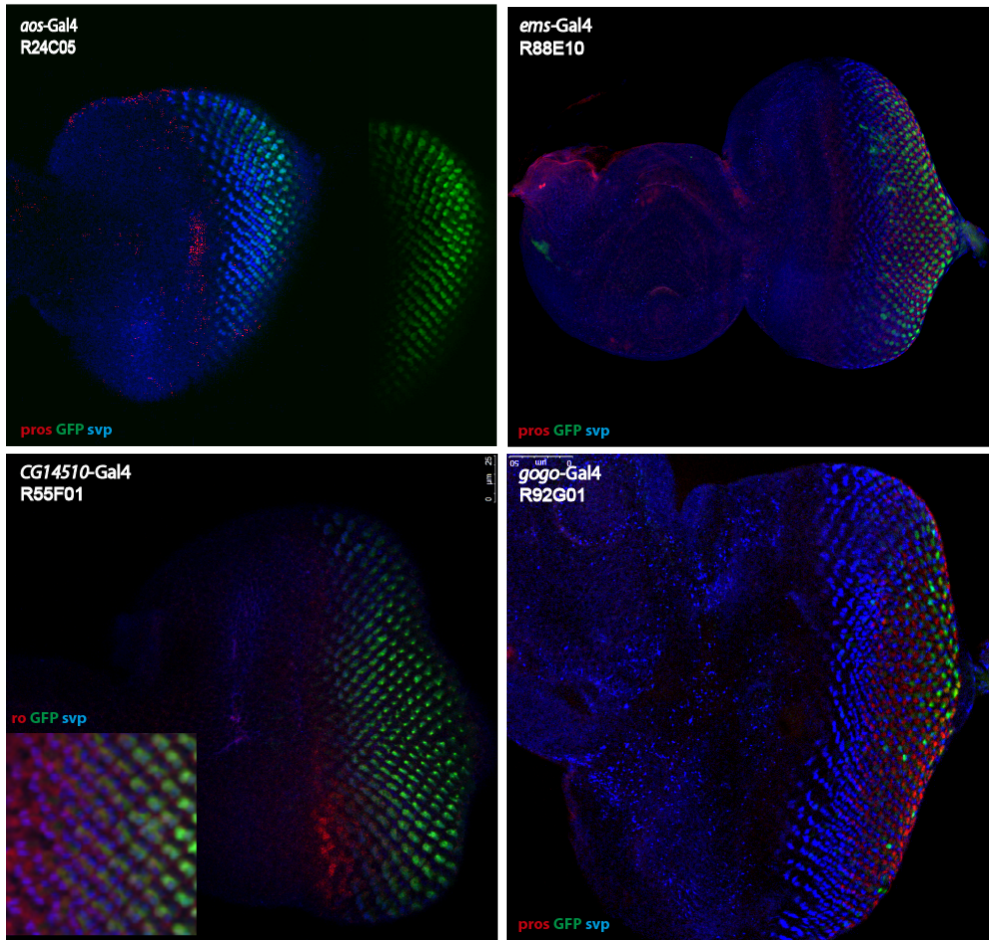
Furthermore, we tried to validate several predicted targets of the TF Svp. In our analysis expression levels of putative targets Cpo, Brp, and Futsch did not change in the absence of Svp; however, in R3/R4 PRs, Peb levels slightly decreased. Therefore, we concluded that Svp might be activating Peb expression in R3/R4 PRs.

APPENDIX A: EXPRESSION PATTERNS OF THE ENHANCER TRAP GAL4 LINES



APPENDIX B: EXPRESSION PATTERNS OF THE SCREENED FLYLIGHT GAL4 LINES





REFERENCES

- Adryan, B., and S. A. Teichmann, 2006, "FlyTF: A Systematic Review of Site-Specific Transcription Factors in the Fruit Fly *Drosophila Melanogaster*", *Bioinformatics*, Vol. 22, No. 12, pp. 1532-1533.
- Amcheslavsky, A., N. Ito, J. Jiang, and Y. T. Ip, 2011, "Tuberous Sclerosis Complex and Myc Coordinate the Growth and Division of *Drosophila* Intestinal Stem Cells", *The Journal of Cell Biology*, Vol. 193, No. 4, pp. 695-710.
- Anders, S., and W. Huber, 2010, "Differential Expression Analysis for Sequence Count Data", *Genome Biology*, Vol. 11, No. 10, p. R106.
- Bao, S., 2010, "Two Themes on the Assembly of the *Drosophila* Eye", *Current Topics in Developmental Biology*, Vol. 93, No. 10, pp. 85-127.
- Bayly, R., and J. D. Axelrod, 2011, "Pointing in the Right Direction : New Developments in the Field of Planar Cell Polarity", *Nature*, Vol. 12, No. 6, pp. 385-391.
- Bejarano, F., and A. Busturia, 2004, "Function of the Trithorax-like Gene during *Drosophila* Development", *Developmental Biology*, Vol. 268, No. 2, pp. 327-341.
- Bellen, H. J., S. Kooyer, D. D'Evelyn, and J. Pearlman, 1992, "The *Drosophila* Couch Potato Protein Is Expressed in Nuclei of Peripheral Neuronal Precursors and Shows Homology to RNA-Binding Proteins", *Genes & Development*, Vol. 6, No.11, pp. 2125-2136.
- Bellen, H., H. Vaessin, and E. Bier, 1992, "The *Drosophila* Couch Potato Gene: An Essential Gene Required for Normal Adult Behavior", *Genetics Society of America*, Vol. 131, No. 2, pp. 365-375.

- Berger, C., H. Harzer, T. R. Burkard, J. Steinmann, S. van der Horst, A.-S. Laurenson, M. Novatchkova, H. Reichert, and J. A. Knoblich, 2012, "FACS Purification and Transcriptome Analysis of *Drosophila* Neural Stem Cells Reveals a Role for Klumpfuss in Self-Renewal", *Cell Reports*, Vol. 2, No. 2, pp. 407-418.
- Bonner, W. A., H. R. Hulett, R. G. Sweet, and L. A. Herzenberg, 1972, "Fluorescence Activated Cell Sorting", *The Review of Scientific Instruments*, Vol. 43, pp. 404-409.
- Brand, A. H., and N. Perrimon, 1993, "Targeted Gene Expression as a Means of Altering Cell Fates and Generating Dominant Phenotypes", *Development*, Vol. 118, No. 2, pp. 401-415.
- Cagan, R. L., and D. F. Ready, 1989, "The Emergence of Order in the *Drosophila* Pupal Retina", *Developmental Biology*, Vol. 136, pp. 346-362.
- Carmona-Saez, P., M. Chagoyen, F. Tirado, J. M. Carazo, and A. Pascual-Montano, 2007, "GENECODIS: A Web-Based Tool for Finding Significant Concurrent Annotations in Gene Lists", *Genome Biology*, Vol.8, No. 1, p. R3.
- Charlton-Perkins, M., and T. A. Cook, 2010, "Building a Fly Eye: Terminal Differentiation Events of the Retina, Corneal Lens, and Pigmented Epithelia", *Current Topics in Developmental Biology*, Vol. 93, pp. 129-173.
- Choi, K., and S. Benzer, 1994, "Rotation of Photoreceptor Clusters in the Developing *Drosophila* Eye Requires the Nemo Gene", *Cell*, Vol.78, No. 1, pp. 125-136.
- Chou, Y.-H., and C.-T. Chien, 2002, "Scabrous Controls Ommatidial Rotation in the *Drosophila* Compound Eye", *Developmental Cell*, Vol. 3, No. 6, pp. 839-850.
- Cooper, M., and S. Bray, 1999, "Frizzled Regulation of Notch Signalling Polarizes Cell Fate in the *Drosophila* Eye", *Nature*, Vol. 397, No.2, pp. 526-530.

- Daga, a, C. a Karlovich, K. Dumstrei, and U. Banerjee, 1996, "Patterning of Cells in the Drosophila Eye by Lozenge, Which Shares Homologous Domains with AML1", *Genes & Development*, Vol. 10, No. 10, pp. 1194-1205.
- Das, G., J. Reynolds-Kenneally, and M. Mlodzik, 2002, "The Atypical Cadherin Flamingo Links Frizzled and Notch Signaling in Planar Polarity Establishment in the Drosophila Eye", *Developmental Cell*, Vol. 2, pp. 655-666.
- Dietzl, G., D. Chen, F. Schnorrer, K.-C. Su, Y. Barinova, M. Fellner, B. Gasser, K. Kinsey, S. Oettel, ... B. J. Dickson, 2007, "A Genome-Wide Transgenic RNAi Library for Conditional Gene Inactivation in Drosophila", *Nature*, Vol. 448, No. 7150, pp. 151-156.
- Domingos, P. M., M. Mlodzik, C. S. Mendes, S. Brown, H. Steller, and B. Mollereau, 2004, "Spalt Transcription Factors Are Required for R3/R4 Specification and Establishment of Planar Cell Polarity in the Drosophila Eye", *Development*, Vol. 131, No. 22, pp. 5695-5702.
- Dos-Santos, N., T. Rubin, F. Chalvet, P. Gandille, F. Cremazy, J. Leroy, E. Boissonneau, and L. Théodore, 2008, "Drosophila Retinal Pigment Cell Death Is Regulated in a Position-Dependent Manner by a Cell Memory Gene", *The International Journal of Developmental Biology*, Vol. 52, No. 1, pp. 21-31.
- Duffy, J. B., 2002, "GAL4 System in Drosophila: A Fly Geneticist's Swiss Army Knife", *Genesis*, Vol. 34, No. 1-2, pp. 1-15.
- Dutta, D., J. Xiang, and B. a Edgar, 2013, "RNA Expression Profiling from FACS-Isolated Cells of the Drosophila Intestine", *Current Protocols in Stem Cell Biology*, Vol. 27, Unit 2F.2.
- Dynlacht, B. D., T. Hoey, and R. Tjian, 1991, "Isolation of Coactivators Associated with the TATA-Binding Protein That Mediate Transcriptional Activation", *Cell*, Vol. 66, No. 3, pp. 563-576.

Eaton, S., 1997, "Planar Polarization of *Drosophila* and Vertebrate Epithelia", *Current Opinion in Cell Biology*, Vol. 9, No. 6, pp. 860-866.

Eden, E., R. Navon, I. Steinfeld, D. Lipson, and Z. Yakhini, 2009, "GORilla: A Tool for Discovery and Visualization of Enriched GO Terms in Ranked Gene Lists", *BMC Bioinformatics*, Vol. 10, p. 48.

Fanto, M., C. A. Mayes, and M. Mlodzik, 1998, "Linking Cell-Fate Specification to Planar Polarity: Determination of the R3/R4 Photoreceptors is a Prerequisite for the Interpretation of the Frizzled Mediated Polarity Signal", *Mechanisms of Development*, Vol. 74, No. 1-2, pp. 51-58.

Fanto, M., and H. Mcneill, 2004, "Planar Polarity from Flies to Vertebrates", *Journal of Cell Science*, Vol. 117, No. 4, pp. 527-533.

Fanto, M., and M. Mlodzik, 1999, "Asymmetric Notch Activation Specifies Photoreceptors R3 and R4 and Planar Polarity in the *Drosophila* Eye", *Nature*, Vol. 397, No. 6719, pp. 523-526.

Farkas, G., J. Gausz, M. Galloni, G. Reuter, H. Gyurkovics, and F. Karch, 1994, "The Trithorax-like Gene Encodes the *Drosophila* GAGA Factor", *Nature*, Vol. 371 No. 6500, pp. 806-808.

Fiehler, R. W., and T. Wolff, 2007, "*Drosophila* Myosin II, Zipper, Is Essential for Ommatidial Rotation", *Developmental Biology*, Vol. 310, pp. 348-362.

Frankfort, B., R. Nolo, Z. Zhang, H. Bellen, and G. Mardon, 2001, "Senseless Repression of Rough Is Required for R8 Photoreceptor Differentiation in the Developing *Drosophila* Eye", *Neuron*, Vol.32, No. 3, pp. 403-414.

- Gaengel, K., and M. Mlodzik, 2003, "Egfr Signaling Regulates Ommatidial Rotation and Cell Motility in the *Drosophila* Eye via MAPK/Pnt Signaling and the Ras Effector Canoe/AF6", *Development*, Vol. 130, No.22, pp. 5413-5423.
- Gambis, A., P. Dourlen, H. Steller, and B. Mollereau, 2011, "Two-Color in Vivo Imaging of Photoreceptor Apoptosis and Development in *Drosophila*", *Developmental Biology*, Vol 351, No.1, pp. 128-134.
- Gibson, M. C., and G. Schubiger, 2001, "Drosophila Peripodial Cells, More than Meets the Eye?", *BioEssays*, Vol. 23, No. 8, pp. 691-697.
- Golic, K. G., 1991, "Site-Specific Recombination between Homologous Chromosomes in *Drosophila*", *Science*, Vol. 252, No. 5008, pp. 958-961.
- Golic, K. G., and S. Lindquist, 1989, "The FLP Recombinase of Yeast Catalyzes Site-Specific Recombination in the *Drosophila* Genome", *Cell*, Vol. 59, No. 3, pp. 499-509.
- Green, E. W., G. Fedele, F. Giorgini, and C. P. Kyriacou, 2014, "A *Drosophila* RNAi Collection Is Subject to Dominant Phenotypic Effects", *Nature Methods*, Vol. 11, No. 3, pp. 222-223.
- Grether, M. E., J. M. Abrams, J. Agapite, K. White, and H. Steller, 1995, "The Head Involution Defective Gene of *Drosophila melanogaster* Functions in Programmed Cell Death", *Genes & Development*, Vol. 9, No. 14, pp. 1694-1708.
- Haag, T. A., N. P. Haag, A. C. Lekven, and V. Hartenstein, 1999, "The Role of Cell Adhesion Molecules in *Drosophila* Heart Morphogenesis: Faint Sausage, Shotgun/DE-Cadherin, and Laminin Are Required for Discrete Stages in Heart Development", *Developmental Biology*, Vol. 208, No. 1, pp. 56-69.

- Harzer, H., C. Berger, R. Conder, G. Schmauss, and J. A. Knoblich, 2013, "FACS Purification of *Drosophila* Larval Neuroblasts for Next-Generation Sequencing", *Nature Protocols*, Vol.8, No. 6, pp. 1088-1099.
- Heberlein, U., and K. Moses, 1995, "Mechanisms of *Drosophila* Retinal Morphogenesis: The Virtues of Being Progressive", *Cell*, Vol. 81, No. 7, pp. 987-990.
- Herrmann, C., B. Van de Sande, D. Potier, and S. Aerts, 2012, "i-cisTarget: An Integrative Genomics Method for the Prediction of Regulatory Features and Cis-Regulatory Modules", *Nucleic Acids Research*, Vol. 40, No. 15, p. e114.
- Higashijima, S., T. Kojima, T. Michiue, S. Ishimaru, Y. Emori, and K. Saigo, 1992, "Dual Bar Homeo Box Genes of *Drosophila* Required in Two Photoreceptor Cells, R1 and R6, and Primary Pigment Cells for Normal Eye Development", *Genes & Development*, Vol. 6, pp. 50-60.
- Hirose, F., N. Ohshima, and M. Shiraki, 2001, "Ectopic Expression of DREF Induces DNA Synthesis, Apoptosis, and Unusual Morphogenesis in the *Drosophila* Eye Imaginal Disc: Possible Interaction with Polycomb and Trithorax Group Proteins", *Molecular and Cellular Biology*, Vol. 21, No. 21, pp. 7231-7242.
- Horn, C., N. Offen, S. Nystedt, U. Häcker, and E. E. A. Wimmer, 2003, "piggyBac-Based Insertional Mutagenesis and Enhancer Detection as a Tool for Functional Insect Genomics", *Genetics*, Vol. 163, No. 2, pp. 647-661.
- Hummel, T., K. Krukkert, J. Roos, G. Davis, and C. Klämbt, 2000, "*Drosophila* Futsch/22C10 Is a MAP1B-like Protein Required for Dendritic and Axonal Development", *Neuron*, Vol. 26, No. 2, pp. 357-370.
- Huynh-Thu, V. A., A. Irrthum, L. Wehenkel, and P. Geurts, 2010, "Inferring Regulatory Networks from Expression Data Using Tree-Based Methods", *Plos One*, Vol. 5, No. 9, pp. 1-10.

- Iyer, E. P. R., and D. N. Cox, 2010, "Laser Capture Microdissection of Drosophila Peripheral Neurons", *Journal of Visualized Experiments : Jove*, Vol. May 24, No. 39, pp. 1-6.
- Janky, R., A. Verfaillie, B. Van de Sande, L. Standaert, V. Christiaens, G. Hulselmans, K. Herten, M. Naval Sanchez, D. Potier, S. Aerts, 2013, "Detection of Cis-Regulatory Master Regulators Enables Reverse Engineering Human Regulons From Cancer Gene Signatures", <http://iregulon.aertslab.org/>, [Accessed May 2014].
- Jenett, A., G. M. Rubin, T.-T. B. Ngo, D. Shepherd, C. Murphy, H. Dionne, B. D. Pfeiffer, A. Cavallaro, D. Hall, C. T. Zugates, 2012, "A GAL4-Driver Line Resource for Drosophila Neurobiology", *Cell Reports*, Vol. 2, No. 4, pp. 991-1001.
- Jenny, A., 2010, "Planar Cell Polarity Signaling in the Drosophila Eye", *Current Topics in Developmental Biology*, Vol. 93, pp. 189-227.
- Jones, W. D., 2009, "The Expanding Reach of the GAL4/UAS System into the Behavioral Neurobiology of Drosophila", *BMB Reports*, Vol. 42, No. 11, pp. 705-712.
- Jory, A., C. Estella, M. W. Giorgianni, M. Slattery, T. R. Laverty, G. M. Rubin, and R. S. Mann, 2012, "A Survey of 6,300 Genomic Fragments for Cis-Regulatory Activity in the Imaginal Discs of Drosophila Melanogaster.", *Cell Reports*, Vol. 2, No. 4, pp. 1014-1024.
- Karpen, G. H., and A. C. Spradling, 1992, "Analysis of Subtelomeric Heterochromatin in the Drosophila Minichromosome Dp1187 by Single P Element Insertional Mutagenesis", *Genetics Society of America*, Vol. 753, No. 1990, pp. 737-753.
- Kauffmann, R. C., S. Li, P. a Gallagher, J. Zhang, and R. W. Carthew, 1996, "Ras1 Signaling and Transcriptional Competence in the R7 Cell of Drosophila", *Genes & Development*, Vol. 10, No. 17, pp. 2167-2178.

- Kimmel, B. E., U. Heberlein, and G. M. Rubin, 1990, "The Homeo Domain Protein Rough Is Expressed in a Subset of Cells in the Developing Drosophila Eye Where It Can Specify Photoreceptor Cell Subtype", *Genes and Development*, Vol. 4, No. 5, pp. 712-727.
- King-Jones, K., G. Korge, and M. Lehmann, 1999, "The Helix-Loop-Helix Proteins dAP-4 and Daughterless Bind Both in Vitro and in Vivo to SEBP3 Sites Required for Transcriptional Activation of the Drosophila Gene Sgs-4", *Journal of Molecular Biology*, Vol. 291, No. 1, pp. 71-82.
- Krupp, G., 2005, "Stringent RNA Quality Control Using the Agilent 2100 Bioanalyzer", *Agilent Technologies*.
- Krystel, J., and K. Ayyanathan, 2013, "Global Analysis of Target Genes of 21 Members of the ZAD Transcription Factor Family in Drosophila Melanogaster", *Gene*, Vol. 512, No. 2, pp. 1-22.
- Kumar, J., 2011, "My What Big Eyes You Have: How the Drosophila Retina Grows", *Developmental Neurobiology*, Vol. 71, No. 12, pp. 1133-1152.
- Lachke, S. A., A. W. Higgins, M. Inagaki, I. Saadi, Q. Xi, M. Long, B. J. Quade, M. E. Talkowski, J. F. Gusella, R. L. Maas, 2012, "The Cell Adhesion Gene PVRL3 Is Associated with Congenital Ocular Defects", *Human Genetics*, Vol. 131, No. 2, pp. 235-250.
- Lawrence, P. a, and J. Casal, 2013, "The Mechanisms of Planar Cell Polarity, Growth and the Hippo Pathway: Some Known Unknowns", *Developmental Biology*, Vol. 377, No. 1, pp. 1-8.
- Lee, H., and P. N. Adler, 2004, "The Grainy Head Transcription Factor Is Essential for the Function of the Frizzled Pathway in the Drosophila Wing", *Mechanisms of Development*, Vol. 121, No. 1, pp. 37-49.

- Lekven, A. C., U. Tepass, M. Keshmeshian, and V. Hartenstein, 1998, "Faint Sausage Encodes a Novel Extracellular Protein of the Immunoglobulin Superfamily Required for Cell Migration and the Establishment of Normal Axonal Pathways in the *Drosophila* Nervous System", *Development*, Vol. 125, No. 14, pp. 2747-2758.
- Li, H., B. Handsaker, A. Wysoker, T. Fennell, J. Ruan, N. Homer, G. Marth, G. Abecasis, and R. Durbin, 2009, "The Sequence Alignment/Map Format and SAMtools", *Bioinformatics*, Vol. 25, No. 16, pp. 2078-2079.
- Liaw, G. J., K. M. Rudolph, J. D. Huang, T. Dubnicoff, A. J. Courey, and J. A. Lengyel, 1995, "The Torso Response Element Binds GAGA and NTF-1/Elf-1, and Regulates Tailless by Relief of Repression", *Genes & Development*, Vol. 9, No. 24, pp. 3163-3176.
- Litzinger, T. C., and K. Del Rio-Tsonis, 2002, *Eye Anatomy, eLS*, John Wiley & Sons, Ltd.
- Lopes, C. S., and F. Casares, 2010, "Hth Maintains the Pool of Eye Progenitors and Its Downregulation by Dpp and Hh Couples Retinal Fate Acquisition with Cell Cycle Exit", *Developmental Biology*, Vol. 339, No. 1, pp. 78-88.
- Marti, G. E., M. Stetler-Stevenson, J. J. Bleesing, and T. A. Fleisher, 2001, "Introduction to Flow Cytometry", *Seminars in Hematology*, Vol. 38, pp. 93-99.
- Marty, F., C. Rockel-Bauer, N. Simigdala, E. Brunner, and K. Basler, 2014, "Large-Scale Imaginal Disc Sorting: A Protocol for "Omics"-Approaches", *Methods*, Vol. 68, No. 1, pp. 260-264.
- Matis, M., and J. D. Axelrod, 2013, "Regulation of PCP by the Fat Signaling Pathway", *Genes & Development*, Vol. 27, No. 20, pp. 2207-2220.
- Matsukage, A., 1995, "The DRE Sequence TATCGATA, a Putative Promoter-Activating Element for *Drosophila* *Melanogaster* Cell-Proliferation-Related Genes", *Gene*, Vol. 166, pp. 233-236.

- Miller, M. R., K. J. Robinson, M. D. Cleary, and C. Q. Doe, 2009, "TU-Tagging : Cell Type-Specific RNA Isolation from Intact Complex Tissues", *Nature Methods*, Vol. 6, No. 6, pp. 439-441.
- Mirkovic, I., W. J. Gault, M. Rahnama, A. Jenny, K. Gaengel, D. Bessette, C. J. Gottardi, E. M. Verheyen, and M. Mlodzik, 2011, " Nemo Kinase Phosphorylates β -catenin to promote ommatidial rotation and connects core PCP factors to E-cadherin- β -catenin", *Nature Structural & Molecular Biology*, Vol. 18, No. 6, pp. 665-672.
- Mirkovic, I., and M. Mlodzik, 2006, "Cooperative Activities of Drosophila DE-Cadherin and DN-Cadherin Regulate the Cell Motility Process of Ommatidial Rotation", *Development*, Vol. 133, No. 17, pp. 3283-3293.
- Mlodzik, M., 1999, "Planar Polarity in the Drosophila Eye: A Multifaceted View of Signaling Specificity and Cross-Talk", *The EMBO Journal*, 18(24), 6873-6879.
- Mlodzik, M. (Ed.), 2005, *Planar Cell Polarization During Development*, Elsevier, San Diego, pp. 15-54.
- Mlodzik, M., Y. Hiromi, U. Weber, C. S. Goodman, and G. M. Rubin, 1990, "The Drosophila Seven-up Gene, A Member of the Steroid Receptor Gene Superfamily, Controls Photoreceptor Cell Fates", *Cell*, Vol. 60, No. 2, pp. 211-224.
- Mukherjee, T., U. Schäfer, and M. P. Zeidler, 2006, "Identification of Drosophila Genes Modulating Janus Kinase/signal Transducer and Activator of Transcription Signal Transduction", *Genetics*, Vol. 172, No. 3, pp. 1683-1697.
- Muñoz-Soriano, V., C. Ruiz, M. Pérez-Alonso, M. Mlodzik, and N. Paricio, 2013, "Nemo Regulates Cell Dynamics and Represses the Expression of Miple, a Midkine/pleiotrophin Cytokine, During Ommatidial Rotation", *Developmental Biology*, Vol. 377, No. 1, pp. 113-138.

- Nagy, A., H. Hegyi, K. Farkas, H. Tordai, E. Kozma, L. Bányai, and L. Patthy, 2008, "Identification and Correction of Abnormal, Incomplete and Mispredicted Proteins in Public Databases", *BMC Bioinformatics*, Vol. 9, p. 353.
- Nagy, A., and L. Patthy, 2013, "MisPred: A Resource for Identification of Erroneous Protein Sequences in Public Databases", *Database: The Journal Of Biological Databases And Curation*, Vol. 2013, p. bat053.
- Neufeld, T. P., a F. de la Cruz, L. a Johnston, and B. a Edgar, 1998, "Coordination of Growth and Cell Division in the Drosophila Wing", *Cell*, Vol. 93, No. 7, pp. 1183-1193.
- Niwa, N., Y. Hiromi, and M. Okabe, 2004, "A Conserved Developmental Program for Sensory Organ Formation in Drosophila Melanogaster", *Nature Genetics*, Vol. 36, pp. 293-297.
- Nogales-Cadenas, R., P. Carmona-Saez, M. Vazquez, C. Vicente, X. Yang, F. Tirado, J. M. Carazo, and A. Pascual-Montano, 2009, "GeneCodis: Interpreting Gene Lists through Enrichment Analysis and Integration of Diverse Biological Information", *Nucleic Acids Research*, Vol. 37, pp. W317-322.
- Nüsslein-Volhard, C., E. Wieschaus, and G. Jürgens, 1984, "Mutations Affecting the Pattern of the Larval Cuticle in Drosophila Melanogaster", *Wilhelm Roux's Archives of Developmental Biology*, Vol. 193, No. 5, pp. 296-307.
- O'Neill, E. M., I. Rebay, R. Tjian, and G. M. Rubin, 1994, "The Activities of Two Ets-Related Transcription Factors Required for Drosophila Eye Development Are Modulated by the Ras/MAPK Pathway", *Cell*, Vol. 78, No. 1, pp. 137-147.
- Özkan, E., R. a Carrillo, C. L. Eastman, R. Weiszmann, D. Waghray, K. G. Johnson, K. Zinn, S. E. Celniker, and K. C. Garcia, 2013, "An Extracellular Interactome of Immunoglobulin and LRR Proteins Reveals Receptor-Ligand Networks", *Cell*, Vol. 154, No. 1, pp. 228-239.

Özsolak, F., and P. M. Milos, 2011, "RNA Sequencing: Advances, Challenges and Opportunities", *Nature Reviews Genetics*, Vol. 12, No. 2, pp. 87-98.

Öztürk, A., 2010, *Characterization of Genes Involved in Photoreceptor Differentiation*, M.Sc. Thesis, Boğaziçi University.

Pavlidis, P., and W. S. Noble, 2001, "Analysis of Strain and Regional Variation in Gene Expression in Mouse Brain.", *Genome Biology*, Vol. 2, No. 10, p. 42.

Peng, Y., and J. D. Axelrod, 2012, "Asymmetric Protein Localization In Planar Cell Polarity: Mechanisms, Puzzles, And Challenges", *Current Topics in Developmental Biology*, Vol. 101, pp. 33-53.

Pepple, K., M. Atkins, and K. Venken, 2008, "Two-Step Selection of a Single R8 Photoreceptor: A Bistable Loop between Senseless and Rough Locks in R8 Fate", *Development*, Vol. 135, No. 24, pp. 4071-4079.

Perfetto, S. P., P. K. Chattopadhyay, L. Lamoreaux, R. Nguyen, D. Ambrozak, R. a Koup, and M. Roederer, 2006, "Amine Reactive Dyes: An Effective Tool to Discriminate Live and Dead Cells in Polychromatic Flow Cytometr.", *Journal of Immunological Methods*, Vol. 313, No. 1-2, pp. 199-208.

Pfeiffer, B. D., A. Jenett, A. S. Hammonds, T.-T. B. Ngo, S. Misra, C. Murphy, A. Scully, J. W. Carlson, K. H. Wan, G. M. Rubin, 2008, "Tools for Neuroanatomy and Neurogenetics in Drosophila", *Proceedings of the National Academy of Sciences of the United States of America*, Vol. 105, No. 28, pp. 9715-9720.

Pichaud, F., and C. Desplan, 2001, "A New Visualization Approach for Identifying Mutations That Affect Differentiation and Organization of the Drosophila Ommatidia", *Development*, Vol. 128, pp. 815-826.

- Pickup, A. T., M. L. Lamka, Q. Sun, M. L. R. Yip, and H. D. Lipshitz, 2002, "Control of Photoreceptor Cell Morphology, Planar Polarity and Epithelial Integrity during *Drosophila* Eye Development", *Development*, Vol. 129, No. 9, pp. 2247-2258.
- Raabe, T., 2000, "The Sevenless Signaling Pathway: Variations of a Common Theme", *Biochimica et Biophysica Acta*, Vol. 1496, No. 1-2, pp. 151-163.
- Rebay, I., and G. M. Rubin, 1995, "Yan Functions as a General Inhibitor of Differentiation and Is Negatively Regulated by Activation of the Ras / MAPK Pathway", *Cell*, Vol. 81, pp. 857-866.
- Reinke, R., and S. L. Zipursky, 1988, "Cell-Cell Interaction in the *Drosophila* Retina: The Bride of Sevenless Gene Is Required in Photoreceptor Cell R8 for R7 Cell Development", *Cell*, Vol. 55, No. 2, pp. 321-330.
- Rikitake, Y., K. Mandai, and Y. Takai, 2012, "The Role of Nectins in Different Types of Cell-Cell Adhesion", *Journal of Cell Science*, Vol. 125, No. 16, pp. 3713-3722.
- Robinson, J. T., H. Thorvaldsdóttir, W. Winckler, M. Guttman, E. S. Lander, G. Getz, and J. P. Mesirov, 2011, "Integrative Genomics Viewer", *Nature Biotechnology*, Vol. 29, No. 1, pp. 24-26.
- Robinson, M. D., D. J. McCarthy, and G. K. Smyth, 2010, "edgeR: A Bioconductor Package for Differential Expression Analysis of Digital Gene Expression Data", *Bioinformatics*, Vol. 26, No. 1, pp. 139-140.
- Rogers, E. M., C. a Brennan, N. T. Mortimer, S. Cook, A. R. Morris, and K. Moses, 2005, "Pointed Regulates an Eye-Specific Transcriptional Enhancer in the *Drosophila* Hedgehog Gene, Which Is Required for the Movement of the Morphogenetic Furrow", *Development*, Vol. 132, No. 21, pp. 4833-4843.

- Roignant, J.-Y., and J. E. Treisman, 2009, "Pattern Formation in the Drosophila Eye Disc", *The International Journal of Developmental Biology*, Vol. 53, No. 5-6, pp. 795-804.
- Rubin, G. M., and A. C. Spradling, 1982, "Genetic Transformation of Drosophila with Transposable Element Vectors", *Science*, Vol. 218, No. 4570, pp. 348-353.
- Ryder, E., and S. Russell, 2003, "Transposable Elements as Tools for Genomics and Genetics in Drosophila", *Briefings in Functional Genomics & Proteomics*, Vol. 2, No. 1, pp. 57-71.
- Safarik, I., and M. Safariková, 1999, "Use of Magnetic Techniques for the Isolation of Cells", *Journal of Chromatography*, Vol. 722, No.1-2, pp. 33-53.
- Schneiderman, J. I., S. Goldstein, and K. Ahmad, 2010, "Perturbation Analysis of Heterochromatin-Mediated Gene Silencing and Somatic Inheritance", *PLoS Genetics*, Vol. 6, No. 9, p. e1001095.
- Schroeder, A., O. Mueller, S. Stocker, R. Salowsky, M. Leiber, M. Gassmann, S. Lightfoot, W. Menzel, M. Granzow, and T. Ragg, 2006, "The RIN: An RNA Integrity Number for Assigning Integrity Values to RNA Measurements", *BMC Molecular Biology*, Vol. 7, No. 3.
- Seppa, M. J., R. I. Johnson, S. Bao, and R. L. Cagan, 2008, "Polychaetoid Controls Patterning by Modulating Adhesion in the Drosophila Pupal Retina", *Developmental Biology*, Vol. 318, No. 1, pp. 1-16.
- Simons, M., and M. Mlodzik, 2008, "Planar Cell Polarity Signaling: From Fly Development to Human Disease.", *Annual Review of Genetics*, Vol. 42, No. 517.
- Singh, J., and M. Mlodzik, 2012, "Planar Cell Polarity Signaling: Coordination of Cellular Orientation Across Tissues", *Wiley Interdisciplinary Reviews Developmental Biology*, Vol. 1, No. 4, pp. 479-499.

- Sipe, C. W., L. Liu, J. Lee, C. Grimsley-Myers, and X. Lu, 2013, "Lis1 Mediates Planar Polarity of Auditory Hair Cells through Regulation of Microtubule Organization", *Development*, Vol. 140, No. 8, pp. 1785-1795.
- Southall, T. D., K. S. Gold, B. Egger, C. M. Davidson, E. E. Caygill, O. J. Marshall, and A. H. Brand, 2013, "Cell-Type-Specific Profiling of Gene Expression and Chromatin Binding without Cell Isolation: Assaying RNA Pol II Occupancy in Neural Stem Cells", *Developmental Cell*, Vol. 26, No. 1, pp.101-112.
- Spinelli, L., P. Gambette, C. E. Chapple, B. Robisson, A. Baudot, H. Garreta, L. Tichit, A. Guénoche, and C. Brun, 2013, "Clust&See: A Cytoscape Plugin for the Identification, Visualization and Manipulation of Network Clusters", *Bio Systems*, Vol. 113, No. 2, pp. 91-95.
- St Johnston, D., 2002, "The Art and Design of Genetic Screens: *Drosophila Melanogaster*", *Nature Reviews Genetics*, Vol. 3, No. 3, pp. 176-188.
- Strutt, D., R. Johnson, K. Cooper, and S. Bray, 2002, "Asymmetric Localization of Frizzled and the Determination of Notch-Dependent Cell Fate in the *Drosophila* Eye", *Current Biology*, Vol. 12, No. 10, pp. 813-824.
- Strutt, H., and D. Strutt, 2002, "Nonautonomous Planar Polarity Patterning in *Drosophila*: Dishevelled-Independent Functions of Frizzled", *Developmental Cell*, Vol. 3, No. 6, pp. 851-863.
- Şahin, H. B., and A. Çelik, 2013, *Drosophila Eye Development and Photoreceptor Specification*, *eLS*, John Wiley & Sons, Ltd., pp. 1-12.
- Tabas-Madrid, D., R. Nogales-Cadenas, and A. Pascual-Montano, 2012, "GeneCodis3: A Non-Redundant and Modular Enrichment Analysis Tool for Functional Genomics", *Nucleic Acids Research*, Vol. 40, pp. W478-W483.

- Takahashi, K., T. Matsuo, T. Katsube, R. Ueda, and D. Yamamoto, 1998, "Direct Binding between Two PDZ Domain Proteins Canoe and ZO-1 and Their Roles in Regulation of the Jun N-Terminal Kinase Pathway in Drosophila Morphogenesis", *Mechanisms of Development*, Vol. 78, No. 1-2, pp. 97-111.
- Thomas, C., and D. Strutt, 2012, "The Roles of the Cadherins Fat and Dachshous in Planar Polarity Specification in Drosophila", *Developmental Dynamics*, Vol. 241, No. 1, pp. 27-39.
- Tirouvanziam, R., C. J. Davidson, J. S. Lipsick, and L. a Herzenberg, 2004, "Fluorescence-Activated Cell Sorting (FACS) of Drosophila Hemocytes Reveals Important Functional Similarities to Mammalian Leukocytes", *Proceedings of the National Academy of Sciences of the United States of America*, Vol. 101, No. 9, pp. 2912-2917.
- Tissir, F., and A. M. Goffinet, 2013, "Shaping the Nervous System: Role of the Core Planar Cell Polarity Genes", *Nature Reviews Neuroscience*, Vol. 14, No. 8, pp. 525-535.
- Togashi, H., K. Kominami, M. Waseda, H. Komura, J. Miyoshi, M. Takeichi, and Y. Takai, 2011, "Nectins Establish a Checkerboard-like Cellular Pattern in the Auditory Epithelium.", *Science*, Vol. 333, pp. 1144-1147.
- Tomlinson, A., and G. Struhl, 1999, "Decoding Vectorial Information from a Gradient: Sequential Roles of the Receptors Frizzled and Notch in Establishing Planar Polarity in the Drosophila Eye.", *Development*, Vol. 126, No. 24, pp. 5725-5738.
- Tomlinson, M. J., S. Tomlinson, X. B. Yang, and J. Kirkham, 2013, "Cell Separation: Terminology and Practical Considerations.", *Journal of Tissue Engineering*, Vol. 4, pp. 2041731412472690.
- Topczewski, J., D. Sepich, and D. Myers, 2001, "The Zebrafish Glypican Knypek Controls Cell Polarity During Gastrulation Movements of of Convergent Extension", *Developmental Cell*, Vol. 1, pp. 251-264.

- Trapnell, C., L. Pachter, and S. L. Salzberg, 2009, "TopHat: Discovering Splice Junctions with RNA-Seq", *Bioinformatics*, Vol. 25, No. 9, pp. 1105-1111.
- Tree, D., D. Ma, and J. Axelrod, 2002, "A Three-Tiered Mechanism for Regulation of Planar Cell Polarity", *Seminars in Cell & Developmental Biology*, Vol. 306, No. 2, pp. 1-8.
- Vogel, C., S. a Teichmann, and C. Chothia, 2003, "The Immunoglobulin Superfamily in *Drosophila Melanogaster* and *Caenorhabditis Elegans* and the Evolution of Complexity", *Development*, Vol. 130, No. 25, pp. 6317-6328.
- Wagh, D. a, T. M. Rasse, E. Asan, A. Hofbauer, I. Schwenkert, H. Dürbeck, S. Buchner, M.-C. Dabauvalle, M. Schmidt, E. Buchner, 2006, "Bruchpilot, a Protein with Homology to ELKS/CAST, Is Required for Structural Integrity and Function of Synaptic Active Zones in *Drosophila*.", *Neuron*, Vol. 49, No. 6, pp. 833-844.
- Wang, X., M. Starz-Gaiano, T. Bridges, and D. Montell, 2008, "Purification of Specific Cell Populations from *Drosophila* Tissues by Magnetic Bead Sorting, for Use in Gene Expression Profiling", *Protocol Exchange (Online)*. doi:10.1038/nprot.2008.28.
- Wang, Z., M. Gerstein, and M. Snyder, 2009, "RNA-Seq: A Revolutionary Tool for Transcriptomics", *Nature Reviews Genetics*, Vol. 10, No. 1, pp. 57-63.
- Weber, U., C. Pataki, J. Mihaly, and M. Mlodzik, 2008, "Combinatorial Signaling by the Frizzled/PCP and Egfr Pathways during Planar Cell Polarity Establishment in the *Drosophila* Eye", *Developmental Biology*, Vol. 316, No. 1, pp. 110-123.
- White, N. M., and A. P. Jarman, 2000, "*Drosophila* Atonal Controls Photoreceptor R8-Specific Properties and Modulates Both Receptor Tyrosine Kinase and Hedgehog Signalling", *Development*, Vol. 127, No. 8, pp. 1681-1689.

- Wigglesworth, B. Y. V. B., 1940, "Local and General Factors in the Development of "Pattern" in *Rhodnius Prolixus* (Hemiptera)", *Journal of Experimental Biology*, Vol. 17, pp. 180-200.
- Wilhelm, B. T., and J.-R. Landry, 2009, "RNA-Seq-Quantitative Measurement of Expression through Massively Parallel RNA-Sequencing.", *Methods*, Vol. 48, No. 3, pp. 249-257.
- Winnebeck, E. C., C. D. Millar, and G. R. Warman, 2010, "Why Does Insect RNA Look Degraded?", *Journal of Insect Science*, Vol. 10, No. 159, p. 159.
- Winter, C. G., B. Wang, A. Ballew, A. Royou, R. Karess, J. D. Axelrod, and L. Luo, 2001, "Drosophila Rho-Associated Kinase (Drok) Links Frizzled-Mediated Planar Cell Polarity Signaling to the Actin Cytoskeleton.", *Cell*, Vol. 105, No. 1, pp. 81-91.
- Wolff, T., and G. M. Rubin, 1998, "Strabismus, a Novel Gene That Regulates Tissue Polarity and Cell Fate Decisions in *Drosophila*", *Development*, Vol. 125, No. 6, pp. 1149-1159.
- Wong, L., and P. Adler, 1993, "Tissue Polarity Genes of *Drosophila* Regulate the Subcellular Location for Prehair Initiation in Pupal Wing Cells", *The Journal of Cell Biology*, Vol. 123, No. 1, pp. 209-221.
- Wu, J., and M. Mlodzik, 2008, "The Frizzled Extracellular Domain Is a Ligand for Van Gogh/Stbm during Nonautonomous Planar Cell Polarity Signaling", *Developmental Cell*, Vol. 15, No. 3, pp. 462-469.
- Yamada, T., 2003, "EDL/MAE Regulates EGF-Mediated Induction by Antagonizing Ets Transcription Factor Pointed", *Development*, Vol. 130, No. 17, pp. 4085-4096.
- Yang, C., J. D. Axelrod, and M. a Simon, 2002, "Regulation of Frizzled by Fat-like Cadherins During Planar Polarity Signaling in the *Drosophila* Compound Eye", *Cell*, Vol. 108, No. 5, pp. 675-688.

Zeidler, M. P., N. Perrimon, and D. I. Strutt, 1999, "Polarity Determination in the Drosophila Eye: A Novel Role for Unpaired and JAK/STAT Signaling", *Genes & Development*, Vol. 13, No. 10, pp. 1342-1353.

Zheng, L., J. Zhang, and R. Carthew, 1995, "Frizzled Regulates Mirror-Symmetric Pattern Formation in the Drosophila Eye", *Development*, Vol. 121, No. 9, pp. 3045-3055.

Zhu, Y. Y., E. M. Machleder, A. Chenchik, R. Li, and P. D. Siebert, 2001, "Reverse Transcriptase Template Switching: A SMART Approach for Full-Length cDNA Library Construction", *BioTechniques*, Vol. 30, No. 4, pp. 892-897.